University of Naples Federico II

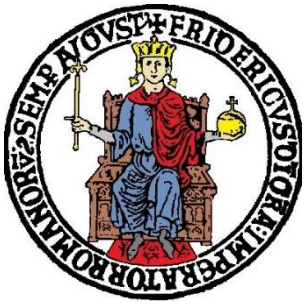

Department of Agricultural Sciences

32nd Cycle of Doctorate in
Agricultural and Food Sciences

An industrial oriented technology for core-shell alginate microbeads production.

Supervisor:
Prof. Fabrizio Sarghini

PhD Candidate:
Angela De Vivo

PhD Program Coordinator:
Prof. Guido D'Urso

Years 2017/2020

Thesis submitted for the degree of PhD in Food Engineering
Napoli, March 2020

PhD Candidate: Angela De Vivo

Supervisor: Prof. Fabrizio Sarghini

PhD Program Coordinator (XXXII Cycle): Prof. Guido D'Urso

Reading Committee:

Prof. Pieter Verboven, University of Leuven

Prof. Maria Charalambides, Imperial College London

Table of Contents

1 Introduction

Ionotropic alginate microgels are commonly used as an encapsulation medium for biomedical, bioprocessing, pharmaceutical and food applications. The purpose is to encapsulate several substances, which in their raw form may be sensitive to heat, light, moisture, pH, toxins, oxidation, mechanical shear, or pressure (Lee et al., 2004; Lin, 2012; Zhang et al., 2007). Microgels are produced via ionotropic cross-linking gelation resulting from the interaction between alginate molecules and calcium or barium cations (Cerveró et al., 2011; Rodríguez-Rivero et al., 2013). The mechanism of cross-linking described by the egg-box model leads to a 3D hydrogel network formation (Simpson et al., 2003) that reduces the space occupied by the alginate because of the water loss (syneresis phenomenon) (Chrastil, 1991; Velings and Mestdagh, 1995). The result is the volume reduction of Ca-alginate beads of 50–60% (Yotsuyanagi et al., 1987) . Thus, normally an alginate bead shrinks during gelation.

Control of the shape, as well as the size and distribution of the microgels is a key factor for their successful application (Lee et al., 2013). The bead size controls the diffusion rate of substrates and products, which is limited in larger beads leading to a lower

process productivity or yield. Sphericity is also an important requisite for the mechanical and chemical stability of the Ca-alginate beads and for the aesthetic quality, which could be a desirable characteristic for pharmaceutical and food products. It has been reported that a non-spherical shape reduce capsule strength (Al-Hajry et al., 1999) and can lead to a breakage of the capsules, resulting in the encapsulant release (Woo et al., 2007). The optimal size range of the microbeads varies depending on the specific application. Large microgels with sizes greater than 1000 μm are favorable for fermentation processes because they allow easy handling, recovery, and purification. A larger particle size (i.e., 500–2000 μm) gives a more distinct texture in the mouth compared to those of smaller particle sizes (i.e., 50–100 μm) and is clearly seen in the functional foods by the consumers, thus promoting marketing strategies for product differentiation (Champagne and Fustier, 2007; Chan et al., 2012). Besides, small microgels (5–25 μm) are also important for controlled and sustained release of an active substance (Burey et al., 2008).

In order to obtain microgels with right-sized for the desired application, various considerations come into play in designing phase including high efficiency and production rates, the scale-up possibilities with no quality concerns, possibility of contamination and the cost constraints if any. The extrusion dripping method has been well classified as relatively simple, size-controlled, low-cost, and scalable formation method for microgels. This method involve the extrusion of a liquid encapsulating material through a nozzle and thus the detachment from the dripping tip in droplet form due to the influence of gravitational force or the use of external force (Lee et al., 2013). In the first case, reference is made to the simple extrusion dripping in which the droplet grows to its maximum volume at the dripping tip prior to detachment. In the second case, reference is made to the use of an external force (e.g. electrostatic potential, coaxial air, vibration) to separate the premature droplet from the dripping tip prior it reaches its maximum volume. By applying these external forces, an improvement of the production rate and a reduction of the bead diameter can be achieved (Leong et al., 2016, Poncelet et al., 1999). Among these methods, the setup of the extrusion method using pressurized air is less complicated and can handle relatively higher viscosity. Hence, the air extrusion method is one of the common methods employed to provide shear force in order to reduce the size of the droplets and eventually the size of the microgels produced, and to increase the production rate of the microgels (Lee et al., 2016).

This chapter will provide i) a description of the general equipment of an air extrusion system including the different design alternatives of the extrusion nozzle ii) an in-depth discussion of the theoretical aspects behind droplet formation and breakup regimes iii) an explanation of the different possibile innovative aspects to improve the existing air extrusion method and iiii) an overview on the production conditions and the properties and formulation of the alginate and gelling solutions that may influence the bead size, size dispersion and shape.

1.1 Setup of an Air Extrusion Method

A typical alginate microgel formation setup includes air or gas supply source, an extrusion nozzle, and a gelation bath, as shown in *Figure 1*.

Generally an air compressor generates the air/gas and its flow rate is controlled by a pressure regulator and monitored by a pressure gauge or a rotameter (Rehg et al., 1986). Before being supplied to the extrusion system, the gas is to be treated to remove humidity and impurities. A battery of filters can be used to remove dust and the microscopic droplets of oil that can be generated by the air compressor (Cocchietto et al., 2013; Yu et al., 2001). The humidity of the gas can also be removed by a filter containing activated carbon (Lee et al., 2016).

Nitrogen can be applied for the bioencapsulation processes, i.e. those processes involving bioactive materials such as microbial bacteria, yeast, animal o plant cells, food bioactives or micronutrients like fish oil and polyphenols, or pharmaceuticals, since sterile or anaerobic conditions are required. Aftel et al. (1996) pointed out that the substitution of air in an air-assisted nozzle with nitrogen do not result in significant differences in droplet mean size.

The typical concentration of calcium chloride prepared for Ca-alginate bead formation is 0.1 M and the acceptable range is from 0.001 to 2.0 M (Lee et al., 2013). Increasing the gelling ion concentration leads to the tightening of the gel network and thus results in a decrease in bead size (Klokk and Melvik, 2002; Ouwerx et al., 1998).

The use of air/gas allows the alginate solution to be conveyed through a tube, from a reservoir to the extrusion nozzle minimizing the incorporation of air bubbles caused by the peristaltic pump and thus, ensuring the production of beads with narrow size distribution (Brandenberger and Widmer, 1998). Moreover, alginate solutions with low viscosity are required to use the peristaltic pump. However, in order to reduce the risk of contamination from the air supply on the final product for bioencapsulation application, a piston pump can be used to deliver alginate solution to the extrusion nozzle (Cocchietto et al., 2013). This avoids the direct contact of the air with the alginate solution.

A different setup with the pressurized air connected to the bottom of the gelation bath can be adopted, where air sprinkling creates continuous stirring in the bath avoiding the microgels from aggregating and ensuring the uniform suspension of microcapsules (Abraham et al., 1996). However, the effect of stirring/mixing in the gelation bath is desirable in order to reduce the concentration gradient between the solution and microgel surface and thus to obtain a more homogeneously gelled alginate microgel. To this end, mechanical devices such as magnetic stirrers, overhead agitation, or the use of a rotating table (*Figure 1*) perform better than the application of pressurized air.

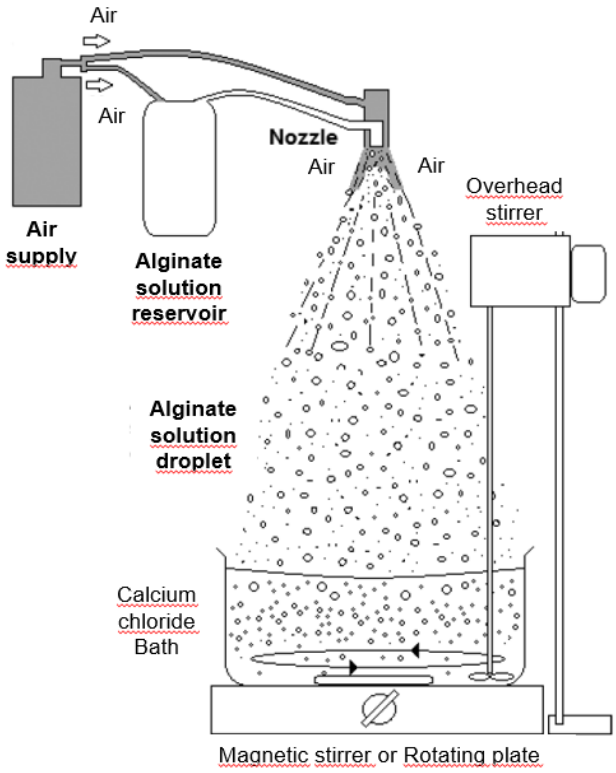

Figure 1. General setup of an air extrusion system.

1.2 Types of Air Extrusion Nozzle

The air extrusion nozzle describes the interaction between the air and the alginate solution. Since the Ca-alginate bead size is primarily defined by the size of the alginate droplets generated at the edge of the dripping, the design of the nozzle is the most important consideration in an extrusion system.

The nozzles in an air extrusion system are typically made from stainless steel, glass, or polyetheretherketone to keep them sterile, as they are easy to clean and sanitize. This is an important requirement when the nozzles are used for bioencapsulation applications. For example, Sugiura et al. (2007) developed a silicon micro-airflow nozzle (60 µm internal diameter) to produce 100 to 300 µm alginate microcapsules with a narrow size distribution.

1.2.1 Simple Air Shear Extrusion Nozzle

The design of these types of nozzle is very simple and include the insertion of a hypodermic needle into a tube where the air flows promoting the detachment of the alginate droplet extruded through the needle (Bressel et al., 2008; Chen et al., 2014) . The needle can be inserted in parallel with the air flow (*Figure 2 a*) (Gåserød et al., 1998), at 45° to the air flow (*Figure 2 b*) (Fiszman et al., 2002; Gåserød et al., 1998), or perpendicular to the direction of the air flow (*Figure 2 c*). The first configuration is expected to lead to the largest alginate droplet and finally the largest alginate microgel.

Typically, air at low pressure and low volumetric flow rate is used since the air force applied on the pendant droplet is a shear force resulting in its detachment before it reaches the maximum size.

This apparatus can be used for low alginate microgel production rates at the laboratory scale. In order to obtain the higher production rate and to move from the small-scale, the use of the coaxial air nozzle can be introduced.

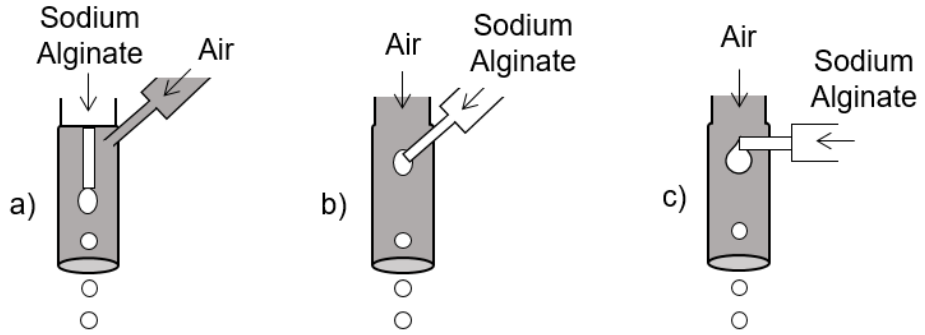

Figure 2. Simple air shear extrusion using a needle into a tube inserted a) parallel with the air flow, b) at 45°to the air flow, c) perpendicular to the air flow.

1.2.2 Air-Liquid Jet Extrusion Nozzle

These types of nozzle enable to pressurize the air up to 0.5 MPa, which is higher than that supplied to the simple air shear extrusion nozzle, described above (< 0.05 MPa). Thus, the flow rate of alginate solution through these nozzle types is increased allowing to move to large-scale.

The apparatus used can be a commercially available or custom-made nozzle such as a coaxial air nozzle (Narsaiah et al., 2014; Prüsse et al., 2008) (*Figure 3*, left side), an atomizing nozzle (Turbotak) (Cui et al., 2006, 2001; Klokk and Melvik, 2002), a fan jet nozzle (Cerveró et al., 2011; Rodríguez-Rivero et al., 2013), or an air-blast atomization nozzle (*Figure 3*, right side) (E. P. Herrero et al., 2006; Edgar P. Herrero et al., 2006).

The technology based on the formation of drops from fluids sprayed through fan jet nozzles allows overcoming clogging problems arising from the use of high viscosity fluids. This is because the alginate solution is subjected to a tensile and stress forces caused by the air that has a velocity much higher that the liquid one. Cerveró et al. (2011) have employed a fan jet nozzle to develop an atomization process with a good productivity working with a viscosity ranging from 90 to 4000 mPa s.

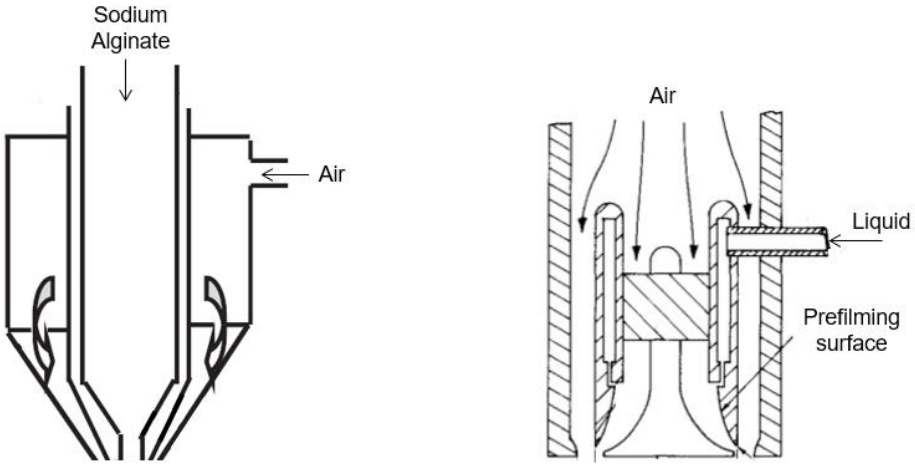

Figure 3. Coaxial air nozzle (left side) and prefilming air blast nozzle (right side).

1.2.3 Flow-Focusing Extrusion Nozzle

Flow focusing extrusion system is a process in which the polymer or inner dispersed phase flows into a central nozzle and an immiscible or outer continuous phase is conveyed through two side channels (as illustrated in *Figure 4*) in order to pressurize the inner phase at the tip of the flow-focusing nozzle (Schneider et al., 2008). The inner phase, i.e., alginate solution is called "focused fluid" while the outer phase, i.e., air is called "focusing fluid". The flow rate of the outer continuous phase is several orders of magnitude higher than the inner disperse phase one. Thus, the central stream is forced into a stationary micro jet-like stream much smaller than the orifice of the nozzle. Considering the high shear stress and the prevailing rapid pressure drop at the orifice, the jet eventually breaks-up into monodisperse and homogeneous droplets with a smaller size than the nozzle orifice. Depending on whether the focusing fluid is a gas or a liquid, flow focusing process is defined as aerodynamic or hydrodynamic respectively (Schneider et al., 2008).

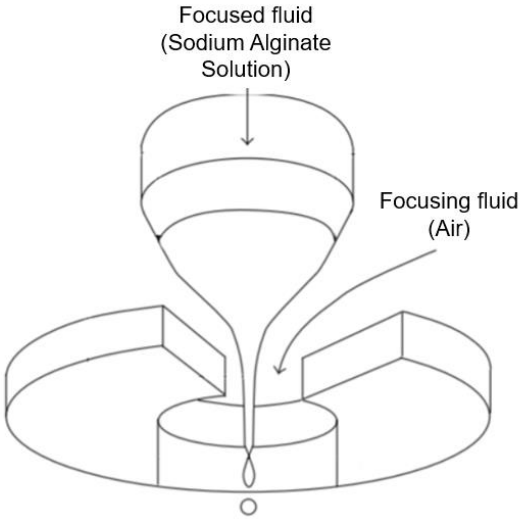

Figure 4. Scheme of functioning of a flow-focusing nozzle. (Reproduced from Martín-Banderas et al., *J. Nanomater.* 2011, 1–10, 2011)

The technology described can be applied to develop an air extrusion nozzle with microchannels. The inner and external diameters are lower compared to the conventional macronozzles in order to further decrease the size of microgels and improve their uniformity. The microfabricated nozzle, known as micro-air flow extrusion nozzle, is advantageous in terms of precision and low pressure loss. This type of nozzle, was successfully employed from Sugiura et al. (2007) to prepare Ca-alginate beads with diameters ranging from 120 to 300 μm.

The flow focusing technique is advantageous to produce micro and nanoparticle. Smaller microcapsules create new prospects for the advancement of microencapsulation technology. Salient features of the flow focusing technology are immediately clear: a) the process consist of a simple one-step without external excitation source, b) the size of the droplets is not determined by nozzle dimension (droplet diameter is smaller than the orifice size), c) particle size can be controlled and adjusted by modifying the fluid flow

velocity of the two phases, d) the flow focusing process leads to high-rates particle and thus, its microfluidic topology can be scaled-up for the industrial production.

1.3 Extrusion Modes of Liquid Droplet Formation

When a droplet is formed at the orifice of a nozzle, five different formation processes of the droplet occurring at the discharge point of the nozzle can be distinguished, depending on the velocity of the extruded liquid (Heinzen et al., 2004):

- The extruded liquid sticks to the edge of the nozzle until the gravitational force, determined by the mass of the droplet, is no longer balanced by the surface tension and the droplet detaches directly from the orifice of the nozzle ($v < v_1$) (*Figure 5 a*).
- An increase in the velocity causes the amount of droplets to increase (*Figure 5 b*) and a further small rise can lead to coalescent droplets resulting in an increased beads size distribution.
- *Figure 5 c* depicts the formation of an undisturbed laminar jet because of the extruded liquid velocity increase, which finally breaks by axial symmetrical vibration and the surface tension.
- With an additional escalation of the jet velocity ($v > v_2$), spiral symmetrical vibrations (*Figure 5 d*) or high frictional forces resulting from the spray jet (*Figure* 5 *e*) produce droplets with large size distribution and less sphericity.

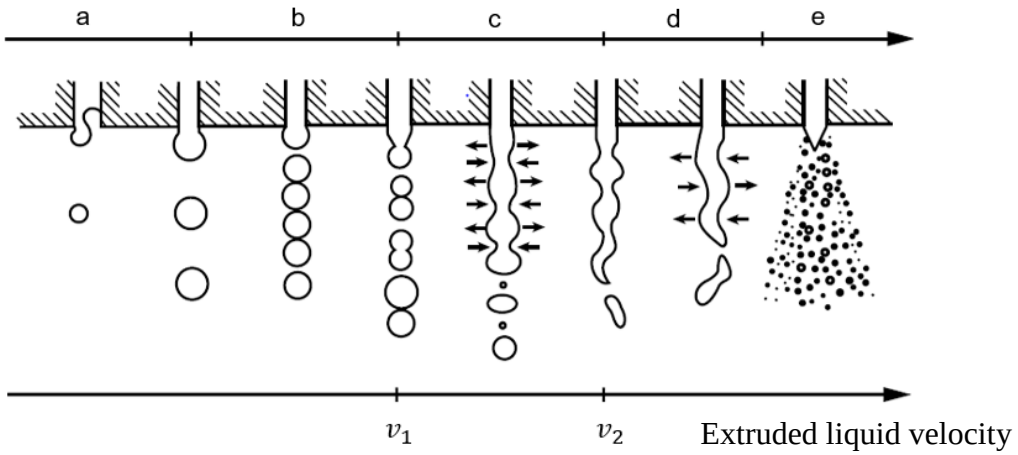

Figure 5. Different mechanisms of droplet formation as a function of the extruded liquid velocities.

(Heinzen et al., 2004) reported that the mechanisms of droplet formation is inter-influenced by the dripping tip diameter and physical properties and flow rate of the extruded liquid solution. The interrelationship is described by the Reynolds (*Re*) and Ohnesorge (*Oh*) numbers characterizing the working conditions (*Figure 6*). The following (2)equations define the dimensionless Reynolds (*Re*) and Ohnesorge (*Oh*) numbers:

$$Re = \frac{v_{\text{liq}} d_d \rho_{\text{liq}}}{\eta} = \frac{\text{inertial forces}}{\text{viscous forces}} \qquad (1)$$

$$Oh = \frac{\eta_{\text{liq}}}{\left(\rho_{\text{liq}} d_d \sigma_{\text{liq}}\right)^{1/2}} = \frac{\text{viscous forces}}{\text{surface tension}} \qquad (2)$$

with

v : velocity of the extruded liquid solution at the point of impact (m s^{-1})

η : viscosity of the extruded liquid solution (Pa s)

ρ : density of the extruded liquid solution (kg m^{-3})

d_d : diameter of the extruded liquid solution droplet (m)

σ : surface tension of the extruded liquid solution (N m^{-1})

Mechanisms *a*, *b*, and *c* are involved in bead production by dripping and jet breakup techniques so called because the droplet detachment at the dripping tip can take dripping or jetting mode as can be seen in *Figure 5* when the velocity is less than the v_2. The boundary transition between the two regimes is highly dependent on the viscosity (or *Oh*) of the liquid solution. Moreover, at constant *Oh*, an increase in the polymer liquid flow rate (*Re*) causes the transition of the detachment mechanism from dripping to jetting (Lee et al., 2013). The formation control of mono-dispersed droplets is only possible via mechanisms *b* and *c* although only the latter is of industrial importance (Whelehan and Marison, 2011).

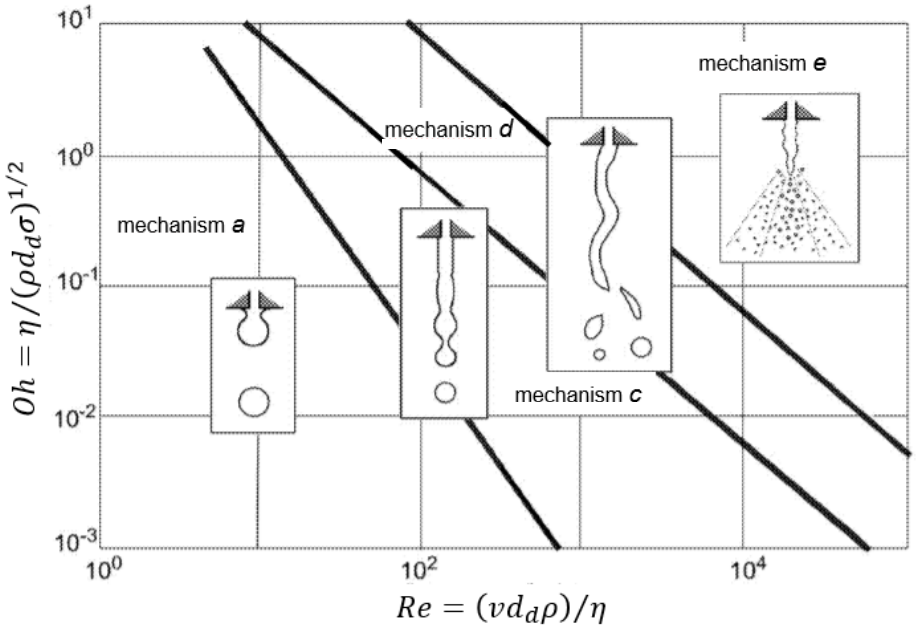

Figure 6. The mechanisms of droplet formation by varying the operating conditions (Ohnesorge number and Reynolds number).

However, using an air extrusion system, it is critical also to control the Weber number (*We*), known as the aerodynamic Weber number which expresses the ratio between inertial and surface tension forces (Lasheras and Hopfinger, 2000):

$$We = \frac{\rho_{air} v_{air}^2 d_j}{\sigma_{\text{liq}}} \qquad (3)$$

with

ρ_g : density of the air/gas (kg m^{-3})

d_j : diameter of the jet (m)

v_g : air/gas velocity measured at the orifice (m s^{-1})

Re_{liq} and We_{air} are the principal dimensionless groups in the Lasheras and Hopfinger's regime diagram (*Figure 7*) and they are calculated for the water-air system. Accordingly, the regime diagram can be used as a reference to establish the extrusion mode of liquid droplets during the formation process provided an alginate solution of low viscosity is used, i.e., water-like solution. This is typical in an atomization system in order to avoid clogging problems (Rodríguez-Rivero et al., 2013). At low Re_{liq} ($Re_{\text{liq}} < 1000$), monodispersed droplets are generated (see mechanism *b* in *Figure 5*). As the flow rate of extruded liquid through the nozzle is increased, the extrusion mode of the liquid transit from dripping to jetting mode (moving along y-axis in *Figure 7*).

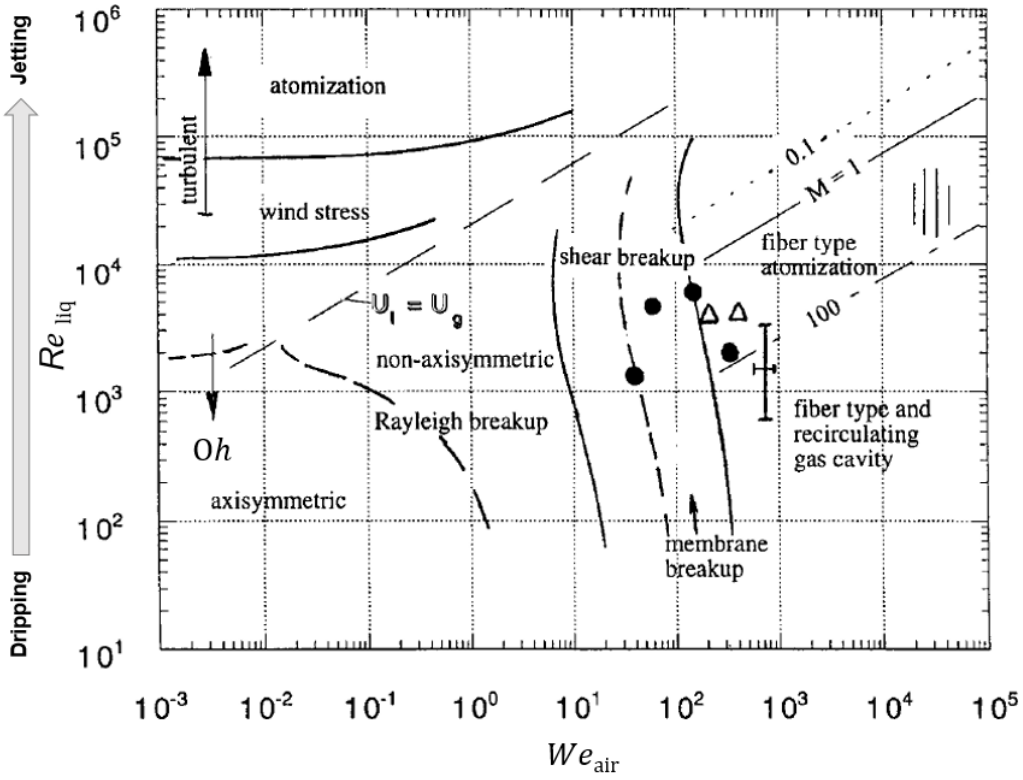

Figure 7. Extrusion modes and breakup regimes presented in the parameter space of the liquid Reynolds number and the aerodynamic Weber number.
(Reproduced from Lasheras, J.C., Hopfinger, E.J., 2000. *Liquid Jet Instability and Atomization in a Coaxial Gas Stream. Annual Review of Fluid Mechanics.* Annu. Rev. Fluid Mech. 32, 275–308)

In the region of low We_{air}, the shear forces exerted from the coaxial air at the air-liquid interface lead to the liquid jet disintegration into fine droplets close to the nozzle. This near-nozzle primary break-up is known as a primary atomization. Moving along x-axis,

a further We_{air} increase causes the droplets to atomize due to the deformation forces exerted on the droplets by the turbulent motion of surrounding air, a process known as secondary atomization (far-nozzle secondary break-up) (Lasheras et al., 1998).
In conclusion, the extrusion mode of alginate solution droplets using an air extrusion system is interinfluenced by the forces and velocity of the fluids figured in the assessment of *Re*, *Oh* and *We* numbers. The first two are based on the process variables of the extruded liquid and the *We* number is related to the process variables of the air/gas.

1.3.1 Deepening of Simple Dripping Detachment

Simple dripping is currently used at lab-scale due to the low liquid volumetric rate. The extruded liquid sticks to the edge of the nozzle until the gravitational force is high enough to overcome the surface tension, resulting in the release of a drop and thus single droplets are directly formed at the orifice outlet (mechanism *a* and *b*). The main factor, which determines the size of the droplet, is the diameter of the pendant droplet neck i.e. the nozzle diameter (as can be seen in Equation(5)).
The equilibrium condition between the two main forces present, gravitational force and surface tension is given by:

$$mg = d_n \sigma \qquad (4)$$

with
m : the critical mass of the droplet (kg)
g : the gravity constant (m s^{-2})
d_n : the diameter of the nozzle (m)
σ : surface tension of the extruded liquid solution (N m^{-1})

Considering the volume of the falling droplet:

$$V = \frac{\pi {d_d}^3}{6} = \frac{m}{\rho} = \frac{d_n\, \sigma}{g\, \rho} \qquad (5)$$

its diameter can be estimated from the following equation:

$$d_d = \sqrt[3]{\frac{6 d_n \sigma}{\rho g}} \qquad (6)$$

However, for systems producing alginate drops which are subsequently gelified into beads by landing in a bath of calcium chloride, it has been reported in the literature (Chan et al., 2009; Whelehan and Marison, 2011) that the diameter of the produced Ca-alginate bead after gelation is different than the diameter of the alginate drop (d_d). More specifically, the actual size of the Ca-alginate beads was found to be smaller than predicted and thus an overall size correction factor (K) was introduced in the Equation (5) in order to improve the size prediction of the Ca-alginate beads. This factor accounts

for the liquid loss factor (k_{LF}) and the shrinkage factor (k_{SF}). The first factor quantifies the partial detachment of alginate liquid pendant from the dripping tip.

$$d_{cab} = K \sqrt[3]{\frac{6 d_n \sigma}{\rho g}} \qquad (7)$$

with
d_{cab} : the diameter of the produced Ca-bead
K : the overall size corrector factor ($K = k_{LF} \cdot k_{SF}$)

The Equation (6) enables a good approximation of d_{cab} to be obtained. It was found that K were between 0.73 and 0.85 under the experimental conditions.
The main drawbacks of this technique are the very low quantities of droplets produced insufficient for industrial application (the production rate is less than 0.5 mL min^{-1}) and the diameter of the produced bead larger than 1000 µm (Lee et al., 2013; Zhang et al., 2007). By introducing an additional force. i.e., the pressurized air, on the droplet formation, the laminar jet breaks up in droplets, which can be released before their maximum volume and thus the size can be chosen in a certain range depending on the applied force. This is in contrast to the droplet formation described in Equation (5), where the droplet diameter depends on the nozzle diameter.

1.4 Coaxial Air-Liquid Jet Disintegration

The complexity of the jet breakup mechanism of liquid droplets during the formation process is due to influence of large number of parameters, such as, the details of the nozzle design, the liquid jet and the air velocity and turbulence, and the physical and thermodynamic states of both liquid and gas.
Jet breakup phenomena have been divided into regimes that reflect differences in the appearance of jets as the operating conditions are changed. The regimes correspond to different combinations of dominant forces (liquid inertia, surface tension, and aerodynamic forces) acting on the jet, leading to its breakup. Lin and Reitz (1998) classified jet breakup in coaxial flows into three main categories (illustrated in *Figure 7*):

- Rayleigh-type breakup. The criteria for assigning jet disintegration to this category are *a)* the mean drop diameter is of the order of the jet diameter and the maximum drop diameter is about twice the jet diameter *b)* the liquid jet breaks up without any liquid membrane or liquid fiber ligament formation. Both axisymmetric breakup ($We_{\text{air}} < 15$) (*Figure 8, left side*) and non-axisymmetric Rayleigh breakup ($15 < We_{\text{air}} < 25$) (*Figure 8, right side*) patterns can be observed.
- Jet disintegration via membrane-type ligaments ($25 < We_{\text{air}} < 70$). At higher airflow rates, the jet develops into a thin liquid sheet (membrane) before breaking into drops. Liquid accumulates at the edges of the thin sheet forming a liquid

frame. The diameter of the frame is smaller than the diameter of the emerging intact liquid jet. The thick frame breaks into drops via the non-axisymmetric Rayleigh mechanism. The diameter of the drops is smaller than the diameter of the jet (*Figure 9*).

– Jet breakup via fiber-type ligaments ($100 < We_{\text{air}} < 500$) (*Figure 10*). At even higher airflow rates, fibers are formed and peel off the jet. Breakup occurs via the non-axisymmetric Rayleigh mechanism, or by breakup into ligaments. The drop diameter is much smaller than the jet diameter.

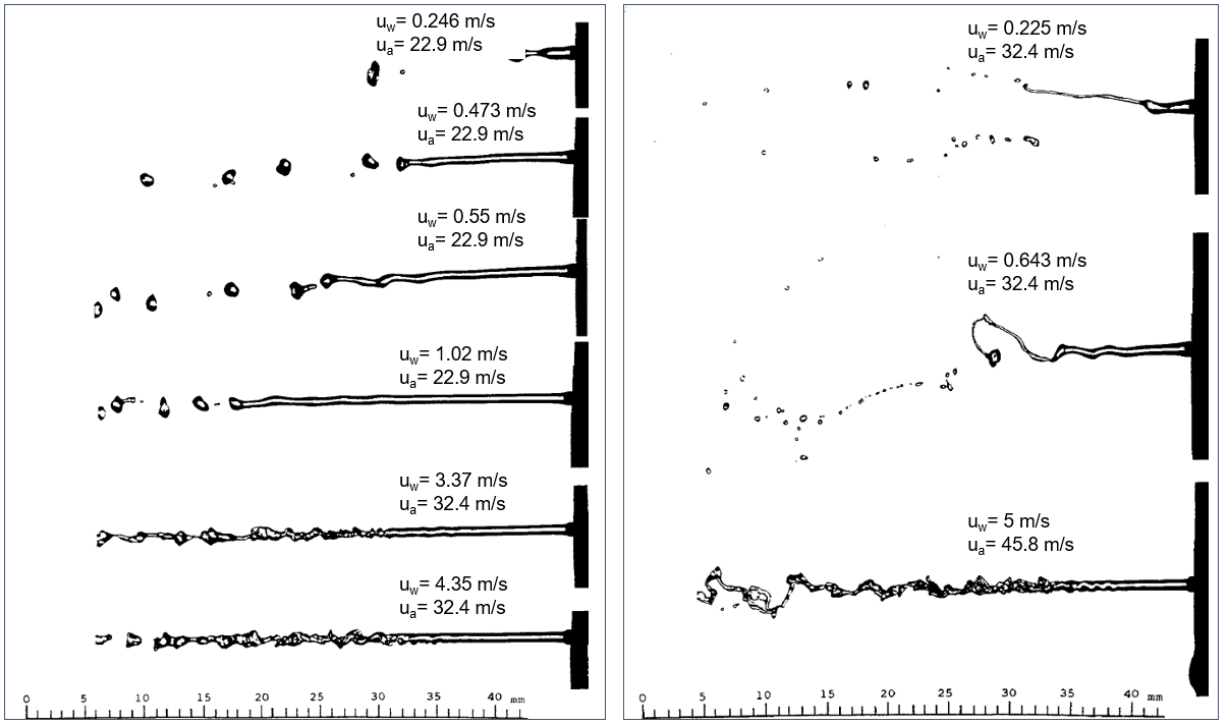

Figure 8. Rayleigh-type axisymmetric (left side) and non-axisymmetric breakup of coaxial jet disintegration (right side). Reproduced from Chigier and Reitz, Regimes of Jet Breakup and Breakup Mechanisms (Physical Aspects), in: Kuo, K. (Ed.), *Recent Advances in Spray Combustion: Spray Atomization and Drop Burning Phenomena.* American Institute of Aeronautics and Astronautics, Inc., Reston, USA, 1996, pp. 109–135)

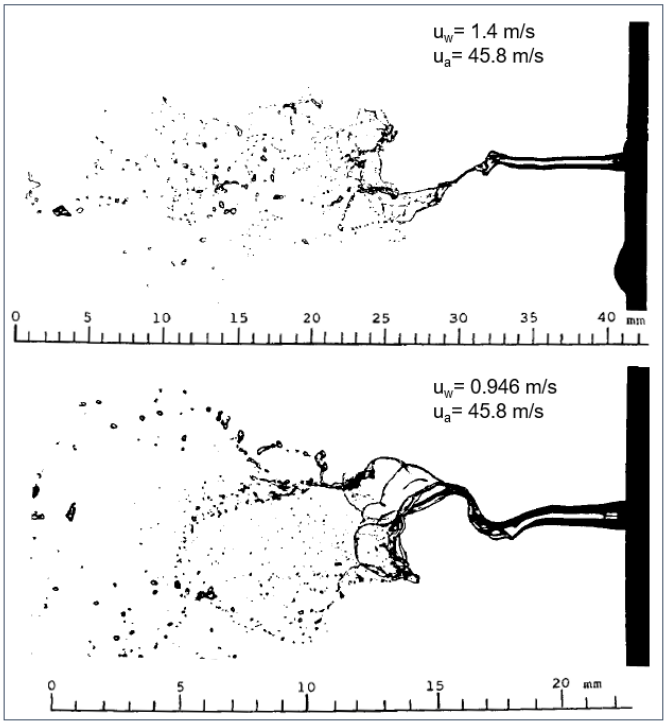

Figure 9. Jet breakup via membrane-type. (Reproduced from Chigier and Reitz, Regimes of Jet Breakup and Breakup Mechanisms (Physical Aspects), in: Kuo, K. (Ed.), *Recent Advances in Spray Combustion: Spray Atomization and Drop Burning Phenomena.*

American Institute of Aeronautics and Astronautics, Inc., Reston, USA, 1996, pp. 109–135)

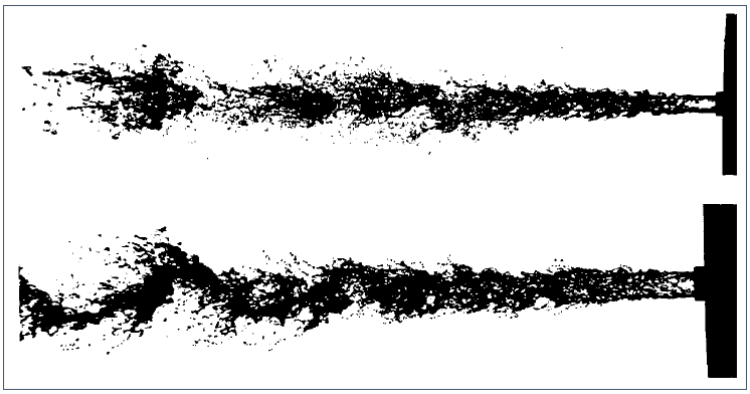

Figure 10. Jet breakup via fiber-type. (Reproduced from Chigier and Reitz, Regimes of Jet Breakup and Breakup Mechanisms (Physical Aspects), in: Kuo, K. (Ed.), *Recent Advances in Spray Combustion: Spray Atomization and Drop Burning Phenomena.* American Institute of Aeronautics and Astronautics, Inc., Reston, USA, 1996, pp. 109–135)

For example, using an air extrusion system coupled with flow-focusing nozzle, Gañán-Calvo (1998) showed that the breakup pattern is regular axisymmetric and the arising droplet stream is monodispersed when the experimental Weber number (We_{air}) is less than 40 (*Figure 11*, left side). However, when the gas stream reaches a fully developed turbulent profile around the liquid jet breakup region, the fluctuations of the gas flow contribute to droplet coalescence and, as a consequence, there is no uniformity in the size of the produced droplets. It has been pointed out that when the focusing inertia per unit mass is very high (as in the case of using a gas) compared to that of a focused liquid, above the critical *We* value of 40, the jet-break up showed a less regular pattern due to the appearing of the non-axisymmetric disturbances coupled to the axisymmetric ones. For larger *We* numbers, the breakup evolve into turbulent (*Figure 11*, right side) since the non-axisymmetric disturbances become dominant compared to the axisymmetric ones and the droplet size distribution shows a significant polydispersity (Martín-Banderas et al., 2005).

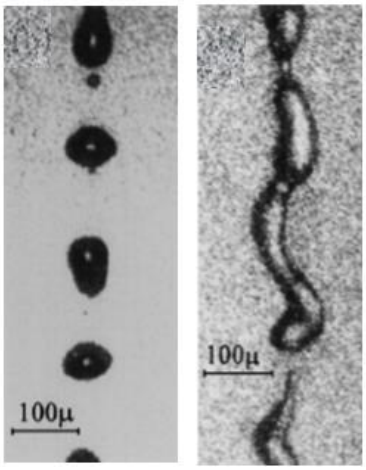

Figure 11. Axisymmetric breakup mode for $We < 40$ *(left side) and nonlinear growth rate of the nonaxisymmetric disturbances for larger* We *numbers (right side).* (Reproduced from Gañán-Calvo, A. M., PRL, 80(2), 285–288, 1998)

In the case of monodispersed microparticles ($We_{\text{air}} < 40$), the corresponding diameter (d_p) is calculated by taking into account the polymer concentration (C, mass of polymer per volume of solution), the polymer solution density (ρ_P), the nozzle diameter (D), the focused and focusing fluid flow rate (Q_d and Q_t) (Martín-Banderas et al., 2011):

$$d_p = \left(\frac{3\pi C}{2k\rho_P}\right)^{1/2} \cdot \left(\frac{Q_d}{Q_t}\right)^{1/2} \cdot D \qquad (8)$$

where k is the wave number of the fastest growing perturbation on the jet (approximately $k \approx 0.5$ for most liquid–liquid combinations) depending on the viscosity and density ratio between the inner and outer liquids.

The Equation (8) can be used to predict the final particle diameter with a remarkable accuracy, given the stream flow rates and the physical properties, or, contrarily, it is possible to define the experimental conditions in order to obtain particles with a desired final diameter. The particle diameter is generally 1/10 up to 1/30 the diameter of the orifice and decreases when as the carrier stream flow rate increases and the polymer flow rate decreases, as reported in the study of Gañán-Calvo et al. (2006) and Tran et al. (2011). In contrast, when the external flow remains constant, as the polymer flow grows, the particle diameter increases.

An interesting area for future research would be the understanding of the formation of sprays and droplets from a liquid jet when the liquid used is a concentrated solution with high viscosity. Different rheological properties may result in different breakup mechanism and thus, the validity of the regime diagram, i.e., the regions where the experimental conditions fall is needed to be investigated.

Before impacting on the surface of a gelation bath, during its fall, the alginate droplet travels at high velocity especially in air extrusion system. As a result, the droplet can be deformed due to the drag forces induced by the surrounding air, droplets oscillation, the collision and the eventual coalescence between droplets due to the atomization. A further shape distortion occurs when the droplet hits the surface of the gelation bath due to its

surface tension and the gelation process (Lee et al., 2013). Specifically, when the droplet penetrates into the gelling solution, viscous forces within the droplet act to retain the spherical droplet shape while the drag forces exerted on the droplet surface from the surrounding solution tend to disrupt the gelled alginate solution droplet (bead). Finally, the residence time in the gelation bath (curing time) affects the degree of bead shrinkage and thus, the size of the Ca-alginate beads. In conclusion, the bead size, size distribution and the final shape of the microgels is determined by the distortions experienced by the droplets in the whole process from atomization to complete gelation.

1.5 Innovative Modifications to Air Extrusion System

1.5.1 Electrostatic Droplet Charging System

Different drawbacks can result from the use of an extrusion air system. Jets of liquids, especially jets of solution with a relatively high viscosity may break up into monodisperse droplets but due to the drag forces induced by surrounding air during traveling and to irregularities in the filament contraction after break-up, distortion of the droplets shape and size occur (Brandenberger et al., 1999). Droplets with different size will move at different velocities resulting in a likely coalescence between the one slower traveling and faster one. Moreover, the coalesced droplets may break up and form satellite droplets. As a result, the sample of alginate microgels has a heterogeneous size distribution. A droplet dispersion system based on electrostatic repulsion forces can be developed to prevent the coalescence and thus, to guarantee the monodispersity. An electrostatic voltage system apply an electrical potential between the nozzle and an electrode, placed directly underneath the nozzle in order to charge negatively the alginate solution droplets (Brandenberger et al., 1999; Whelehan et al., 2010) as illustrated in *Figure 12*. Due to the charge leading to repulsive forces between the droplets, the distance between the droplets in the droplet chain is stabilized. Thus, coalescence is less probable and hence alginate microgels with a narrow size distribution can be produced (Prüsse et al., 2008).

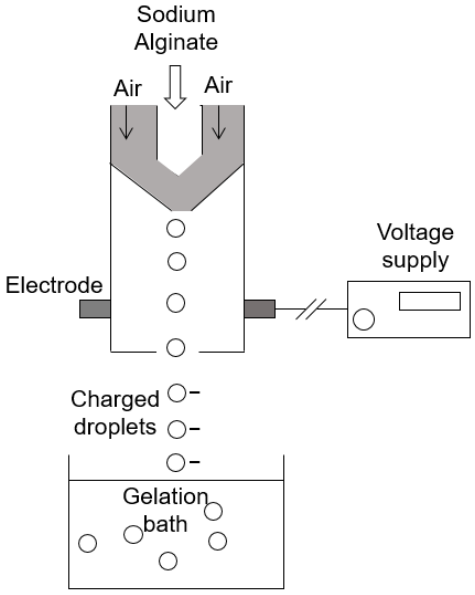

Figure 12. Eletrostatic Droplet Charging Method.

1.5.2 Novel Gelation Methods

The deformation of the droplet due to impact on the gelation bath-air interface and to the following penetration into the gelation bath as well as the inhomogeneous gelation due to the limited diffusion of cross-linking cations represent limitations of the external gelation in a typical air extrusion system. In order to overcome this limitation, innovative gelation methods has been developed to solidify the alginate solution droplets while they are moving in the air with or without the use of a gelation bath. They will be discussed in more detail in this paragraph.

1.5.2.1 Gelation Methods without Gelation Bath

Gelation techniques without gelation bath can concern an in situ gelation or an immediate gelation. In situ gelation (also known as spray evaporation method) enables spray-dry encapsulation in cross-linked alginates in a single step (Santa-Maria et al., 2012), as depicted in *Figure 13*. The alginate solution is infused with ammonia and $CaHPO_4$. During spraying, the volatile base, i.e., ammonia evaporates from the droplet, thus decreasing the spraying solution pH and allowing the calcium ions to be released from the base-insoluble $CaHPO_4$ to cross-link the alginates when the particles dry. In other words, calcium ions needed for cross-linking become available during spray drying by volatilization of ammonia and consequent drop in the pH of the spraying solution. It has been reported (Santa-Maria et al., 2012) that the cross-linking achieved by internal gelation results in small particle sizes and is easily scaled-up for industrial applications. However, only a moderate excess of $CaHPO_4$ can be added in the formulation because the excess of $CaHPO_4$ could contribute to toxicity (Weiner et al., 2001) to the product when the alginate microgel is used as additive for food production. Moreover, this method may not be appropriate in biological applications because of acid conditions required by this method to allow the gelation.

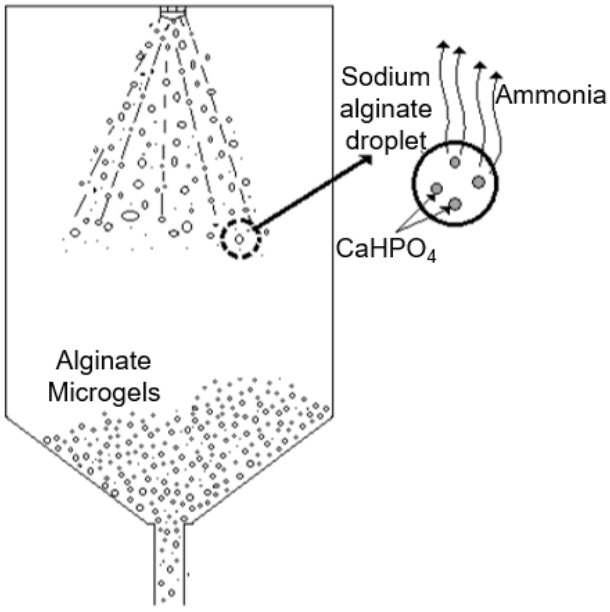

Figure 13. Gelation of alginate solution droplets via spray ecvaporation, i.e., via pH change.

An immediate gelation based on the impinging aerosols technique is a recent advance (Ching et al., 2015; Hariyadi et al., 2012, 2010; Sohail et al., 2012, 2011) involving dual aerosols of alginate solution and $CaCl_2$ cross-linking solution to increase the surface area for cross-linking reactions, resulting in high production of microgels. Alginate gel microparticles were produced by spraying sodium alginate solution into an aerosol mist of $CaCl_2$ solution contained within a closed chamber. Thus, they are solidified upon impinging with the mist of salt solution. Alginate solution and $CaCl_2$ solution are pumped through separate peristaltic pumps to upper and lower spray nozzles, as illustrated in *Figure 14*. In conclusion, this innovative technique allows the production of microgels in batch mode as the microgels do not need to be cured in a gelation bath for a period of time. The impinging aerosols technique showed potential for producing alginate gel microparticles of utility for protection and controlled delivery of a range of therapeutic molecules (Hariyadi et al., 2010). Moreover, this gelation method can minimize the encapsulated bioactive materials leakage that occurs during curing in the gelation bath. The issue is more severe when the released material is valuable (Lee et al., 2016).

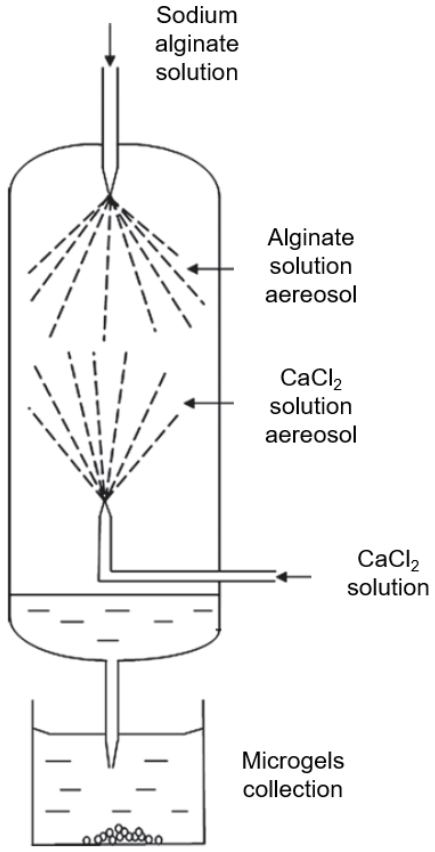

Figure 14. Schematic of the impinging aerosol technique for production of alginate microgels. (Reproduced from Hariyadi et al., J. Drug Target., 18, 831–841, 2010)

1.5.2.2 Gelation with Gelation Bath: Pre-Gelation Methods

Crystal gun method is one of method developed to pre-gel the alginate solution droplet internally during traveling in the air. Tiny $BaCl_2$ crystals were injected into the fluid alginate droplets before they come into contact with external gelation bath. The air-jet extrusion nozzle is equipped with a "crystal gun" arranged perpendicularly to the droplet stream at about one-third of the distance between the droplet generator and the gelation

bath (see schematic diagram in *Figure 15 a*) (Zimmermann et al., 2003). Compared to the conventional gelation, this method allows an instantaneous uniform cross-linking throughout the bead due to the injection of the crystals into the interior of the alginate droplets. The conventional curing process occurs "externally", i.e., in the gelation bath and involve the gel structure rearrangement through the cations diffusion in the microgels in order to allow them to reach an equilibrium size. Therefore, due to the diffusion limitation, the inner part of the microgel may be incompletely gelled compromising the achievement of beads with uniform size and spherical shape. However, the method is only suitable for an air extrusion system that produces alginate solution droplets in a chain pattern, which operates in the regime of Rayleigh breakup. This is to ensure all alginate solution droplets that passed through the crystal gun are injected with an equal amount of $BaCl_2$ crystals. It has been reported that the beads formed by the crystal gun method are more spherical, compact, and mechanically stable compared to beads formed by conventional methods (Lee et al., 2013).

A pre-gelation technique has been developed using a liquid sheet of a $CaCl_2$ solution, as presented in *Figure 15 b*. The alginate solution droplets are shot through a vertically liquid sheet of the gelling agent (obtained using a slot in a polycarbonate horizontal tube) that continuously flows downward in order to induce a fast gelation "on the fly" allowing the droplet to preserve their shape before reaching the gelation bath (Dávalos-Saucedo et al., 2013). The results of the first phase of study demonstrated a loss of spherical shape in the produced beads using this method probably because of the aerodynamic effect on the alginate droplets, which are "flying" perpendicularly to the falling sheet. Moreover, it appears that the most of the microgels were captured by the liquid sheet rather than passed through it.

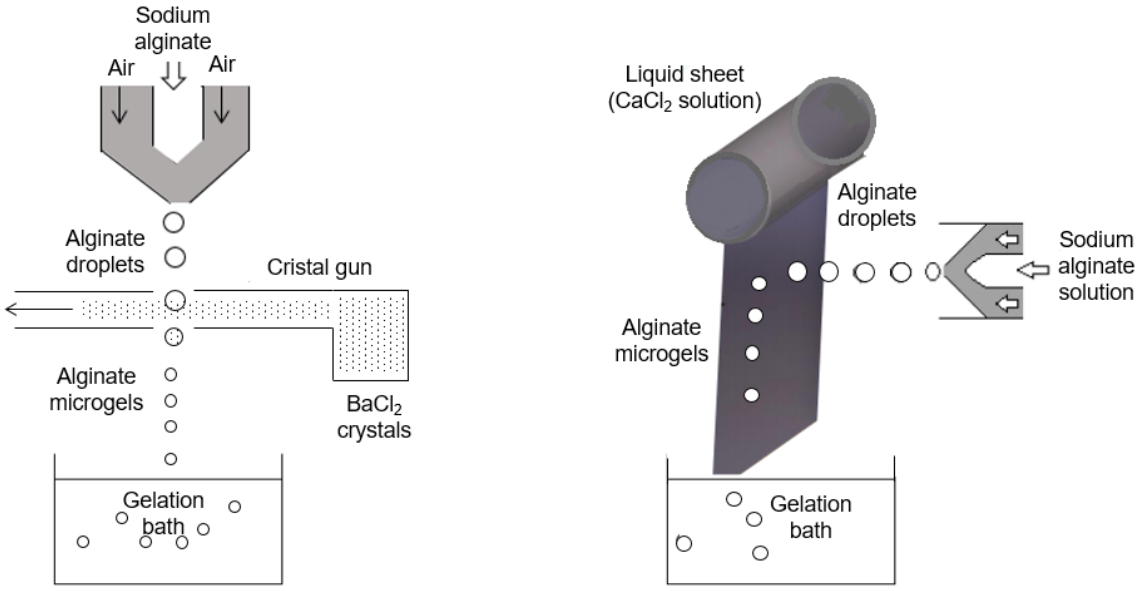

Figure 15. Apparatus setup to pre-gel the alginate solution droplets using a) the crystal gun method and b) the liquid sheet method.

1.6 Influence of Process Variables on Bead Size and Shape

An air extrusion system requires strict control of a number of process variables that are changed to suit an intended application and thus, to produce spherical Ca-alginate beads within the desired size range. This is mostly achieved based on empirical knowledge or trial and error approach according to which various attempts concerning the liquid formulation and experimental setup are required in order to estimate the suitable process variables.

The process variables influence the extrusion modes and the break up regimes of the liquid jet and hence size distribution and shape of the droplets produced. However, the alginate solution droplets experience the strongest shape deformation and size change when they hit the surface of the gelation bath and during gelation (i.e., cross-linking reaction) than when travel in the air between the nozzle and the gelation bath. In the latter case, coalescence and collision phenomena can occur affecting the shape and size change, as explained above.

The main process variables are:

- concentration and physical properties of the alginate solution (density, viscosity, and surface tension)
- diameter and design of the air extrusion nozzle
- air and alginate solution flow rate
- distance between nozzle and gelation bath, i.e. spraying distance
- gelation method
- air temperature only investigated in the spray-drying process since it is determinant for droplet drying and, as a consequence, it has a strong influence on the particle size.

Finally Gelation formulation (amount of Ca^{2+}) and solution properties of the gelation bath are usually not included in the parameters study that affect the bead size and shape of microgels produced using an air extrusion system because they are kept constant.

1.6.1 Alginate Properties and Solution Formulation

The range of the physical proprieties of alginate solution used to produce microgels via air extrusion method is 992–1000 kg m^{-3} for the density, 54–76 mN m^{-1} for the surface tension and 8–5500 mPa s for the viscosity.

Among the physical properties of alginate solution, viscosity is reported to greatly influence mean diameter and shape of alginate microgels. The study of E. P. Herrero et al., 2006 showed that the microcapsules average diameter increases as the alginate viscosity increases. On the other hand, the viscous force within the droplet is important to ensure that the droplet retains its spherical shape against the impact force upon hitting the surface of the gelation bath (Seifert and Phillips, 1997). Moreover, the use of viscous alginate solutions allows to improve mechanical and chemical stability of the microgels. This is because as the viscosity or concentration increases, the number of alginate molecules per volume available for the cross-linking reaction increases resulting in a more strong and compact microgels. However, alginate solutions with a high viscosity

are not suitable for air extrusion encapsulation method since the bead forming process may encounter difficulties related to the pumping of highly viscous solution and the blockage at the dripping nozzle. The permissible upper limit for alginate viscosity is determined by the type of the nozzle. For example, this value is about 5500 mPa s for the coaxial air nozzle. A further increase of the alginate solution can be achieved using a heated nozzle (Voo et al., 2015) to break up the alginate solution jet at the air nozzle.

1.6.2 Air Extrusion Nozzle

1.6.2.1 Diameter

The Ca-alginate bead diameter is mainly dependent and proportional on the external diameter of the extrusion nozzle tip when the flow rate of alginate solution is low. It is well known that the disintegration of the pendant droplets occurs near the nozzle tip at low Reynolds numbers (Rayleigh breakup regime, see *Figure 7*) due to the shear forces exerted from the coaxial air at the air-liquid interface. As the flow rate of alginate solution jet is increased, the diameter of the microgels becomes less dependent on the nozzle tip size since the droplets are formed from far-nozzle secondary atomization break up that occurs away from the nozzle. In this case, the deformation forces exerted on the droplets are due to the turbulent motion of surrounding air.

1.6.2.2 Types

In the air extrusion methods, the air is used to break up the extruded liquid jet into fine droplets and hence to assist the droplet atomization. As the flow rate of the air pressurized increase, the extrusion mode transit from the dripping of monodispersed droplets to the spraying regime resulting in the increase of size dispersion of the droplets. The size variation is commonly expressed by measures of span or coefficient of variance (CV, defined as the ratio of the standard deviation to the mean).

The influence of the different types of air extrusion nozzle on the size and shape of alginate microgels produced from an air extrusion system has been extensively investigated by Lee et al. (2016). In the *Table 1*, reproduced from his study, the range of mean diameter, description of size distribution and shape of alginate microgels are given. The viscosity limit, a typical throughput and the breakup regime of the alginate solution droplets related to the each system connected with a targeted type of nozzle are also available in the *Table 1*.

The throughput is determined by the amount of alginate microgels produced per nozzle per production time for the air extrusion system.

The simple air shear nozzle produce the largest alginate microgels (diameters in the range 180–3170 μm) compared to the other nozzles. Among the air-liquid jet extrusion nozzles, the air blast one can produce fine microgels with diameters lower than 50 μm. Small microgels can also be obtained using flow-focusing or micro-air flow nozzle.

The systems for which the typical production rates are provided (see *Table 1*) can be categorized as a low-throughput system and thus they are suitable for laboratory and pilot-scale applications. On the other hand, the throughput is correlated to the size distribution of alginate microgels as meaning that a low-throughput system results in a narrow distribution with low coefficients of variance (CV). Consequently, a monodisperse and

well-controlled distribution characterize the microgels produced by the different types nozzle with the exception of the coaxial air extrusion nozzle for which monodispersed droplets can be formed only within the primary atomization regime.

Table 1. Summary of the range of mean diameter, size distribution and sphericity of the microgels produced when different types of air extrusion nozzles are used.

Air extrusion nozzle	Microgels mean diameter (μm)	Size distribution description	CV (%)	Sphericity	Viscosity limit (mPa s)	Throughput	Breakup regimes
Simple air shear	180–3170	controlled	<5	++	<4000	~30 ml h^{-1}	RB or PA
Coaxial air	50–2300	narrow	3–50	++	<5500	25 g h^{-1}	PA or SA
Turbotak	3–130	narrow	33	+	<2000	NA	PA or SA
Fan jet	18–450	narrow	NA	+	<4000	NA	PA or SA
Air-blast atomization	1– 50	narrow	NA	+	~190	NA	PA or SA
Flow-focusing	2–50	controlled	<10	++	NA	~0.25 ml h^{-1}	RB
Micro-air flow	130–300	controlled	<8	++	~100	0.33 ml h^{-1}	RB

NA: data not available; ++ spherical shape; + oval shape; Rayleigh breakup = RB; Primary atomization = PA; Secondary atomization = SA.

1.6.3 Air/Liquid Mass Flow Rate Ratio

The findings of the previous investigations confirm the effect of the ratio of liquid flow rate to air flow rate ($\dot{m}_{liq}/\dot{m}_{air}$) on the mean diameter of microgels (Edgar P. Herrero et al., 2006; Mansour and Chigier, 1995). In particular, the atomized microgels size has been expressed in terms of the $\dot{m}_{liq}/\dot{m}_{air}$ ratio, the Weber number (related to the air) and the Ohnesorge number (related to the sodium alginate). It was found that the increase in the $\dot{m}_{air}/\dot{m}_{liq}$ ratio results in a decrease in the mean diameter but in an increase in the particle size distribution (the coefficient of variance rises) (Chan et al., 2012). Moreover, as increase the $\dot{m}_{air}/\dot{m}_{liq}$ the microgels become more spherical. It was also reported that the minimum $\dot{m}_{air}/\dot{m}_{liq}$ to achieve atomization conditions is 0.0011 for 20 g/L sodium alginate. For a value lower than 0.0011, the air could not have had sufficient aerodynamic and shear forces to create instabilities on the liquid surface that could cause the liquid to breakup into smaller droplets. As a general rule, the recommended $\dot{m}_{air}/\dot{m}_{liq}$ ratio operating range is from 3.0 to 5.0 in order to obtain finely atomized sprays. Below the lower limit the mean drop size increases rapidly, and above a value of about 5.0 insignificant improvement can be achieved (El-Shanawany and Lefebvre, 1980).

1.6.4 Spraying distance

The spraying distance between the atomization device and reaction bath is also an important factor that has influence on the mean diameter and the size variation of the microgels produced. Too short or too large distances lead to beads characterized by not controlled size distribution (Cui et al., 2001; El-Shanawany and Lefebvre, 1980). In the former case, aggregation phenomena of droplets in the gelation bath occur since the atomization regime achievement is limited by the small distance. On the other hand, with increasing the spraying distance, the probability of that the alginate droplets will coalesce is increased. However, if the droplets are pre-gelled during traveling in the air, the

probability of coalescing decreases. This can be achieved using gelation methods without the use of gelation bath in order to ensure the instantaneous solidification of the droplets as soon as they come into contact with the Ca^{2+} cations (as previously described).
Finally, beyond the suitable spraying distance range, the alginate droplets could be lost. The most commonly selected distance ranges are between 0.20 and 0.25 m.

1.6.5 Gelation methods

Microgels in the size range of 400–2000 μm (Zimmermann et al., 2003) and 20–1000 μm (Dávalos-Saucedo et al., 2013) are produced using crystal gun method and liquid sheet method, respectively, as gelation methods. The order of magnitude is comparable to the one reported for the extrusion system connected with the coaxial air nozzle without pre-gelation step (see *Table 1*). In other words, the pre-gelation methods do not seem to affect the mean diameter of the microgels since they only help to retain the spherical shape of the droplets after entering the gelation bath.
On the contrary, the gelation methods proposed in this study without gelation bath can produce fine microgels with mean diameter <120 μm for the spray evaporation method (Santa-Maria et al., 2012) and mean diameter <80 μm for the impinging aerosols method (Lee et al., 2016). However, the microgels produced by these gelation methods show a not perfectly spherical shape. This is a reasonable since the required nozzle is a spray nozzle where the atomized alginate solution droplets have a high tendency to coalesce with each other and to become deformed during traveling in the spraying chamber. Despite the irregular shape, the microgels are produced at high throughputs making the spray evaporation method and the impinging aerosols method suitable for the food and agricultural applications where precise control in terms of shape, size, size distribution and encapsulation efficiency is not required compared to biological, medical and pharmaceutical applications. The production rates of these methods are primarily limited by the capacity of the spraying chamber.

1.6.6 Air Temperature

Most applications employing air extrusion systems use the ambient air. Only in the spray-drying process, hot inlet air in the range of 135–180 °C is applied to allow the liquid jet atomization into fine particles (Santa-Maria et al., 2012; Schoubben et al., 2010). Schoubben et al. (2010) investigated the influence of the inlet temperature (in the range 130°C–145°C) on the alginate particle size distributions at controlled outlet temperature (70 °C). The results showed that the highest inlet temperature produced the largest amount of particle aggregations resulting in the increase of mean diameter compared to the other inlet temperatures considered. This is because as the inlet temperature increases, the gap between inlet and outlet temperatures is increased leading to higher residual moisture in the new-extruded particles. The residual humidity promotes particle aggregation resulting in wider size distribution of the particles. Therefore, the inlet temperature has to be selected according to the used solvent minimizing, as much as possible, the gap between inlet and outlet temperatures.

1.7 Objectives

In the previously described framework, the aim of this thesis is the development of an extrusion air system connected with a micro-air flow nozzle resulting in an integration of a feed pump and a co-flow microfluidic device in order to obtain size-controlled droplets and eventually alginate microgels. The microfluidic device is made of hybrid 3D printing technology for the scale-up ability based on the massive parallelization.
As emerged from the literature review, air is generally used in the extrusion system to encapsulate active food ingredients in matrix configuration because of the low cost availability. Moreover, the use of air as a continuous phase covers a series of industrial problems such as like droplet gelation and oil separation making the air extrusion technology implementable on industrial scale compared to the liquid-liquid configuration. The air assisted microfluidic extrusion system is poorly investigated in previous literature for the core-shell encapsulation applications, where liquid jet breakup and droplet atomization including the formation of satellites (secondary) droplets exhibit more complex dynamics.
The specific research questions of this thesis are referred to the:

- optimization of the geometrical parameter of the two different microfluidic devices designed for microencapsulation in matrix and core-shell configuration, respectively
- influence of the process conditions on the size and size dispersion of the microgels produced
- analysis of the physical effects linked to the polymer carrier (alginate) viscosity
- understanding of the fundamental phenomena involved in the formation of a pendant droplet or a jet at the nozzle by coupling the experimental approach and the numerical modeling.

The scientific publications related to this Doctoral thesis are listed below:

I. Marra, F., De Vivo, A., Sarghini, F., 2017. Virtualization of fluid-dynamics in micro-air assisted extruders for food microfluidic based encapsulation. J. Food Eng. 213, 89–98. https://doi.org/10.1016/j.jfoodeng.2017.04.030.

II. Sarghini, F., De Vivo, A., 2019. Effect of process parameters on microencapsulation of active compounds by co-flow air assisted microfluidic extrusion. Chem. Eng. Trans. 75, 439–444. https://doi.org/10.3303/CET1975074.

III. De Vivo, A., Marra F., Sarghini F., submitted. An industrial oriented technology for core-shell alginate microcapsule. Submitted to J. Food Eng. on January 2019, under revision.

Chapter 2 is directly based on publication I, Chapter 3 is directly based on publication II and Chapter 4 is directly based on publication III.

References

Abraham, S.M., Vieth, R.F., Burgess, D.J., 1996. Novel technology for the preparation of sterile alginate-poly-l-lysine microcapsules in a bioreactor. Pharm. Dev. Technol. 1, 63–68. https://doi.org/10.3109/10837459609031419

Acero, A.J., Montanero, J.M., Ferrera, C., Herrada, M.A., Gañán-Calvo, A.M., 2012. Enhancement of the stability of the flow focusing technique for low-viscosity liquids. J. Micromechanics Microengineering 22. https://doi.org/10.1088/0960-1317/22/11/115039

Aftel, R., Gupta, A.K., Cook, C., Presser, C., 1996. Gas property effects on droplet atomiation and combustion in an air-assist atomier. Symp. Combust. 26, 1645–1651. https://doi.org/10.1016/S0082-0784(96)80388-2

Al-Hajry, H.A., Al-Maskry, S.A., Al-Kharousi, L.M., El-Mardi, O., Shayya, W.H., Goosen, M.F.A., 1999. Electrostatic encapsulation and growth of plant cell cultures in alginate. Biotechnol. Prog. 15, 768–774. https://doi.org/10.1021/bp990069e

Babak, V.G., Skotnikova, E.A., Lukina, I.G., Pelletier, S., Hubert, P., Dellacherie, E., 2000. Hydrophobically associating alginate derivatives: Surface tension properties of their mixed aqueous solutions with oppositely charged surfactants. J. Colloid Interface Sci. 225, 505–510. https://doi.org/10.1006/jcis.2000.6788

Belalia, F., Djelali, N.E., 2014. Rheological properties of sodium alginate solutions. Rev. Roum. Chim. 59, 135–145.

Brandenberger, H., Nüssli, D., Piëch, V., Widmer, F., 1999. Monodisperse particle production: A method to prevent drop coalescence using electrostatic forces. J. Electrostat. 45, 227–238. https://doi.org/10.1016/S0304-3886(98)00052-7

Brandenberger, H., Widmer, F., 1998. A new multinozzle encapsulation/immobilisation system to produce uniform beads of alginate. J. Biotechnol. 63, 73–80. https://doi.org/10.1016/S0168-1656(98)00077-7

Bressel, T.A.B., Paz, A.H., Baldo, G., Lima, E.O.C., Matte, U., Saraiva-Pereira, M.L., 2008. An effective device for generating alginate microcapsules. Genet. Mol. Biol. 31, 136–140. https://doi.org/10.1590/S1415-47572008000100023

Burey, P., Bhandari, B.R., Howes, T., Gidley, M.J., 2009. Gel particles from spray-dried disordered polysaccharides. Carbohydr. Polym. 76, 206–213. https://doi.org/10.1016/j.carbpol.2008.10.001

Burey, P., Bhandari, B.R., Howes, T., Gidley, M.J., 2008. Hydrocolloid gel particles: Formation, characterization, and application. Crit. Rev. Food Sci. Nutr. 48, 361–377. https://doi.org/10.1080/10408390701347801

Ceausoglu, I., Hunkeler, D., 2002. A new microencapsulation device for controlled membrane and capsule size distributions. J. Microencapsul. 19, 725–735. https://doi.org/10.1080/02652040210144261

Cerveró, J.M., Nogareda, J., Valle, E.M.M. del, Galán, M.A., 2011. Development of a technology to produce monodispersed microparticles based on the formation of drops from viscous non-Newtonian liquids sprayed through a fan jet nozzle. Chem. Eng. J. 174, 699–708. https://doi.org/10.1016/j.cej.2011.09.063

Champagne, C.P., Fustier, P., 2007. Microencapsulation for the improved delivery of bioactive compounds into foods. Curr. Opin. Biotechnol. 18, 184–190. https://doi.org/10.1016/j.copbio.2007.03.001

Champagne, C.P., Gardner, N.J., Roy, D., 2005. Challenges in the addition of probiotic cultures to foods. Crit. Rev. Food Sci. Nutr. 45, 61–84. https://doi.org/10.1080/10408690590900144

Chan, E.S., Lee, B.B., Ravindra, P., Poncelet, D., 2009. Prediction models for shape and size of ca-alginate macrobeads produced through extrusion-dripping method. J. Colloid Interface Sci. 338, 63–72. https://doi.org/10.1016/j.jcis.2009.05.027

Chan, E.S., Lim, T.K., Ravindra, P., Mansa, R.F., Islam, A., 2012. The effect of low air-to-liquid mass flow rate ratios on the size, size distribution and shape of calcium alginate particles produced using the atomization method. J. Food Eng. 108, 297–303. https://doi.org/10.1016/j.jfoodeng.2011.08.010

Chen, C., Ye, S., Wang, D., Hatting, J.L., Yu, X., 2014. Alginate embedding and subsequent sporulation of in vitro-produced Conidiobolus thromboides hyphae using a pressurised air-extrusion method. Biol. Control 69, 52–58. https://doi.org/10.1016/j.biocontrol.2013.10.016

Chigier, N., Reitz, R.D., 1996. Regimes of Jet Breakup and Breakup Mechanisms (Physical Aspects), in: Kuo, K. (Ed.), Recent Advances in Spray Combustion: Spray Atomization and Drop Burning Phenomena. American Institute of Aeronautics and Astronautics, Inc., Reston, USA, pp. 109–135.

Ching, S.H., Bhandari, B., Webb, R., Bansal, N., 2015. Visualizing the interaction between sodium caseinate and calcium alginate microgel particles. Food Hydrocoll. 43, 165–171. https://doi.org/10.1016/j.foodhyd.2014.05.013

Chrastil, J., 1991. Gelation of Calcium Alginate. Influence of Rice Starch or Rice Flour on the Gelation Kinetics and on the Final Gel Structure. J. Agric. Food Chem. 39, 874–876. https://doi.org/10.1021/jf00005a012

Chu, L.Y., Utada, A.S., Shah, R.K., Kim, J.W., Weitz, D.A., 2007. Controllable monodisperse multiple emulsions. Angew. Chemie - Int. Ed. 46, 8970–8974. https://doi.org/10.1002/anie.200701358

Cocchietto, M., Blasi, P., Lapasin, R., Moro, C., Gallo, D., Sava, G., 2013. Microencapsulation of Bioactive Principles with an Airless Spray-Gun Suitable for Processing High Viscous Solutions. J. Funct. Biomater. 4, 312–328. https://doi.org/10.3390/jfb4040312

Cohen, I., Li, H., Hougland, J.L., Mrksich, M., Nagel, S.R., 2001. Using selective withdrawal to coat microparticles. Science (80-.). 292, 265–267. https://doi.org/10.1126/science.1059175

Cramer, C., Fischer, P., Windhab, E.J., 2004. Drop formation in a co-flowing ambient fluid. Chem. Eng. Sci. 59, 3045–3058. https://doi.org/10.1016/j.ces.2004.04.006

Cubaud, T., Mason, T.G., 2008. Capillary threads and viscous droplets in square microchannels. Phys. Fluids 20. https://doi.org/10.1063/1.2911716

Cui, J.H., Cao, Q.R., Choi, Y.J., Lee, K.H., Lee, B.J., 2006. Effect of additives on the viability of bifidobacteria loaded in alginate poly-l-lysine microparticles during the freeze-drying process. Arch. Pharm. Res. 29, 707–711. https://doi.org/10.1007/BF02968256

Cui, J.H., Goh, J.S., Park, S.Y., Kim, P.H., Lee, B.J., 2001. Preparation and physical characterization of alginate microparticles using air atomization method. Drug Dev. Ind. Pharm. 27, 309–319. https://doi.org/10.1081/DDC-100103730

Dávalos-Saucedo, C.A., Sarghini, F., Masi, P., 2013. Alginate beads production using a liquid sheet pregelification technique, in: Proc. of the Inside Food Symposium. KU Leuven, Leuven, pp. 1–6.

Deshpande, S.S., Anumolu, L., Trujillo, M.F., 2012. Evaluating the performance of the two-phase flow solver interFoam. Comput. Sci. Discov. 5. https://doi.org/10.1088/1749-4699/5/1/014016

Devi, N., Hazarika, D., Deka, C., Kakati, D.K., 2012. Study of complex coacervation of gelatin a and sodium alginate for microencapsulation of olive oil. J. Macromol. Sci. Part A Pure Appl. Chem. 49, 936–945. https://doi.org/10.1080/10601325.2012.722854

Dimotakis, P.E., 2000. The mixing transition in turbulent flows. J. Fluid Mech. 409, 69–98. https://doi.org/10.1017/S0022112099007946

Dulieu, C., Poncelet, D., Neufeld, R.J., 1999. Encapsulation and Immobilization Techniques, in: Ktihtreiber, W.M., Lanza, R.P., Chick, W.L. (Eds.), Cell Encapsulation Technology and Therapeutics. Springer, New York, pp. 3–17.

Eggers, J., Villermaux, E., 2008. Physics of liquid jets. Reports Prog. Phys. 71. https://doi.org/10.1088/0034-4885/71/3/036601

El-Shanawany, M.S., Lefebvre, A.H., 1980. Airblast Atomization: the Effect of Linear Scale on Mean Drop Size. Am. Soc. Mech. Eng. 4, 184–189.

Errico, A., Lama, G.F.C., Francalanci, S., Chirico, G.B., Solari, L., Preti, F., 2019. Flow dynamics and turbulence patterns in a drainage channel colonized by common reed (Phragmites australis) under different scenarios of vegetation management. Ecol. Eng. 133, 39–52. https://doi.org/10.1016/j.ecoleng.2019.04.016

Fijan, R., Šostar-Turk, S., Lapasin, R., 2007. Rheological study of interactions between non-ionic surfactants and polysaccharide thickeners used in textile printing. Carbohydr. Polym. 68, 708–717. https://doi.org/10.1016/j.carbpol.2006.08.006

Fiszman, G.L., Karara, A.L., Finocchiaro, L.M.E., Glikin, G.C., 2002. A laboratory scale device for microencapsulation of genetically engineered cells into alginate beads. Electron. J. Biotechnol. 5, 279–283. https://doi.org/10.2225/vol5-issue3-fulltext-5

Friso, D., 2017. Meccanica dei solidi e dei fluidi alimentari, in: Friso, D. (Ed.), Ingegneria Dell'industria Agroalimentare. CLEUP sc - Cooperativa Libraria Editrice Università di Padova, Padova, pp. 1–62.

Fundueanu, G., Nastruzzi, C., Carpov, A., Desbrieres, J., Rinaudo, M., 1999. Physico-chemical characterization of Ca-alginate microparticles produced with different methods. Biomaterials 20, 1427–1435. https://doi.org/10.1016/S0142-9612(99)00050-2

Gañán-Calvo, A.M., 1998. Generation of Steady Liquid Microthreads and Micron-Sized Monodisperse Sprays in Gas Streams. Phys. Rev. Lett. 80, 285–288. https://doi.org/10.1103/PhysRevLett.80.285

Gañán-Calvo, A.M., Martín-Banderas, L., González-Prieto, R., Rodríguez-Gil, A., Berdún-Álvarez, T., Cebolla, A., Chávez, S., Flores-Mosquera, M., 2006. Straightforward production of encoded microbeads by Flow Focusing: Potential applications for biomolecule detection. Int. J. Pharm. 324, 19–26. https://doi.org/10.1016/j.ijpharm.2006.05.032

Gañán-Calvo, A.M., Montanero, J.M., 2009. Revision of capillary cone-jet physics: Electrospray and flow focusing. Phys. Rev. E - Stat. Nonlinear, Soft Matter Phys. 79, 1–18. https://doi.org/10.1103/PhysRevE.79.066305

Gåserød, O., Smidsrød, O., Skjåk-Bræk, G., 1998. Microcapsules of alginate-chitosan - I. A quantitative study of the interaction between alginate and chitosan. Biomaterials 19, 1815–1825. https://doi.org/10.1016/S0142-9612(98)00073-8

Gordillo, J.M., Ganán-Calvo, A.M., Pŕez-Saborid, M., 2001. Monodisperse microbubbling: Absolute instabilities in coflowing gas-liquid jets. Phys. Fluids 13, 3839–3842. https://doi.org/10.1063/1.1416188

Gouin, S., 2004. Microencapsulation: Industrial appraisal of existing technologies and trends. Trends Food Sci. Technol. 15, 330–347. https://doi.org/10.1016/j.tifs.2003.10.005

Gundabala, V.R., Martinez-Escobar, S., Marquez, S.M., Marquez, M., Fernandez-Nieves, A., 2013. Celloidosomes® via glass-based microfluidics. J. Phys. D. Appl. Phys. 46. https://doi.org/10.1088/0022-3727/46/11/114006

Haeberle, S., Naegele, L., Burger, R., Stetten, F. Von, Zengerle, R., Ducree, J., 2008. Alginate bead fabrication and encapsulation of living cells under centrifugally induced artificial gravity conditions. J. Microencapsul. 25, 267–274. https://doi.org/10.1080/02652040801954333

Hardikar, A.A., Risbud, M. V., Bhonde, R.R., 1999. A simple microcapsule generator design for islet encapsulation. J. Biosci. 24, 371–376. https://doi.org/10.1007/BF02941251

Hariyadi, D.M., Lin, S.C.Y., Wang, Y., Bostrom, T., Turner, M.S., Bhandari, B., Coombes, A.G.A., 2010. Diffusion loading and drug delivery characteristics of alginate gel microparticles produced by a novel impinging aerosols method. J. Drug Target. 18, 831–841. https://doi.org/10.3109/1061186X.2010.525651

Hariyadi, D.M., Wang, Y., Lin, S.C.Y., Bostrom, T., Bhandari, B., Coombes, A.G.A., 2012. Novel alginate gel microspheres produced by impinging aerosols for oral delivery of proteins. J. Microencapsul. 29, 250–261. https://doi.org/10.3109/02652048.2011.646329

Heinzen, C., Berger, A., Marison, I., 2004. Technology for Jet Break-Up for Encapsulation of Cells and Liquids in Monodisperse Microcapsules, in: Nedovic, V., Willaert, R. (Eds.), Fundamentals of Cell Immobilisation Biotechnology. Kluwer Academic Publishers, pp. 257–275.

Herrada, M.A., Gañán-Calvo, A.M., Ojeda-Monge, A., Bluth, B., Riesco-Chueca, P., 2008. Liquid flow focused by a gas: Jetting, dripping, and recirculation. Phys. Rev. E - Stat. Nonlinear, Soft Matter Phys. 78, 1–16. https://doi.org/10.1103/PhysRevE.78.036323

Herrero, Edgar P., Del Valle, E.M.M., Galán, M.A., 2006. Modelling prediction of the microcapsule size of polyelectrolyte complexes produced by atomization. Chem. Eng. J. 121, 1–8. https://doi.org/10.1016/j.cej.2006.04.003

Herrero, E. P., Martín Del Valle, E.M., Galán, M.A., 2006. Development of a new technology for the production of microcapsules based in atomization processes. Chem. Eng. J. 117, 137–142. https://doi.org/10.1016/j.cej.2005.12.022

Hirt, C.W., Nichols, B.D., 1981. Volume of Fluid (VOF) Method for the Dynamics of Free Boundaries*. J. Comput. Phys. 39, 201–225. https://doi.org/10.1016/0021-9991(81)90145-5

Klokk, T.I., Melvik, J.E., 2002. Controlling the size of alginate gel beads by use of a high electrostatic potential. J. Microencapsul. 19, 415–424. https://doi.org/10.1080/02652040210144234

Kontturi, L.S., Yliperttula, M., Toivanen, P., Määttä, A., Määttä, A.M., Urtti, A., 2011. A laboratory-scale device for the straightforward production of uniform, small sized cell microcapsules with long-term cell viability. J. Control. Release 152, 376–381. https://doi.org/10.1016/j.jconrel.2011.03.005

Krasaekoopt, W., Bhandari, B., Deeth, H., 2004. The influence of coating materials on some properties of alginate beads and survivability of microencapsulated probiotic bacteria. Int. Dairy J. 14, 737–743. https://doi.org/10.1016/j.idairyj.2004.01.004

Lakkis, J.M., 2016. Encapsulation and controlled release in bakery applications, in: Lakkis, J.M. (Ed.), Encapsulation and Controlled Release Technologies in Food Systems. John Wiley & Sons, Inc., United Kingdom, pp. 204–235.

Lasheras, J.C., Hopfinger, E.J., 2000. Liquid Jet Instability and Atomization in a Coaxial Gas Stream. Annual Review of Fluid Mechanics. Annu. Rev. Fluid Mech. 32, 275–308. https://doi.org/10.1146/annurev.genom.1.1.409

Lasheras, J.C., Villermaux, E., Hopfinger, E.J., 1998. Break-up and atomization of a round water jet by a high-speed annular air jet. J. Fluid Mech. 30, 85–105.

Lee, B.B., Bhandari, B.R., Howes, T., 2016. Air Extrusion System for Ionotropic Alginate Microgel Particle Formation: A Review. Chem. Eng. Technol. 39, 2355–2369. https://doi.org/10.1002/ceat.201600088

Lee, B.B., Ravindra, P., Chan, E.S., 2013. Size and shape of calcium alginate beads produced by extrusion dripping. Chem. Eng. Technol. 36, 1627–1642.

https://doi.org/10.1002/ceat.201300230
Lee, J.S., Cha, D.S., Park, H.J., 2004. Survival of freeze-dried Lactobacillus bulgaricus KFRI 673 in chitosan-coated calcium alginate microparticles. J. Agric. Food Chem. 52, 7300–7305. https://doi.org/10.1021/jf040235k
Leong, J.Y., Lam, W.H., Ho, K.W., Voo, W.P., Lee, M.F.X., Lim, H.P., Lim, S.L., Tey, B.T., Poncelet, D., Chan, E.S., 2016. Advances in fabricating spherical alginate hydrogels with controlled particle designs by ionotropic gelation as encapsulation systems. Particuology 24, 44–60. https://doi.org/10.1016/j.partic.2015.09.004
Lin, S.P., Reitz, R.D., 1998. Drop and Spray Formation from a Liquid Jet. Annu. Rev. Fluid Mech. 30, 85–105. https://doi.org/10.1146/annurev.fluid.30.1.85
Lin, T.C., 2012. Performance of a Micro Atomizer Under Single-Fluid and Twin-Fluid Micro-Encapsulation Process. Int. J. Mod. Phys. Conf. Ser. 19, 219–226. https://doi.org/10.1142/s2010194512008781
Ma, J., Lin, Y., Chen, X., Zhao, B., Zhang, J., 2014. Flow behavior, thixotropy and dynamical viscoelasticity of sodium alginate aqueous solutions. Food Hydrocoll. 38, 119–128. https://doi.org/10.1016/j.foodhyd.2013.11.016
Mansour, A., Chigier, N., 1995. Air-blast atomization of non-Newtonian liquids. J. Nonnewton. Fluid Mech. 58, 161–194. https://doi.org/10.1016/0377-0257(95)01356-Z
Marra, F., De Vivo, A., Sarghini, F., 2018. Air Assisted Production of Alginate Beads Using Focusing Flow Microfluidic Devices: Numerical Modeling of Beads Formation. Lect. Notes Bioeng. 119–127. https://doi.org/10.1007/978-3-319-62027-5_11
Marra, F., De Vivo, A., Sarghini, F., 2017. Virtualization of fluid-dynamics in micro-air assisted extruders for food microfluidic based encapsulation. J. Food Eng. 213, 89–98. https://doi.org/10.1016/j.jfoodeng.2017.04.030
Martín-Banderas, L., Flores-Masquera, M., Riesco-Chueca, P., Rodríguez-Gil, A., Cebolla, Á., Chávez, S., Gañán-Calvo, A.M., 2005. Flow focusing: A versatile technology to produce size-controlled and specific-morphology microparticles. Small 1, 688–692. https://doi.org/10.1002/smll.200500087
Martín-Banderas, L., González-Prieto, R., Rodríguez-Gil, A., Fernández-Arévalo, M., Flores-Mosquera, M., Chávez, S., Gaņán-Calvo, A.M., 2011. Application of flow focusing to the break-up of a magnetite suspension jet for the production of paramagnetic microparticles. J. Nanomater. 2011, 1–10. https://doi.org/10.1155/2011/527437
Martins, E., Poncelet, D., Rodrigues, R.C., Renard, D., 2017. Oil encapsulation techniques using alginate as encapsulating agent: applications and drawbacks. J. Microencapsul. 34, 754–771. https://doi.org/10.1080/02652048.2017.1403495
Montanero, J.M., Rebollo-Muņoz, N., Herrada, M.A., Gaņán-Calvo, A.M., 2011. Global stability of the focusing effect of fluid jet flows. Phys. Rev. E - Stat. Nonlinear, Soft Matter Phys. 83, 1–7. https://doi.org/10.1103/PhysRevE.83.036309
Murakami, R., Takashima, R., 2003. Mechanical properties of the capsules of chitosan-soy globulin polyelectrolyte complex. Food Hydrocoll. 17, 885–888. https://doi.org/10.1016/S0268-005X(03)00109-7
Narsaiah, K., Jha, S.N., Wilson, R.A., Mandge, H.M., Manikantan, M.R., 2014. Optimizing microencapsulation of nisin with sodium alginate and guar gum. J. Food Sci. Technol. 51, 4054–4059. https://doi.org/10.1007/s13197-012-0886-6
Nie, Z., Seo, M.S., Xu, S., Lewis, P.C., Mok, M., Kumacheva, E., Whitesides, G.M., Garstecki, P., Stone, H.A., 2008. Emulsification in a microfluidic flow-focusing device: Effect of the viscosities of the liquids. Microfluid. Nanofluidics 5, 585–594. https://doi.org/10.1007/s10404-008-0271-y

Ouwerx, C., Velings, N., Mestdagh, M.M., Axelos, M.A.V., 1998. Physico-chemical properties and rheology of alginate gel beads formed with various divalent cations. Polym. Gels Networks 6, 393–408. https://doi.org/10.1016/S0966-7822(98)00035-5

Peretz, S., 2004. Interaction of alginate with metal ions, cationic surfactants and cationic dyes 49, 857–865.

Perrechil, F.A., Sato, A.C.K., Cunha, R.L., 2011. κ-Carrageenan-sodium caseinate microgel production by atomization: Critical analysis of the experimental procedure. J. Food Eng. 104, 123–133. https://doi.org/10.1016/j.jfoodeng.2010.12.004

Poncelet, D., 2001. Production of Alginate Beads by Emulsification/Internal Gelation. Ann. N. Y. Acad. Sci. 944, 74–82. https://doi.org/10.1111/j.1749-6632.2001.tb03824.x

Poncelet, D., Babak, V.G., Neufeld, R.J., Goosen, M.F.A., Burgarski, B., 1999. Theory of electrostatic dispersion of polymer solutions in the production of microgel beads containing biocatalyst. Adv. Colloid Interface Sci. 79, 213–228. https://doi.org/10.1016/S0001-8686(97)00037-7

Poncelet, D., Poncelet De Smet, B., Beaulieu, C., Neufeld, R.J., 1993. Scale-up of gel bead and microcapsule production in cell immobilization, in: Goosen, M.F.A. (Ed.), Fundamentals of Animal Cell Encapsulation and Immobilization. CRC Press, pp. 113–141.

Prüsse, U., Bilancetti, L., Bučko, M., Bugarski, B., Bukowski, J., Gemeiner, P., Lewińska, D., Manojlovic, V., Massart, B., Nastruzzi, C., Nedovic, V., Poncelet, D., Siebenhaar, S., Tobler, L., Tosi, A., Vikartovská, A., Vorlop, K.D., 2008. Comparison of different technologies for alginate beads production. Chem. Pap. 62, 364–374. https://doi.org/10.2478/s11696-008-0035-x

Rehg, T., Dorger, C., Chau, P.C., 1986. Application of an atomizer in producing small alginate gel beads for cell immobilization. 8, 111–114.

Rodríguez-Rivero, C., Nogareda, J., Martín, M., del Valle, E.M.M., Galán, M.A., 2013. CFD modeling and its validation of non-Newtonian fluid flow in a microparticle production process using fan jet nozzles. Powder Technol. 246, 617–624. https://doi.org/10.1016/j.powtec.2013.05.050

Santa-Maria, M., Scher, H., Jeoh, T., 2012. Microencapsulation of bioactives in cross-linked alginate matrices by spray drying. J. Microencapsul. 29, 286–295. https://doi.org/10.3109/02652048.2011.651494

Sarghini, F., 2015. Microfluidic Encapsulation Process, in: Mishra, M.K. (Ed.), Handbook of Encapsulation and Controlled Release. CRC Press, Boca Raton, USA, pp. 359–378.

Sarghini, F., De Vivo, A., 2019. Effect of process parameters on microencapsulation of active compounds by co-flow air assisted microfluidic extrusion. Chem. Eng. Trans. 75, 439–444. https://doi.org/10.3303/CET1975074

Schneider, T., Chapman, G.H., Häfeli, U.O., 2011. Effects of chemical and physical parameters in the generation of microspheres by hydrodynamic flow focusing. Colloids Surfaces B Biointerfaces 87, 361–368. https://doi.org/10.1016/j.colsurfb.2011.05.040

Schneider, T., Zhao, H., Jackson, J.K., Chapman, G.H., Dykes, J., HaFeli, U.O., 2008. Use of Hydrodynamic Flow Focusing for the Generation of Biodegradable Camptothecin-Loaded Polymer Microspheres. J. Pharm. Sci. 97, 4943–4954. https://doi.org/10.1002/jps.21344

Schoubben, A., Blasi, P., Giovagnoli, S., Rossi, C., Ricci, M., 2010. Development of a scalable procedure for fine calcium alginate particle preparation. Chem. Eng. J. 160, 363–369. https://doi.org/10.1016/j.cej.2010.02.062

Seifert, D.B., Phillips, J.A., 1997. Production of small, monodispersed alginate beads for cell immobilization. Biotechnol. Prog. 13, 562–568. https://doi.org/10.1021/bp9700723

Shah, R.K., Shum, H.C., Rowat, A.C., Lee, D., Agresti, J.J., Utada, A.S., Chu, L.-Y., Kim, J.-W., Fernandez-Nieves, A., Martinez, C.J., Weitz, D.A., 2008. Designer emulsions using microfluidics Open access under CC BY-NC-ND license. Mater. Today 11, 18–27. https://doi.org/10.1016/S1369-7021(08)70053-1

Shilpa, A., Agrawal, S.S., Ray, A.R., 2003. Controlled delivery of drugs from alginate matrix. J. Macromol. Sci. - Polym. Rev. 43, 187–221. https://doi.org/10.1081/MC-120020160

Si, T., Li, F., Yin, X.Y., Yi, X.Z., 2009. Modes in flow focusing and instability of coaxial liquid-gas jets. J. Fluid Mech. 629, 1–23. https://doi.org/10.1017/S0022112009006211

Simpson, N.E., Grant, S.C., Blackband, S.J., Constantinidis, I., 2003. NMR properties of alginate microbeads. Biomaterials 24, 4941–4948. https://doi.org/10.1016/S0142-9612(03)00418-6

Sohail, A., Turner, M.S., Coombes, A., Bostrom, T., Bhandari, B., 2011. Survivability of probiotics encapsulated in alginate gel microbeads using a novel impinging aerosols method. Int. J. Food Microbiol. 145, 162–168. https://doi.org/10.1016/j.ijfoodmicro.2010.12.007

Sohail, A., Turner, M.S., Prabawati, E.K., Coombes, A.G.A., Bhandari, B., 2012. Evaluation of Lactobacillus rhamnosus GG and Lactobacillus acidophilus NCFM encapsulated using a novel impinging aerosol method in fruit food products. Int. J. Food Microbiol. 157, 162–166. https://doi.org/10.1016/j.ijfoodmicro.2012.04.025

Sugiura, S., Oda, T., Aoyagi, Y., Matsuo, R., Enomoto, T., Matsumoto, K., Nakamura, T., Satake, M., Ochiai, A., Ohkohchi, N., Nakajima, M., 2007. Microfabricated airflow nozzle for microencapsulation of living cells into 150 micrometer microcapsules. Biomed. Microdevices 9, 91–99. https://doi.org/10.1007/s10544-006-9011-9

Sugiura, S., Oda, T., Izumida, Y., Aoyagi, Y., Satake, M., Ochiai, A., Ohkohchi, N., Nakajima, M., 2005. Size control of calcium alginate beads containing living cells using micro-nozzle array. Biomaterials 26, 3327–3331. https://doi.org/10.1016/j.biomaterials.2004.08.029

Sun, X.T., Liu, M., Xu, Z.R., 2014. Microfluidic fabrication of multifunctional particles and their analytical applications. Talanta 121, 163–177. https://doi.org/10.1016/j.talanta.2013.12.060

Tabeei, A., Samimi, A., Khorram, M., Moghadam, H., 2012. Study pulsating electrospray of non-Newtonian and thixotropic sodium alginate solution. J. Electrostat. 70, 77–82. https://doi.org/10.1016/j.elstat.2011.10.006

Tran, V.T., Benoît, J.P., Venier-Julienne, M.C., 2011. Why and how to prepare biodegradable, monodispersed, polymeric microparticles in the field of pharmacy? Int. J. Pharm. 407, 1–11. https://doi.org/10.1016/j.ijpharm.2011.01.027

Tryggvason, G., Scardovelli, R., Zaleski, S., 2004. Direct Numerical Simulations of Gas-Liquid Multiphase flows. Cambridge University Press, Cambridge. https://doi.org/10.1142/9781860949609_0009

Utada, A.S., Chu, L., Link, D.R., Holtze, C., Weitz, D.A., 2007. Dripping, Jetting, Drops, and Wetting: The Magic of Microfluidics 32, 702–708.

Utada, A.S., Lorenceau, E., Link, D.R., Kaplan, P.D., Stone, H.A., Weitz, D.A., 2005. Monodisperse double emulsions generated from a microcapillary device. Science (80-.). 308, 537–541. https://doi.org/10.1126/science.1109164

Van Steijn, V., Kleijn, C.R., Kreutzer, M.T., 2009. Flows around confined bubbles and

their importance in triggering pinch-off. Phys. Rev. Lett. 103, 1–4. https://doi.org/10.1103/PhysRevLett.103.214501
Vega, E.J., Montanero, J.M., Herrada, M.A., Gañán-Calvo, A.M., 2010. Global and local instability of flow focusing: The influence of the geometry. Phys. Fluids 22, 1–10. https://doi.org/10.1063/1.3450321
Velings, N.M., Mestdagh, M.M., 1995. Physico-chemical properties of alginate gel beads. Polym. Gels Networks 3, 311–330. https://doi.org/10.1016/0966-7822(94)00043-7
Voo, W.P., Lee, B.B., Idris, A., Islam, A., Tey, B.T., Chan, E.S., 2015. Production of ultra-high concentration calcium alginate beads with prolonged dissolution profile. RSC Adv. 5, 36687–36695. https://doi.org/10.1039/c5ra03862f
Weiner, M.L., Salminen, W.F., Larson, P.R., Barter, R.A., Kranetz, J.L., Simon, G.S., 2001. Toxicological review of inorganic phosphates. Food Chem. Toxicol. 39, 759–786. https://doi.org/10.1016/S0278-6915(01)00028-X
Whelehan, M., Marison, I.W., 2011. Microencapsulation using vibrating technology. J. Microencapsul. 28, 669–688. https://doi.org/10.3109/02652048.2011.586068
Whelehan, M., von Stockar, U., Marison, I.W., 2010. Removal of pharmaceuticals from water: Using liquid-core microcapsules as a novel approach. Water Res. 44, 2314–2324. https://doi.org/10.1016/j.watres.2009.12.036
Wikström, J., Elomaa, M., Syväjärvi, H., Kuokkanen, J., Yliperttula, M., Honkakoski, P., Urtti, A., 2008. Alginate-based microencapsulation of retinal pigment epithelial cell line for cell therapy. Biomaterials 29, 869–876. https://doi.org/10.1016/j.biomaterials.2007.10.056
Woo, J.W., Roh, H.J., Park, H.D., Ji, C.I., Lee, Y.B., Kim, S.B., 2007. Sphericity Optimization of Calcium Alginate Gel Beads and the Effects of Processing Conditions on Their Physical Properties. Food Sci. Biotechnol. 16, 715–721.
Wu, J., Kong, T., Yeung, K.W.K., Shum, H.C., Cheung, K.M.C., Wang, L., To, M.K.T., 2013. Fabrication and characterization of monodisperse PLGA-alginate core-shell microspheres with monodisperse size and homogeneous shells for controlled drug release. Acta Biomater. 9, 7410–7419. https://doi.org/10.1016/j.actbio.2013.03.022
Yotsuyanagi, T., Ohkubo, T., Ohhashi, T., Ikeda, K., 1987. Calcium-Induced Gelation of Alginic Acid and pH-Sensitive Reswelling of Dried Gels. Chem. Pharm. Bull. 35, 1555–1563. https://doi.org/10.1248/cpb.35.1555
Yu, W.K., Yim, T. Bin, Lee, K.Y., Heo, T.R., 2001. Effect of skim milk-alginate beads on survival rate of bifidobacteria. Biotechnol. Bioprocess Eng. 6, 133–138. https://doi.org/10.1007/BF02931959
Zhang, J., Li, X., Zhang, D., Xiu, Z., 2007. Theoretical and experimental investigations on the size of alginate microspheres prepared by dropping and spraying. J. Microencapsul. 24, 303–322. https://doi.org/10.1080/02652040701339098
Zhou, C., Yue, P., Feng, J.J., 2006. Formation of simple and compound drops in microfluidic devices. Phys. Fluids 18, 1–14. https://doi.org/10.1063/1.2353116
Zimmermann, H., Hillgärtner, M., Manz, B., Feilen, P., Brunnenmeier, F., Leinfelder, U., Weber, M., Cramer, H., Schneider, S., Hendrich, C., Volke, F., Zimmermann, U., 2003. Fabrication of homogeneously cross-linked, functional alginate microcapsules validated by NMR-, CLSM- and AFM-imaging. Biomaterials 24, 2083–2096. https://doi.org/10.1016/S0142-9612(02)00639-7

2 Jet Instabilities Dominating the Drops Breakup Dynamics

2.1 Introduction

The application of hydrocolloid gel particles is gaining momentum in several fields, including food, chemical, and pharmaceutical industries. Among several possibilities, alginate gel particles are widely used, being non-toxic, biocompatible, biodegradable, cheap, and relatively simple to produce, particularly appreciated as carrier for microencapsulated compounds. Usually, particle size and their shape are crucial for specific applications.

Alginate is often used in both matrix and drop-in-drop encapsulation, and industrial scale production of possibly monodispersed alginate beads with desirable characteristics such as controlled size and shape is a desirable target in food industry.

In order to design systems and develop methods able to produce microdroplets and microbeads holding the desired characteristics, both in terms of product and process, a suitable microfluidic system must be adopted. Its main feature, beside scalability, ease of operation, ability to keep the production rate while ensuring sterility and avoiding contamination by the solvent, is the rapid, reproducible and controlled formation of uniform droplets.

Microfluidics plays an interesting role in micro-beads production: different approaches have been tried to work quite well on a laboratory scale with fluid mixtures of relatively simple rheology. Nonetheless the transfer of such technology to the industrial scale is often challenging, as several additional characteristics are required: devices should be easy to build, possibly arranged in parallel arrays for mass production with minimal interference length between the single devices, the separation between extrusion fluid and micro-beads should be simple, and possibly cheap (Sarghini, 2015).

Several mechanical and chemical methods had been introduced to produce particles with narrow size distribution in a single step approach, (e.g. milling, oil-water and water-oil emulsions, coacervation, spinning disks, atomization, vibrating nozzles) (Schneider et al., 2011; Prüsse et al., 2008).

Among the proposed methods, extrusion-dripping has been well recognized as relatively simple, size-controlled, low-cost, and scalable formation method for microgels (Burey et al., 2009). In this work, the concept of extrusion has been used in a wider sense, referred to a pressure driven drop shaping at the end of a capillary. In the extrusion-dripping, a biopolymer solution is forced through a nozzle (or a needle) in the form of droplets into hardening solution, where droplets gelation is induced in the hardening solution as a result of crosslinking agents (e.g., mineral ions, glutar-aldehyde, or enzymes, Chan et al., 2009). Gelation can be alternatively induced by applying a temperature change (heating or cooling) in case of thermally setting biopolymers, such as gelatin and whey proteins, or complexation with another polymer (e.g., polysaccharides) may occur (Murakami and Takashima, 2003).

Extrusion-dripping method has been used as well to produce microgel particles of biopolymers such as k-carrageenan injected into a potassium chloride solution (ionic gelation) (Perrechil et al., 2011), pectin injected into a calcium rich solution (ionic gelation), chitosan injected into a tripolyphosphate solution (ionic gelation), whey protein

injected into a hot liquid (heat-set gelation), and gelatin injected into a cold liquid (cold-set gelation).
If production of large microgels, characterized by diameters greater than 1 mm, can be performed by simple gravity extrusion dripping method (in which a pendant droplet is allowed to grow until it reaches the maximum size that can be supported by surface tension forces at the dripping tip, whereupon the droplet detaches and turns into a microgel particle when it falls into the gelation solution), in order to decrease the microgel size, the droplet breakup must be assisted by external forces, such as the ones developed by pressurized air, electrostatic charges, vibration, rotation, or shear flow of two fluids.
Pressurized air have been widely investigated in alginate microgels, with the setup being less complicated, handling higher viscosity solutions. A typical air extrusion system for alginate microgel formation consists of a pressurized air or gas supply source as a continuous phase (CP), an extrusion nozzle, and a gelation bath. In these systems, needle diameter, feed solution viscosity, and the flow rate and properties of the gelling fluid, as the dispersed phase (DP), determine the microgel particles size.
Flow focusing is a microfluidic technique where two or more phases of liquid or gases are co-axially focused and then forced through a small orifice. The flow rate of the CP, usually exceeds that of the inner DP, typically by ten to thousand times depending on the fluid characteristics. The DP is thus forced into a narrow jet and obliged by CP confinement to flow at the orifice. Due to the rapid change in pressure chamber to the outlet and the prevailing effects of shear stress, fluid dynamics instabilities in several forms appear, and the jet breaks up into droplets after passing the orifice (Schneider et al., 2011).
Among the available microfluidic device geometries, the flow-focusing type has been commonly used to make monodisperse polymer particles, both spherical and non-spherical. One of the most important factors influencing droplet formation in such microfluidic devices is the confinement as the propagating thread is restricted within the microchannels and is affected by both the geometry and size of the channel (Van Steijn et al., 2009). The various confinements let microfluidic device, the cross junction geometry and the flow-focusing junction.
A possible flow-focusing configuration, requiring oil as CP, allows a very good control of geometrical properties of beads in the extruding phase, although it involves complicate production processes, as it introduces a barrier to the interaction of alginate solution with the calcium ions solution during external gelation phase and requiring a-posteriori filtering and washing procedure to recover the beads. Moreover, during gelation phase, chain agglomerations of micro-beads can appear (Haeberle et al., 2008).
The possibility of using a gas as CP introduces several advantages if compared with liquid-liquid focusing configuration: easier separations of the different phases, cheaper production and the possibility of using three-dimensional arrays for mass production with minimal interference distance. On the other hand, the reduced shear stress at the phase interface and different inertial properties of the gas-liquid mixture requires relative high gas velocities involving gas flow instabilities (Si et al., 2009) and possibly turbulence, with a more difficult control of drop properties.

In such approach, the pressure gradient induced by an outer gas stream is used to confine and 'focus' a steady liquid jet of the dispersed phase. When the liquid microjet and the co-flowing gas stream cross a discharge outlet whose diameter is much larger than that of the microjet, a jet instability is generated, inducing DP flow break-up and allowing mass production of ultrafine and almost monodispersed spray, microcapsule or microspheres (beads) (Acero et al., 2012).

This technique was used for active compounds microencapsulation (Gundabala et al., 2013) using a configuration in co-focusing flow (gas-liquid) in which viscous (Cohen et al., 2001) and/or pressure (Gañán-Calvo, 1998) forces stretch an interface until small DP jet is emitted.

One of the first application of air-liquid extrusion for alginate micro-beads production was introduced by Hardikar et al., (1999), with the use of a drop generator comprising a needle, a three-way valve, and a swinny filter for encapsulation of islet cells in a matrix of alginate having an average size of 400 μm.

Ceausoglu and Hunkeler (2002) have demonstrated the possibility of producing not only microspheres, but also microcapsules in a shell-and-core configuration. The size obtained was 400 μm. Fiszman et al., (2002) reported the possibility to encapsulate in matrix cells genetically modified in alginate microspheres with a diameter range varying from 300 μm up to 1800 μm. In Sugiura et al. (2007) have created a micro-nozzle which is capable of producing microcapsules with a diameter range of 100-300 μm. In Wikström et al. (2008) reported the possibility to link the alginate to other materials to obtain microcapsules with different porosity, obtained by varying the divalent ions of the hardening solution, and using an air-liquid extrusion system capable of encapsulating cells in microcapsules of 490 μm of average diameter. Kontturi et al. (2011) reported the possibility of using a system of coaxial extrusion in air to produce microcapsules with an average diameter smaller than 200 μm.

Although several application had been published especially for Newtonian mixtures, the technology can be considered still in maturation for real industrial applications, as there are not enough theoretical information to control the shape of the beads, as instabilities dominating jet breakup of complex rheological liquid such those used in food industry still represent a theoretical challenge, especially for generation of small diameter micro-beads, and geometrical parameters play a key role in both the extrusion process (Vega et al., 2010) and jet stability (Montanero et al., 2011).

The physics of liquid jets is quite complex (Eggers and Villermaux, 2008) and several break-up mechanisms, activated by local and global instabilities, can appear depending on characteristics Reynolds and Weber number, the density ratio and the viscosity ratio (Si et al., 2009; for the Newtonian case).

While an extensive bibliography is present for the Newtonian case, in the Non-Newtonian case, a comprehensive theory is still missing, and the laminar jet breakup may cause the presence of large micro-beads depending on viscosity and surface tension of the liquid. Furthermore, in the case of non-Newtonian and highly viscous fluids, it may lead to an irregular jet breakup, causing a wide size distribution of the droplets.

In any case, the micro-beads production is only the first step of the process, as the impact of alginate micro-beads into the divalent Ca^{2+} solution required for gelation can introduce

several modification of the shape and diameters, due to further fragmentation and inertial effects related to the high speed assumed by the alginate beads after jet breakup.
Another possibility is the use of internal gelation (Poncelet, 2001), where alginate microspheres were produced by internal gelation of an emulsion of alginate dispersed within vegetable oil, followed by a reduction in pH to release calcium from an insoluble salt. In the mentioned work, microspheres with mean diameters ranging from 50 to 1000 μm were obtained with standard deviations ranging from 35 to 45% of their mean value.
In this work a mild pre-gelation technique was introduced, interposing a liquid sheet of calcium chloride solution vertically flowing in the path of the liquid alginate drops obtained using a gas-liquid focusing device: the micro-beads shape fixing process starts "on the fly", and eventually the gelation process is completed in a liquid bath or into the flowing screen itself.
The main idea relies on the possibility to control gelation in a confined zone, i.e. the liquid sheet, to reduce not only the uncontrolled inertial effects which are present in high speed gas-liquid extrusion process, but also the dimension of the extruding device.
Moreover, multiple parallel devices could be arranged in a small volume, allowing mass production of alginate beads.
Nonetheless, the high frequency characterizing the physics and possible local effects, for example due to minimum misalignment of geometrical devices, can modify the framework; such phenomena are extremely difficult to be captured experimentally, while an important insight can be obtained using numerical modeling, as will be shown in this work.

2.2 Materials and methods

Micro-beads for experimental test were prepared using alginate, which is a water-soluble linear polysaccharide extracted from brown seaweed. It is composed of alternating blocks of 1e4 linked α-L-guluronic and β-D-mannuronic acid residues. Depending on the source of the alginate, the molecules can be composed of three types of blocks: polymannuronic acid blocks (MM), polyguluronic acid blocks (GG) and mixed blocks (MG). The amount of the elements (MM and GG) varies with the source of alginate (E. P. Herrero et al., 2006). Alginate solution (DP) was obtained by purchasing medium viscosity alginic acid sodium salt from brown algae, for R&D use from Sigma-Aldrich. The aqueous solution was then prepared with a 2% w/v concentration, mixed at 30 °C for 12 h and part of it was then colored using UV activated red florescent Createx water based color for optical inspection. Surface tension for alginate was set to a value of 65 mN m^{-1} (Babak et al., 2000), while rheological properties were obtained experimentally by using a Rheometrics RFS II rheometer, showing a non-Newtonian shear-thinning behavior. In any case, the non-Newtonian effect with seaweed alginate is small compared with the non-linear behavior of bacterial alginate. The aqueous solution of alginates (less than 2% w/v) exhibits a quasi-Newtonian behavior: increasing the sodium alginate concentration enhances the viscosity and shifts the flow behavior from almost Newtonian to pseudoplastic with thixotropy (Tabeei et al., 2012). In this work, referred to an aqueous solution of alginate 2% w/v, a power-law formulation was adopted in numerical simulations, being k=0.2 the consistency index (Pa s^n) and n=0.88 is the power law index

(dimensionless), in agreement with literature (Belalia and Djelali, 2014; Tabeei et al., 2012). Calcium chloride ($CaCl_2$) solution for gelation was prepared using AppliChem GmbH Ottoweg Calcium chloride dried powder pure at 97% in a baker stirred on a warm hot plate at 20 °C until the powder was dispersed in distilled water, using a calcium chloride concentration equal to 2% w/v.

All experiments where performed at least in triplicate, and test were performed in different days. Characterization of alginate micro-beads sizes was quantitatively obtained using a light scattering particle size measuring instrument (Mastersizer 3000, Malvern Instruments), and optically with an optical stereomicroscope equipped with a digital camera with 40x magnifying power. Illumination was provided by using a UV lamp at 390 nm wavelength.

Mastersizer was used with a laser obscuration greater than 10%, experimental test were repeated three times for each run, and micro-beads were characterized as milky particles with particle adsorption index equal to 1.51 and particle refraction index equal to 1.36. Small variation of optical indices did not show significant variation of results. Although the non-spherical option was used, a certain amount of size distribution spread is related to the relative orientation of the particles passing by in the detection area respect to laser light scattering detection sensors. Results were averaged using at least 20 independent measures.

Micro-beads shape and dimensions were also examined by means of a Scanning Electron Microscopy (LEO EVO 40 SEM, Zeiss, Germany) with a 20 KeV acceleration voltage and a magnification of 1500x.

The configuration sketched in *Figure 16 a* represents the experimental setup, where the micro-beads were recovered after a longer flight using an open collector tank positioned at 1.2 m of distance from the microfluidic device.

In gas-liquid focusing devices, the periodic pressure drop Δp generated by the gas stream (which co-flows with the liquid jet across the orifice of diameter D_e of the external geometry as described in *Figure 16 b*) is responsible of the instability of the liquid jet that together with geometrical characteristics drives the droplet formation. The main geometrical parameters considered are the diameters D_i and D_e of the internal and external capillaries and the capillary-to-orifice distance H.

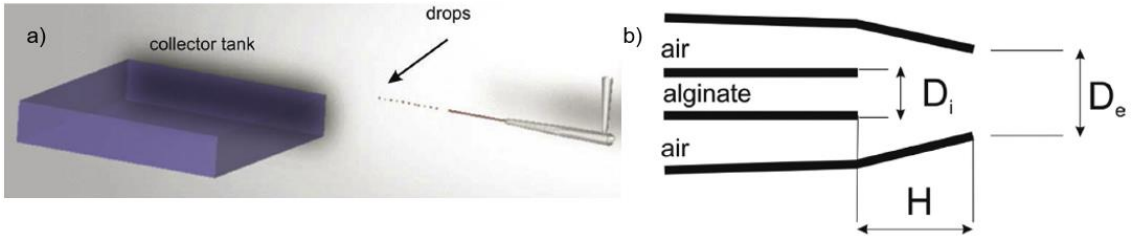

Figure 16. a) Schematic representation and b) flow-focusing device used in the experimental setup.

2.3 Numerical simulation methods for microfluidics flows

In order to gain a mechanistic insight on the dynamics of the drop formation, experiments were complemented with a numerical approach, performed using computational fluid dynamics techniques and results were compared with experimental data.

Numerical results, especially in the case of multiphase flows with large density ratios (Tryggvason et al., 2004), must be handled carefully, as several numerical difficulties arise when performing such simulations: accurate interface representation and advection, mass conservation, spurious currents just to mention a few.

Nonetheless, the reliability of results is quite good when a consistent time step is adopted together with a sufficient fine spatial discretization and an accurate choice of numerical schemes to reduce diffusion errors. The numerical simulation solver adopted in this work is Open-Foam (Openfoam v2.2.0), an open source CFD software package based on a control volumes approach. Several 3D mesh configurations were tested to asses mesh independence, ranging from 150 x 10^3 up to 2 x 10^6 control volumes. The final choice with a characteristic cell length of 2 μm in the jet breakup zone was considered fine enough to provide a mesh independent detail of droplet formation dynamics in term of final droplet diameter.

Continuous Phase-Dispersed Phase interaction was modelled by using a Volume of Fluid (VOF) approach (Hirt and Nichols, 1981), while for the numerical implementation in interFoam see

(Deshpande et al., 2012). The Reynolds number Re_g for the gas phase computed using the velocity of the unperturbed jet (i.e. without considering the restriction due to the passage of the alginate jet) and the external diameter D_e can be as high as 4600, and for this a Large Eddy Simulation was used to model moderate turbulence effects of the gas phase (Dimotakis, 2000). Simulations were performed using a dual Xeon E5 2690v3 processors computer (48 logical cores) with 256 Gb of memory.

The general equation set governing transport phenomena can obtained by applying conservation of mass, momentum and energy laws on a control volume in 3D Cartesian coordinates, and it is described in the following lines:

Continuity equation:

$$\frac{\partial \bar{\rho}}{\partial t} + \frac{\partial \bar{\rho} u_i}{\partial x_i} = 0 \qquad (9)$$

Conservation of momentum (fluid flow equations)

$$\frac{\partial \bar{\rho} u_j}{\partial t} + \frac{\partial \bar{\rho} u_i u_j}{\partial x_i} = \frac{\partial \sigma_{ij}}{\partial x_i} + \bar{\rho} g \qquad j = 1, 2, \dots 3 \qquad (10)$$

For the evolution of the alginate fraction function C (Volume of Fluid)

$$\frac{DC}{Dt} + u_i \frac{\partial C}{\partial x_i} = 0 \qquad (11)$$

where u_i is velocity (m s^{-1}), T is average temperature (K), P is pressure (Pa), ρ is density (kg m^{-3}), $\mu_{\text{eff}} = k\,\dot{\gamma}^n$ is the effective dynamic viscosity for the alginate solution (Pa s), and c_p is the heat capacity (J kg^{-1} K^{-1}) at constant pressure, and C is the fraction function. All the physical quantities are averaged ($\bar{x} = \mathrm{C}\,\bar{x}_{\text{alg}} + (1 - \mathrm{C})\bar{x}_{\text{air}}$) depending on the fraction function C of alginate in the local volume, i.e., for each cell, properties such as density and viscosity are calculated by a volume fraction average of all fluids in the cell. These properties are then used to solve a single momentum equation through the domain, and the numerical velocity field is shared among the fluids.

The device was oriented horizontally so that the liquid sheet could flow downward driven by gravity.

2.4 Results

Droplets can be formed in a dripping or jet schemes. The dripping-jet transition can be obtained either by comparing the capillary collapse time in Rayleigh-Plateau instability and the growth time of the dispersed thread (Utada et al., 2005), or by comparing the capillary time for the interfacial disturbance growth and the time convective fluid flow (Zhou et al., 2006). Therefore, the map of flow models is usually constructed based on the capillary number or the Weber number of the two phases (Cubaud and Mason, 2008). In microfluidic flow-focusing devices, the size of droplets formed in the dripping regime usually depends on the channel size, the viscosities and flow rates, as well as the interfacial tension. However, the effect of the viscosity ratio of both phases on the droplet size is contradictive in the literature (Cramer et al., 2004; Nie et al., 2008). Some results showed that the droplet size is not influenced by the viscosity ratio of both phases in axisymmetric capillary co-flowing device (Cramer et al., 2004), whereas, others found that the viscosity of the dispersed phase affects dramatically the droplet size in microfluidic flow-focusing devices with a small and short orifice (Nie et al., 2008). Moreover, the scaling law varies with droplet size in the dripping regime in microfluidic flow-focusing devices with cross junction geometries (Cubaud and Mason, 2008).

The beads production process can be broadly divided into two steps: the drop production process and gelation process. Although in this work most of the attention is focused on the drop generation process, the effect of the secondary gelation screen is briefly analyzed.

The response of the system can be characterized in this case by the free jet radius R, depending on the control parameters Q (volumetric flow rate), the pressure drop Δp between the inner part of the continuous phase and the external part, and the liquid density ρ, where the liquid viscosity μ and the surface tension γ play an important role for very viscous liquids and very thin jets.

The focusing device adopted in the experiments is described in *Figure 16 b*, and geometrical parameters are the following: D_i= 0.36 mm, D_e= 0.46 mm, H= 2 mm.

The breakup of the liquid jet into discrete drops can be controlled by the application of a periodic disturbance to the jet. Linear stability theory predicts that the disturbance will

grow exponentially and break the jet into drops provided the disturbance wavelength is greater than the jet circumference.
This phenomenon is known as Plateau- Rayleigh instability. This behavior of the liquid jet derives from the existence of small perturbations in any physical system, as in all real-world flows some non-negligible external disturbance that will increase exponentially in unstable systems are present.
In general, this deformation of the column (liquid coaxial jet), called varicose perturbations, is represented as a series of periodic displacement sinusoids. In our case, instabilities are generated by an external forced convection due to the air e liquid jet interactions. Geometry represents an important parameter in the experimental setup.
In the Newtonian case, in presence of moderately or large values of the Weber and Reynolds numbers for the liquid phase ($We > 1$ and $Re_{\mathrm{liq}} \geq 10$), the energy loss associated with the surface tension and viscosity can be neglected (Gañán-Calvo and Montanero, 2009) and the radius (R) of the undisturbed liquid jet can be estimated from the exact balance between the applied pressure and the resulting kinetic energy, according to the formula

$$R = \left(\frac{\rho Q^2}{2\pi^2 \Delta p} \right)^{1/4} \qquad (12)$$

where no geometrical parameters are present (Gañán-Calvo, 1998; Herrada et al., 2008; Gordillo et al., 2001).
The experimental setup adopted in this case is more complex, both from a geometrical and rheological point of view. If we consider the inner diameter of the undisturbed jet (D_i) and $\mathrm{v} = Q/(\pi R^2)$ as the characteristic length and velocity respectively, and using $Q_{\mathrm{air}} = 1\ \mathrm{L\ min^{-1}}$ and $Q_{\mathrm{alg}} = 0.5\ \mathrm{mL\ min^{-1}}$ (using an average value of tested configurations) we obtain $We = 0.10$ and $Re_{\mathrm{liq}} = 30$ where Re_{liq} is the generalized Reynolds number for the liquid phase, far away from conditions in which geometry is not important.
The droplets collected after the splash into the collector tank show a spherical shape as shown in *Figure 17 a* mainly because of the aerodynamic pressure regularization effects during the flight, and they present a wider size dispersion, caused by the impact and fragmentation of the drops on the liquid tank surface. Such fragmentation can be difficult to avoid in this air jet/liquid jet configuration, due to the relative high speed at which micro-beads gas-liquid production takes place. These results are shown in *Figure 17 b*, where the drop size distribution of collected beads is analyzed using the laser scattering equipment. The standard deviation optically computed on a reduced subset of the sample is equal to ±10 μm.

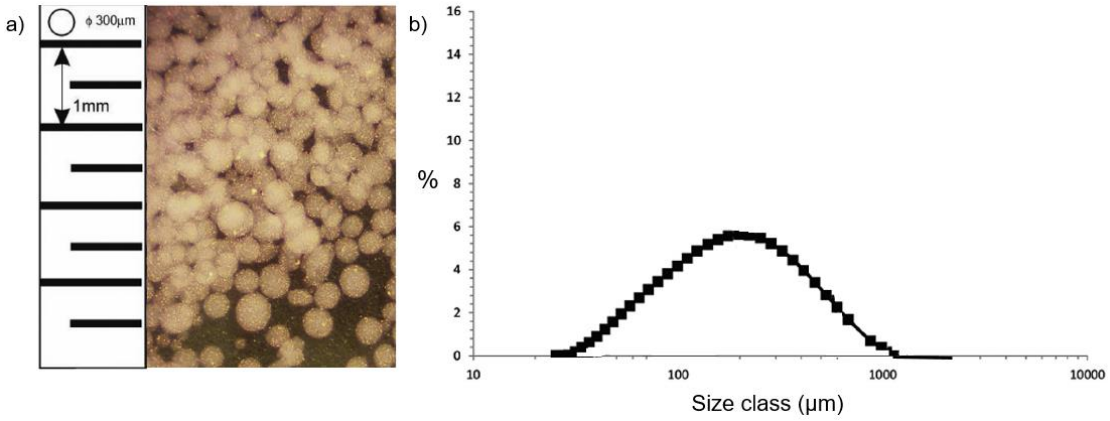

Figure 17. a) Snapshot of alginate micro-beads produced and b) laser scattering particle size distribution.

In order to validate the model, a comparison between volume mean diameter $D_{4/3}$ at fixed (DP $0.5\,\mathrm{mL\,min^{-1}}$) and fixed CP ($0.5\,\mathrm{L\,min^{-1}}$) have been proposed in this study. Experimental and numerical results are reported in *Table 2*. Numerical results are in good agreement with the experimental ones and demonstrate that the model solution is able to provide quite trustable values of the $D_{4/3}$ diameter.

As a matter of fact, the drop formation mechanism resulted to be quite complex, and the possibility to use a numerical model allows to gain a powerful insight into the complex dominating phenomena

involved. The interaction of a high-speed air jet (the continuous phase CP) and the induced instability of a liquid coaxial jet (the discrete phase DP) makes the framework much more complicated and the normal identification of jetting and dripping regimes cannot be simply applied.

Table 2. Comparison between experimental (exp) and numerical (num) volume mean diameter $D_{4/3}$ (µm) at fixed DP (a) and fixed CP (b).

(a) DP= 0.5 (ml min^{-1})				**(b)** CP= 0.5 (l min^{-1})			
CP (l min^{-1})	exp	STD	num	DP (ml min^{-1})	exp	STD	num
0.5	432	8	440	0.5	410	8	390
1	330	10	320	1	432	10	440
1.5	163	8	180	1.5	482	6	500

STD= Standard deviation

To support the previous statement, in *Figure 18* dynamics of jet instability and drop formation is clearly highlighted.

Images from t_1 to t_{12} represent instantaneous snapshots of the alginate jet and drop (magenta) immersed into the velocity field, with a Δt between each snapshot equal to $3{\cdot}10^{-4}$ and a computational time step equal to $1{\cdot}10^{-5}$ s.

The complex periodic drop formation dynamics cane be described in the following way:

1. In the first phase, a Drop D1 is already present in the field of interest, while the liquid jet, detached from the tip of the inner capillary, is elongated due to the effect of external disturbance (t_1).

2. Starting from t_2, a first drop D2M is detached in the frontal part of the jet while the remaining part of the jet undergoes to a secondary elongation and instability (t_3–t_4), ending with a final formation of two droplets of different sizes, DS1 and DS2.
3. However, it is not over. The four droplets have different mass and velocities and they are immersed into a complex fluid dynamics field: droplet D2M is faster than droplet D1 (t_7), as it is accelerated by the presence of a still coherent air jet, and eventually merges with D1, resulting in the new drop D3.
4. Drop DS1 is faster and bigger then DS2, and eventually it will reach the forward one, merging in the final drop D4 (t_9), whose speed is intermediate between those of the original droplets, due to the conservation of momentum.
5. Drop D4 is the new D1 as the process starts again (t_{11}–t_{12}).

The drop merging phenomena involved let us consider that porting this approach to a core shell encapsulation configuration could not be so easy.
The instantaneous differential pressure field generated by the air stream is described in *Figure 19 a*, while in *Figure 19 b* 3d vortex tube for $P = +200$ Pa and $P = -200$ Pa are shown.
Following the work of (Si et al., 2009), although referred to a Newtonian case, the jet seems to be characterized as a coexisting jetting mode, a transition mode between helical and axisymmetric jetting, for which both non-axisymmetric and axisymmetric disturbances exist. The couple of droplets, main and satellite, formed at the end of the liquid jet, move downstream in a whipping way, and the micro-beads average diameter of the main drop is nearly equivalent to that of the jet. In the same work, Si et al. observed that the shape of satellite drops in this regime is elongated from a sphere into a ligament for larger values of Q.

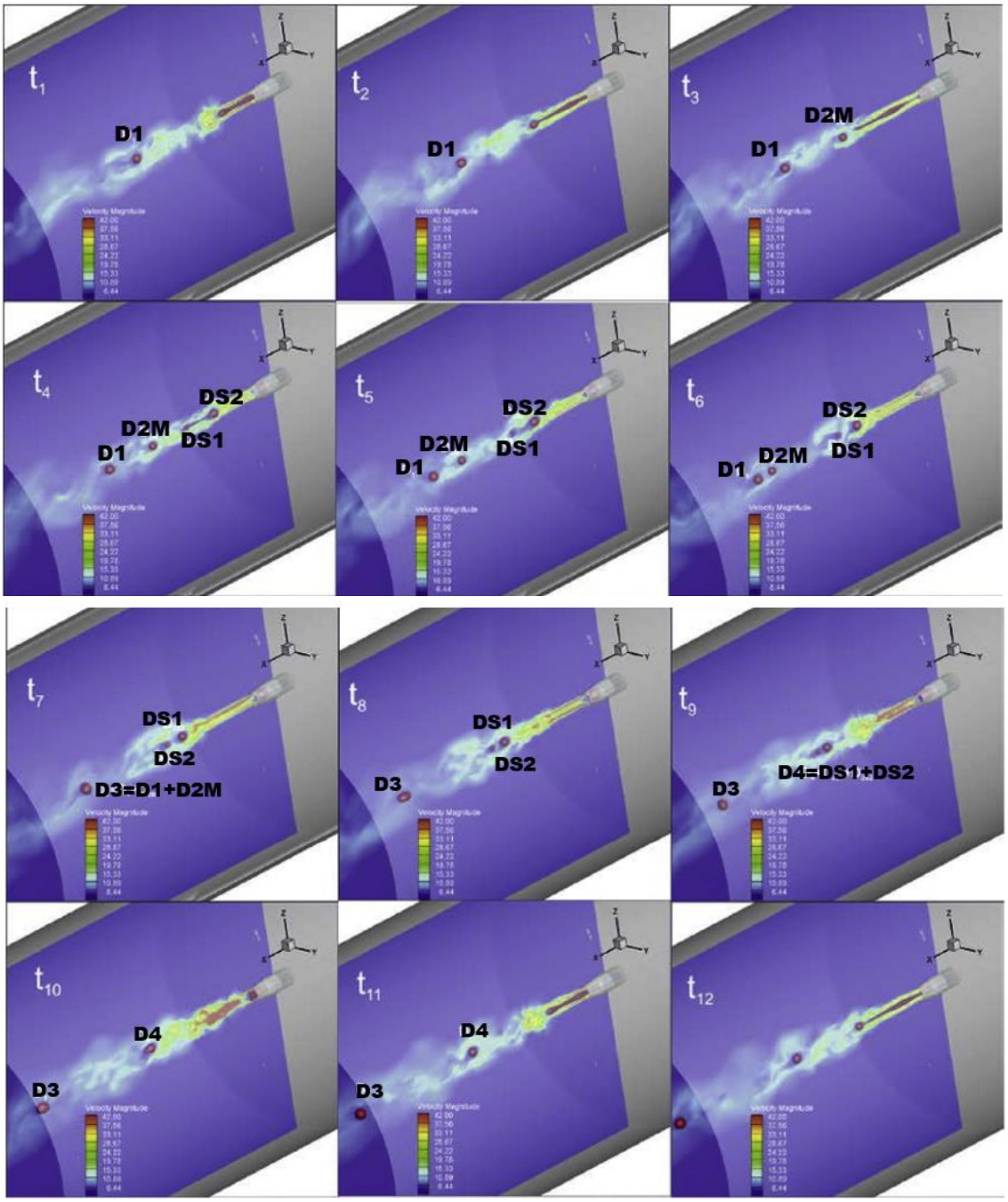

Figure 18. The dynamics of jet breakup, drop formation and merging.

The numerically computed frequency of the disturbance evaluated at point probe P, shown in *Figure 19 a*, is 22 KHz, higher than the drop generation frequency, as shown in Fig. 7. Effects of coupling of pressure disturbance frequency, pressure intensity and proper frequencies of the liquid jet is not known.

The gas velocity (and more precisely the oscillating pattern appearing near the tip, reported in *Figure 20*) is linked to the appearance of pressure oscillations: these pressure oscillations act as an external dynamic force, thus introducing the required external periodic disturbances for the Rayleigh-Plateau instability.

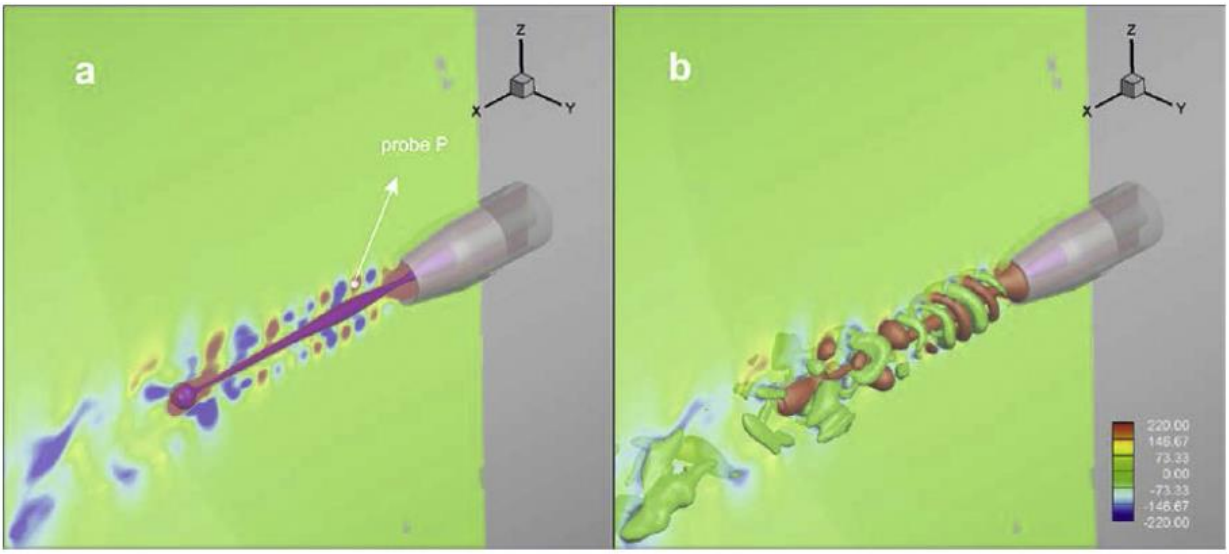

Figure 19. (a) Instantaneous differential pressure field generated by the air stream on a transversal section and (b) isosurfaces for $P{=}{+}200$ Pa *and* $P{=}\ {-}\ 200$ Pa.

The frequency of involved phenomena and the small scales of considered devices make almost impossible to gain an insight using only experimental techniques.
The instability frequencies for Non-Newtonian Rayleigh-Plateau phenomena are not well established and they depend also on the geometrical configuration of devices, since different devices hold different geometrical configurations (including minor misalignments) and it results in different forcing wavelengths. In this framework, numerical tools provide a terrific predictive power, as stressed in *Figure 21*, where drop formation and interaction mechanism show to be dramatically changed by a 15° lateral misalignment of inner capillary axes.
In this case, the axial symmetry of the jet breakup is lost immediately, and the flow field pushes laterally the new formed droplet, changing the size distribution.

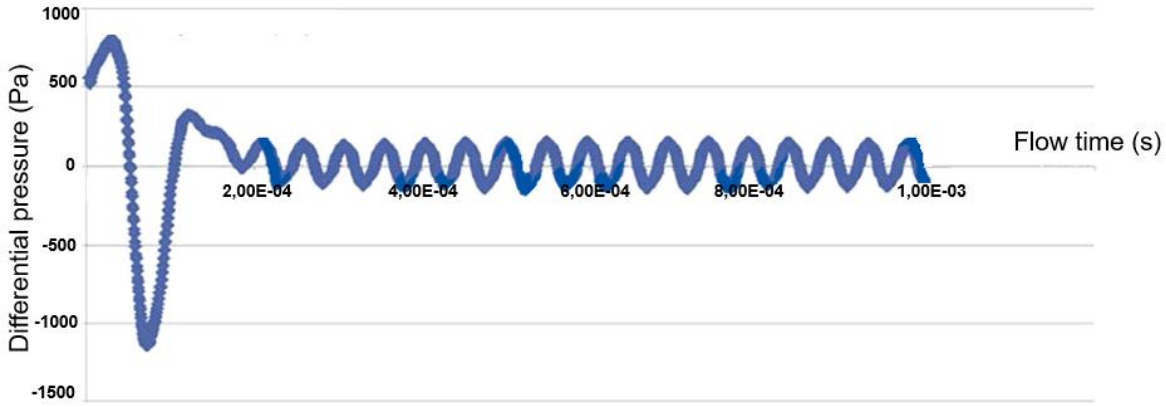

Figure 20. Pressure disturbance frequency and intensity at the exit of the microfluidic nozzle.

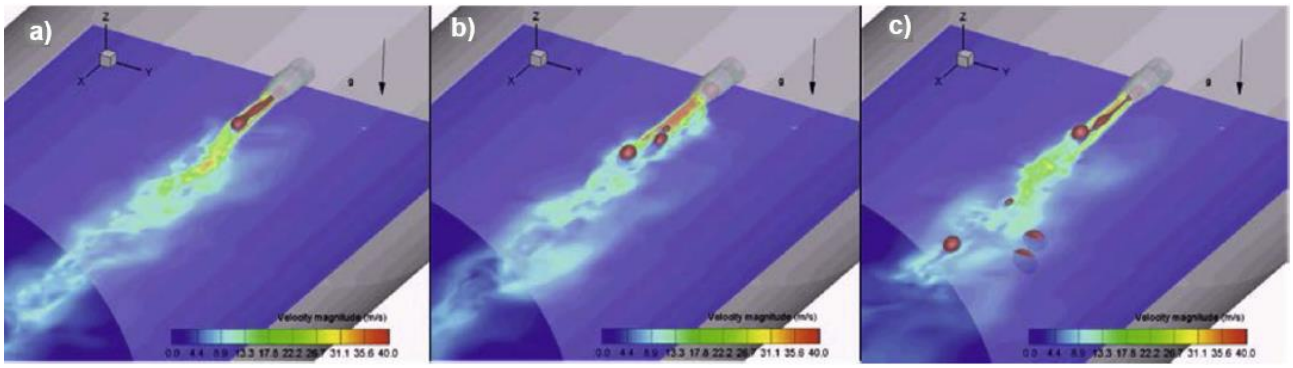

Figure 21. Effect of misalignment of inner capillary axes (15°) on drop formation and interaction mechanism.

2.5 Conclusions

The results obtained showed that the proposed approach (a gas continuous phase plus a liquid sheet to induce an immediate gelation) represents a viable solution for possible mass production of alginate micro-beads, at least for matrix encapsulation. Quite small and regular micro-beads were produced, although the theoretical lower limit of micro-beads diameter for device was not investigated in this work.

Nonetheless, a purely experimental approach is not able to provide all significant data as reference lengths and the dynamics involved make extremely difficult to apply classical measurements technique to control the process.

On one hand the microfluidic device adopted is very simple and cheap (coupling together borosilicate micro capillary, commonly used in a lab and a connecting frame obtained using a 3D printer), and the equivalent low-cost industrial device could be produced by using a highly accurate rapid prototyping machine, reducing the problems related to clogging and fouling by simply replacing the tip.

On the other hand, the simplicity of the device is balanced by the extreme complexity of interactions between air and alginate and drop merging and collisions. Geometric parameters play a fundamental role to control jet instabilities dominating the drops breakup dynamics: small misalignment can dramatically change the jet breakup dynamics, introducing a completely different framework. Newtonian theory of jet breakup does not apply, increasing the complexity of the theoretical framework and support of numerical modeling represents somehow one of the few options available to optimize microfluidic devices for air-liquid encapsulation.

References

Abraham, S.M., Vieth, R.F., Burgess, D.J., 1996. Novel technology for the preparation of sterile alginate-poly-l-lysine microcapsules in a bioreactor. Pharm. Dev. Technol. 1, 63–68. https://doi.org/10.3109/10837459609031419

Acero, A.J., Montanero, J.M., Ferrera, C., Herrada, M.A., Gañán-Calvo, A.M., 2012. Enhancement of the stability of the flow focusing technique for low-viscosity liquids. J. Micromechanics Microengineering 22. https://doi.org/10.1088/0960-1317/22/11/115039

Aftel, R., Gupta, A.K., Cook, C., Presser, C., 1996. Gas property effects on droplet atomiation and combustion in an air-assist atomier. Symp. Combust. 26, 1645–1651. https://doi.org/10.1016/S0082-0784(96)80388-2

Al-Hajry, H.A., Al-Maskry, S.A., Al-Kharousi, L.M., El-Mardi, O., Shayya, W.H., Goosen, M.F.A., 1999. Electrostatic encapsulation and growth of plant cell cultures in alginate. Biotechnol. Prog. 15, 768–774. https://doi.org/10.1021/bp990069e

Babak, V.G., Skotnikova, E.A., Lukina, I.G., Pelletier, S., Hubert, P., Dellacherie, E., 2000. Hydrophobically associating alginate derivatives: Surface tension properties of their mixed aqueous solutions with oppositely charged surfactants. J. Colloid Interface Sci. 225, 505–510. https://doi.org/10.1006/jcis.2000.6788

Belalia, F., Djelali, N.E., 2014. Rheological properties of sodium alginate solutions. Rev. Roum. Chim. 59, 135–145.

Brandenberger, H., Nüssli, D., Piëch, V., Widmer, F., 1999. Monodisperse particle production: A method to prevent drop coalescence using electrostatic forces. J. Electrostat. 45, 227–238. https://doi.org/10.1016/S0304-3886(98)00052-7

Brandenberger, H., Widmer, F., 1998. A new multinozzle encapsulation/immobilisation system to produce uniform beads of alginate. J. Biotechnol. 63, 73–80. https://doi.org/10.1016/S0168-1656(98)00077-7

Bressel, T.A.B., Paz, A.H., Baldo, G., Lima, E.O.C., Matte, U., Saraiva-Pereira, M.L., 2008. An effective device for generating alginate microcapsules. Genet. Mol. Biol. 31, 136–140. https://doi.org/10.1590/S1415-47572008000100023

Burey, P., Bhandari, B.R., Howes, T., Gidley, M.J., 2009. Gel particles from spray-dried disordered polysaccharides. Carbohydr. Polym. 76, 206–213. https://doi.org/10.1016/j.carbpol.2008.10.001

Burey, P., Bhandari, B.R., Howes, T., Gidley, M.J., 2008. Hydrocolloid gel particles: Formation, characterization, and application. Crit. Rev. Food Sci. Nutr. 48, 361–377. https://doi.org/10.1080/10408390701347801

Ceausoglu, I., Hunkeler, D., 2002. A new microencapsulation device for controlled membrane and capsule size distributions. J. Microencapsul. 19, 725–735. https://doi.org/10.1080/02652040210144261

Cerveró, J.M., Nogareda, J., Valle, E.M.M. del, Galán, M.A., 2011. Development of a technology to produce monodispersed microparticles based on the formation of drops from viscous non-Newtonian liquids sprayed through a fan jet nozzle. Chem. Eng. J. 174, 699–708. https://doi.org/10.1016/j.cej.2011.09.063

Champagne, C.P., Fustier, P., 2007. Microencapsulation for the improved delivery of bioactive compounds into foods. Curr. Opin. Biotechnol. 18, 184–190. https://doi.org/10.1016/j.copbio.2007.03.001

Champagne, C.P., Gardner, N.J., Roy, D., 2005. Challenges in the addition of probiotic cultures to foods. Crit. Rev. Food Sci. Nutr. 45, 61–84. https://doi.org/10.1080/10408690590900144

Chan, E.S., Lee, B.B., Ravindra, P., Poncelet, D., 2009. Prediction models for shape and size of ca-alginate macrobeads produced through extrusion-dripping method. J. Colloid Interface Sci. 338, 63–72. https://doi.org/10.1016/j.jcis.2009.05.027

Chan, E.S., Lim, T.K., Ravindra, P., Mansa, R.F., Islam, A., 2012. The effect of low air-to-liquid mass flow rate ratios on the size, size distribution and shape of calcium alginate particles produced using the atomization method. J. Food Eng. 108, 297–303. https://doi.org/10.1016/j.jfoodeng.2011.08.010

Chen, C., Ye, S., Wang, D., Hatting, J.L., Yu, X., 2014. Alginate embedding and subsequent sporulation of in vitro-produced Conidiobolus thromboides hyphae using a pressurised air-extrusion method. Biol. Control 69, 52–58. https://doi.org/10.1016/j.biocontrol.2013.10.016

Chigier, N., Reitz, R.D., 1996. Regimes of Jet Breakup and Breakup Mechanisms (Physical Aspects), in: Kuo, K. (Ed.), Recent Advances in Spray Combustion: Spray Atomization and Drop Burning Phenomena. American Institute of Aeronautics and Astronautics, Inc., Reston, USA, pp. 109–135.

Ching, S.H., Bhandari, B., Webb, R., Bansal, N., 2015. Visualizing the interaction between sodium caseinate and calcium alginate microgel particles. Food Hydrocoll. 43, 165–171. https://doi.org/10.1016/j.foodhyd.2014.05.013

Chrastil, J., 1991. Gelation of Calcium Alginate. Influence of Rice Starch or Rice Flour on the Gelation Kinetics and on the Final Gel Structure. J. Agric. Food Chem. 39, 874–876. https://doi.org/10.1021/jf00005a012

Chu, L.Y., Utada, A.S., Shah, R.K., Kim, J.W., Weitz, D.A., 2007. Controllable monodisperse multiple emulsions. Angew. Chemie - Int. Ed. 46, 8970–8974. https://doi.org/10.1002/anie.200701358

Cocchietto, M., Blasi, P., Lapasin, R., Moro, C., Gallo, D., Sava, G., 2013. Microencapsulation of Bioactive Principles with an Airless Spray-Gun Suitable for Processing High Viscous Solutions. J. Funct. Biomater. 4, 312–328. https://doi.org/10.3390/jfb4040312

Cohen, I., Li, H., Hougland, J.L., Mrksich, M., Nagel, S.R., 2001. Using selective withdrawal to coat microparticles. Science (80-.). 292, 265–267. https://doi.org/10.1126/science.1059175

Cramer, C., Fischer, P., Windhab, E.J., 2004. Drop formation in a co-flowing ambient fluid. Chem. Eng. Sci. 59, 3045–3058. https://doi.org/10.1016/j.ces.2004.04.006

Cubaud, T., Mason, T.G., 2008. Capillary threads and viscous droplets in square microchannels. Phys. Fluids 20. https://doi.org/10.1063/1.2911716

Cui, J.H., Cao, Q.R., Choi, Y.J., Lee, K.H., Lee, B.J., 2006. Effect of additives on the viability of bifidobacteria loaded in alginate poly-l-lysine microparticles during the freeze-drying process. Arch. Pharm. Res. 29, 707–711. https://doi.org/10.1007/BF02968256

Cui, J.H., Goh, J.S., Park, S.Y., Kim, P.H., Lee, B.J., 2001. Preparation and physical characterization of alginate microparticles using air atomization method. Drug Dev. Ind. Pharm. 27, 309–319. https://doi.org/10.1081/DDC-100103730

Dávalos-Saucedo, C.A., Sarghini, F., Masi, P., 2013. Alginate beads production using a liquid sheet pregelification technique, in: Proc. of the Inside Food Symposium. KU Leuven, Leuven, pp. 1–6.

Deshpande, S.S., Anumolu, L., Trujillo, M.F., 2012. Evaluating the performance of the two-phase flow solver interFoam. Comput. Sci. Discov. 5. https://doi.org/10.1088/1749-4699/5/1/014016

Devi, N., Hazarika, D., Deka, C., Kakati, D.K., 2012. Study of complex coacervation of gelatin a and sodium alginate for microencapsulation of olive oil. J. Macromol. Sci. Part A Pure Appl. Chem. 49, 936–945. https://doi.org/10.1080/10601325.2012.722854

Dimotakis, P.E., 2000. The mixing transition in turbulent flows. J. Fluid Mech. 409, 69–98. https://doi.org/10.1017/S0022112099007946

Dulieu, C., Poncelet, D., Neufeld, R.J., 1999. Encapsulation and Immobilization Techniques, in: Ktihtreiber, W.M., Lanza, R.P., Chick, W.L. (Eds.), Cell Encapsulation Technology and Therapeutics. Springer, New York, pp. 3–17.

Eggers, J., Villermaux, E., 2008. Physics of liquid jets. Reports Prog. Phys. 71. https://doi.org/10.1088/0034-4885/71/3/036601

El-Shanawany, M.S., Lefebvre, A.H., 1980. Airblast Atomization: the Effect of Linear Scale on Mean Drop Size. Am. Soc. Mech. Eng. 4, 184–189.

Errico, A., Lama, G.F.C., Francalanci, S., Chirico, G.B., Solari, L., Preti, F., 2019. Flow dynamics and turbulence patterns in a drainage channel colonized by common reed (Phragmites australis) under different scenarios of vegetation management. Ecol. Eng. 133, 39–52. https://doi.org/10.1016/j.ecoleng.2019.04.016

Fijan, R., Šostar-Turk, S., Lapasin, R., 2007. Rheological study of interactions between non-ionic surfactants and polysaccharide thickeners used in textile printing. Carbohydr. Polym. 68, 708–717. https://doi.org/10.1016/j.carbpol.2006.08.006

Fiszman, G.L., Karara, A.L., Finocchiaro, L.M.E., Glikin, G.C., 2002. A laboratory scale device for microencapsulation of genetically engineered cells into alginate beads. Electron. J. Biotechnol. 5, 279–283. https://doi.org/10.2225/vol5-issue3-fulltext-5

Friso, D., 2017. Meccanica dei solidi e dei fluidi alimentari, in: Friso, D. (Ed.), Ingegneria Dell'industria Agroalimentare. CLEUP sc - Cooperativa Libraria Editrice Università di Padova, Padova, pp. 1–62.

Fundueanu, G., Nastruzzi, C., Carpov, A., Desbrieres, J., Rinaudo, M., 1999. Physico-chemical characterization of Ca-alginate microparticles produced with different methods. Biomaterials 20, 1427–1435. https://doi.org/10.1016/S0142-9612(99)00050-2

Gañán-Calvo, A.M., 1998. Generation of Steady Liquid Microthreads and Micron-Sized Monodisperse Sprays in Gas Streams. Phys. Rev. Lett. 80, 285–288. https://doi.org/10.1103/PhysRevLett.80.285

Gañán-Calvo, A.M., Martín-Banderas, L., González-Prieto, R., Rodríguez-Gil, A., Berdún-Álvarez, T., Cebolla, A., Chávez, S., Flores-Mosquera, M., 2006. Straightforward production of encoded microbeads by Flow Focusing: Potential applications for biomolecule detection. Int. J. Pharm. 324, 19–26. https://doi.org/10.1016/j.ijpharm.2006.05.032

Gañán-Calvo, A.M., Montanero, J.M., 2009. Revision of capillary cone-jet physics: Electrospray and flow focusing. Phys. Rev. E - Stat. Nonlinear, Soft Matter Phys. 79, 1–18. https://doi.org/10.1103/PhysRevE.79.066305

Gåserød, O., Smidsrød, O., Skjåk-Bræk, G., 1998. Microcapsules of alginate-chitosan - I. A quantitative study of the interaction between alginate and chitosan. Biomaterials 19, 1815–1825. https://doi.org/10.1016/S0142-9612(98)00073-8

Gordillo, J.M., Ganán-Calvo, A.M., Pŕez-Saborid, M., 2001. Monodisperse microbubbling: Absolute instabilities in coflowing gas-liquid jets. Phys. Fluids 13, 3839–3842. https://doi.org/10.1063/1.1416188

Gouin, S., 2004. Microencapsulation: Industrial appraisal of existing technologies and trends. Trends Food Sci. Technol. 15, 330–347. https://doi.org/10.1016/j.tifs.2003.10.005

Gundabala, V.R., Martinez-Escobar, S., Marquez, S.M., Marquez, M., Fernandez-Nieves, A., 2013. Celloidosomes® via glass-based microfluidics. J. Phys. D. Appl. Phys. 46. https://doi.org/10.1088/0022-3727/46/11/114006

Haeberle, S., Naegele, L., Burger, R., Stetten, F. Von, Zengerle, R., Ducree, J., 2008. Alginate bead fabrication and encapsulation of living cells under centrifugally induced artificial gravity conditions. J. Microencapsul. 25, 267–274. https://doi.org/10.1080/02652040801954333

Hardikar, A.A., Risbud, M. V., Bhonde, R.R., 1999. A simple microcapsule generator design for islet encapsulation. J. Biosci. 24, 371–376. https://doi.org/10.1007/BF02941251

Hariyadi, D.M., Lin, S.C.Y., Wang, Y., Bostrom, T., Turner, M.S., Bhandari, B., Coombes, A.G.A., 2010. Diffusion loading and drug delivery characteristics of alginate gel microparticles produced by a novel impinging aerosols method. J. Drug Target. 18, 831–841. https://doi.org/10.3109/1061186X.2010.525651

Hariyadi, D.M., Wang, Y., Lin, S.C.Y., Bostrom, T., Bhandari, B., Coombes, A.G.A., 2012. Novel alginate gel microspheres produced by impinging aerosols for oral delivery of proteins. J. Microencapsul. 29, 250–261. https://doi.org/10.3109/02652048.2011.646329

Heinzen, C., Berger, A., Marison, I., 2004. Technology for Jet Break-Up for Encapsulation of Cells and Liquids in Monodisperse Microcapsules, in: Nedovic, V., Willaert, R. (Eds.), Fundamentals of Cell Immobilisation Biotechnology. Kluwer Academic Publishers, pp. 257–275.

Herrada, M.A., Gañán-Calvo, A.M., Ojeda-Monge, A., Bluth, B., Riesco-Chueca, P., 2008. Liquid flow focused by a gas: Jetting, dripping, and recirculation. Phys. Rev. E - Stat. Nonlinear, Soft Matter Phys. 78, 1–16. https://doi.org/10.1103/PhysRevE.78.036323

Herrero, Edgar P., Del Valle, E.M.M., Galán, M.A., 2006. Modelling prediction of the microcapsule size of polyelectrolyte complexes produced by atomization. Chem. Eng. J. 121, 1–8. https://doi.org/10.1016/j.cej.2006.04.003

Herrero, E. P., Martín Del Valle, E.M., Galán, M.A., 2006. Development of a new technology for the production of microcapsules based in atomization processes. Chem. Eng. J. 117, 137–142. https://doi.org/10.1016/j.cej.2005.12.022

Hirt, C.W., Nichols, B.D., 1981. Volume of Fluid (VOF) Method for the Dynamics of Free Boundaries*. J. Comput. Phys. 39, 201–225. https://doi.org/10.1016/0021-9991(81)90145-5

Klokk, T.I., Melvik, J.E., 2002. Controlling the size of alginate gel beads by use of a high electrostatic potential. J. Microencapsul. 19, 415–424. https://doi.org/10.1080/02652040210144234

Kontturi, L.S., Yliperttula, M., Toivanen, P., Määttä, A., Määttä, A.M., Urtti, A., 2011. A laboratory-scale device for the straightforward production of uniform, small sized cell microcapsules with long-term cell viability. J. Control. Release 152, 376–381. https://doi.org/10.1016/j.jconrel.2011.03.005

Krasaekoopt, W., Bhandari, B., Deeth, H., 2004. The influence of coating materials on some properties of alginate beads and survivability of microencapsulated probiotic bacteria. Int. Dairy J. 14, 737–743. https://doi.org/10.1016/j.idairyj.2004.01.004

Lakkis, J.M., 2016. Encapsulation and controlled release in bakery applications, in: Lakkis, J.M. (Ed.), Encapsulation and Controlled Release Technologies in Food Systems. John Wiley & Sons, Inc., United Kingdom, pp. 204–235.

Lasheras, J.C., Hopfinger, E.J., 2000. Liquid Jet Instability and Atomization in a Coaxial Gas Stream. Annual Review of Fluid Mechanics. Annu. Rev. Fluid Mech. 32, 275–308. https://doi.org/10.1146/annurev.genom.1.1.409

Lasheras, J.C., Villermaux, E., Hopfinger, E.J., 1998. Break-up and atomization of a round water jet by a high-speed annular air jet. J. Fluid Mech. 30, 85–105.

Lee, B.B., Bhandari, B.R., Howes, T., 2016. Air Extrusion System for Ionotropic Alginate Microgel Particle Formation: A Review. Chem. Eng. Technol. 39, 2355–2369. https://doi.org/10.1002/ceat.201600088

Lee, B.B., Ravindra, P., Chan, E.S., 2013. Size and shape of calcium alginate beads produced by extrusion dripping. Chem. Eng. Technol. 36, 1627–1642.

https://doi.org/10.1002/ceat.201300230
Lee, J.S., Cha, D.S., Park, H.J., 2004. Survival of freeze-dried Lactobacillus bulgaricus KFRI 673 in chitosan-coated calcium alginate microparticles. J. Agric. Food Chem. 52, 7300–7305. https://doi.org/10.1021/jf040235k
Leong, J.Y., Lam, W.H., Ho, K.W., Voo, W.P., Lee, M.F.X., Lim, H.P., Lim, S.L., Tey, B.T., Poncelet, D., Chan, E.S., 2016. Advances in fabricating spherical alginate hydrogels with controlled particle designs by ionotropic gelation as encapsulation systems. Particuology 24, 44–60. https://doi.org/10.1016/j.partic.2015.09.004
Lin, S.P., Reitz, R.D., 1998. Drop and Spray Formation from a Liquid Jet. Annu. Rev. Fluid Mech. 30, 85–105. https://doi.org/10.1146/annurev.fluid.30.1.85
Lin, T.C., 2012. Performance of a Micro Atomizer Under Single-Fluid and Twin-Fluid Micro-Encapsulation Process. Int. J. Mod. Phys. Conf. Ser. 19, 219–226. https://doi.org/10.1142/s2010194512008781
Ma, J., Lin, Y., Chen, X., Zhao, B., Zhang, J., 2014. Flow behavior, thixotropy and dynamical viscoelasticity of sodium alginate aqueous solutions. Food Hydrocoll. 38, 119–128. https://doi.org/10.1016/j.foodhyd.2013.11.016
Mansour, A., Chigier, N., 1995. Air-blast atomization of non-Newtonian liquids. J. Nonnewton. Fluid Mech. 58, 161–194. https://doi.org/10.1016/0377-0257(95)01356-Z
Marra, F., De Vivo, A., Sarghini, F., 2018. Air Assisted Production of Alginate Beads Using Focusing Flow Microfluidic Devices: Numerical Modeling of Beads Formation. Lect. Notes Bioeng. 119–127. https://doi.org/10.1007/978-3-319-62027-5_11
Marra, F., De Vivo, A., Sarghini, F., 2017. Virtualization of fluid-dynamics in micro-air assisted extruders for food microfluidic based encapsulation. J. Food Eng. 213, 89–98. https://doi.org/10.1016/j.jfoodeng.2017.04.030
Martín-Banderas, L., Flores-Masquera, M., Riesco-Chueca, P., Rodríguez-Gil, A., Cebolla, Á., Chávez, S., Gañán-Calvo, A.M., 2005. Flow focusing: A versatile technology to produce size-controlled and specific-morphology microparticles. Small 1, 688–692. https://doi.org/10.1002/smll.200500087
Martín-Banderas, L., González-Prieto, R., Rodríguez-Gil, A., Fernández-Arévalo, M., Flores-Mosquera, M., Chávez, S., Gaņán-Calvo, A.M., 2011. Application of flow focusing to the break-up of a magnetite suspension jet for the production of paramagnetic microparticles. J. Nanomater. 2011, 1–10. https://doi.org/10.1155/2011/527437
Martins, E., Poncelet, D., Rodrigues, R.C., Renard, D., 2017. Oil encapsulation techniques using alginate as encapsulating agent: applications and drawbacks. J. Microencapsul. 34, 754–771. https://doi.org/10.1080/02652048.2017.1403495
Montanero, J.M., Rebollo-Muņoz, N., Herrada, M.A., Gaņán-Calvo, A.M., 2011. Global stability of the focusing effect of fluid jet flows. Phys. Rev. E - Stat. Nonlinear, Soft Matter Phys. 83, 1–7. https://doi.org/10.1103/PhysRevE.83.036309
Murakami, R., Takashima, R., 2003. Mechanical properties of the capsules of chitosan-soy globulin polyelectrolyte complex. Food Hydrocoll. 17, 885–888. https://doi.org/10.1016/S0268-005X(03)00109-7
Narsaiah, K., Jha, S.N., Wilson, R.A., Mandge, H.M., Manikantan, M.R., 2014. Optimizing microencapsulation of nisin with sodium alginate and guar gum. J. Food Sci. Technol. 51, 4054–4059. https://doi.org/10.1007/s13197-012-0886-6
Nie, Z., Seo, M.S., Xu, S., Lewis, P.C., Mok, M., Kumacheva, E., Whitesides, G.M., Garstecki, P., Stone, H.A., 2008. Emulsification in a microfluidic flow-focusing device: Effect of the viscosities of the liquids. Microfluid. Nanofluidics 5, 585–594. https://doi.org/10.1007/s10404-008-0271-y

Ouwerx, C., Velings, N., Mestdagh, M.M., Axelos, M.A.V., 1998. Physico-chemical properties and rheology of alginate gel beads formed with various divalent cations. Polym. Gels Networks 6, 393–408. https://doi.org/10.1016/S0966-7822(98)00035-5

Peretz, S., 2004. Interaction of alginate with metal ions, cationic surfactants and cationic dyes 49, 857–865.

Perrechil, F.A., Sato, A.C.K., Cunha, R.L., 2011. κ-Carrageenan-sodium caseinate microgel production by atomization: Critical analysis of the experimental procedure. J. Food Eng. 104, 123–133. https://doi.org/10.1016/j.jfoodeng.2010.12.004

Poncelet, D., 2001. Production of Alginate Beads by Emulsification/Internal Gelation. Ann. N. Y. Acad. Sci. 944, 74–82. https://doi.org/10.1111/j.1749-6632.2001.tb03824.x

Poncelet, D., Babak, V.G., Neufeld, R.J., Goosen, M.F.A., Burgarski, B., 1999. Theory of electrostatic dispersion of polymer solutions in the production of microgel beads containing biocatalyst. Adv. Colloid Interface Sci. 79, 213–228. https://doi.org/10.1016/S0001-8686(97)00037-7

Poncelet, D., Poncelet De Smet, B., Beaulieu, C., Neufeld, R.J., 1993. Scale-up of gel bead and microcapsule production in cell immobilization, in: Goosen, M.F.A. (Ed.), Fundamentals of Animal Cell Encapsulation and Immobilization. CRC Press, pp. 113–141.

Prüsse, U., Bilancetti, L., Bučko, M., Bugarski, B., Bukowski, J., Gemeiner, P., Lewińska, D., Manojlovic, V., Massart, B., Nastruzzi, C., Nedovic, V., Poncelet, D., Siebenhaar, S., Tobler, L., Tosi, A., Vikartovská, A., Vorlop, K.D., 2008. Comparison of different technologies for alginate beads production. Chem. Pap. 62, 364–374. https://doi.org/10.2478/s11696-008-0035-x

Rehg, T., Dorger, C., Chau, P.C., 1986. Application of an atomizer in producing small alginate gel beads for cell immobilization. 8, 111–114.

Rodríguez-Rivero, C., Nogareda, J., Martín, M., del Valle, E.M.M., Galán, M.A., 2013. CFD modeling and its validation of non-Newtonian fluid flow in a microparticle production process using fan jet nozzles. Powder Technol. 246, 617–624. https://doi.org/10.1016/j.powtec.2013.05.050

Santa-Maria, M., Scher, H., Jeoh, T., 2012. Microencapsulation of bioactives in cross-linked alginate matrices by spray drying. J. Microencapsul. 29, 286–295. https://doi.org/10.3109/02652048.2011.651494

Sarghini, F., 2015. Microfluidic Encapsulation Process, in: Mishra, M.K. (Ed.), Handbook of Encapsulation and Controlled Release. CRC Press, Boca Raton, USA, pp. 359–378.

Sarghini, F., De Vivo, A., 2019. Effect of process parameters on microencapsulation of active compounds by co-flow air assisted microfluidic extrusion. Chem. Eng. Trans. 75, 439–444. https://doi.org/10.3303/CET1975074

Schneider, T., Chapman, G.H., Häfeli, U.O., 2011. Effects of chemical and physical parameters in the generation of microspheres by hydrodynamic flow focusing. Colloids Surfaces B Biointerfaces 87, 361–368. https://doi.org/10.1016/j.colsurfb.2011.05.040

Schneider, T., Zhao, H., Jackson, J.K., Chapman, G.H., Dykes, J., HaFeli, U.O., 2008. Use of Hydrodynamic Flow Focusing for the Generation of Biodegradable Camptothecin-Loaded Polymer Microspheres. J. Pharm. Sci. 97, 4943–4954. https://doi.org/10.1002/jps.21344

Schoubben, A., Blasi, P., Giovagnoli, S., Rossi, C., Ricci, M., 2010. Development of a scalable procedure for fine calcium alginate particle preparation. Chem. Eng. J. 160, 363–369. https://doi.org/10.1016/j.cej.2010.02.062

Seifert, D.B., Phillips, J.A., 1997. Production of small, monodispersed alginate beads for cell immobilization. Biotechnol. Prog. 13, 562–568. https://doi.org/10.1021/bp9700723

Shah, R.K., Shum, H.C., Rowat, A.C., Lee, D., Agresti, J.J., Utada, A.S., Chu, L.-Y., Kim, J.-W., Fernandez-Nieves, A., Martinez, C.J., Weitz, D.A., 2008. Designer emulsions using microfluidics Open access under CC BY-NC-ND license. Mater. Today 11, 18–27. https://doi.org/10.1016/S1369-7021(08)70053-1

Shilpa, A., Agrawal, S.S., Ray, A.R., 2003. Controlled delivery of drugs from alginate matrix. J. Macromol. Sci. - Polym. Rev. 43, 187–221. https://doi.org/10.1081/MC-120020160

Si, T., Li, F., Yin, X.Y., Yi, X.Z., 2009. Modes in flow focusing and instability of coaxial liquid-gas jets. J. Fluid Mech. 629, 1–23. https://doi.org/10.1017/S0022112009006211

Simpson, N.E., Grant, S.C., Blackband, S.J., Constantinidis, I., 2003. NMR properties of alginate microbeads. Biomaterials 24, 4941–4948. https://doi.org/10.1016/S0142-9612(03)00418-6

Sohail, A., Turner, M.S., Coombes, A., Bostrom, T., Bhandari, B., 2011. Survivability of probiotics encapsulated in alginate gel microbeads using a novel impinging aerosols method. Int. J. Food Microbiol. 145, 162–168. https://doi.org/10.1016/j.ijfoodmicro.2010.12.007

Sohail, A., Turner, M.S., Prabawati, E.K., Coombes, A.G.A., Bhandari, B., 2012. Evaluation of Lactobacillus rhamnosus GG and Lactobacillus acidophilus NCFM encapsulated using a novel impinging aerosol method in fruit food products. Int. J. Food Microbiol. 157, 162–166. https://doi.org/10.1016/j.ijfoodmicro.2012.04.025

Sugiura, S., Oda, T., Aoyagi, Y., Matsuo, R., Enomoto, T., Matsumoto, K., Nakamura, T., Satake, M., Ochiai, A., Ohkohchi, N., Nakajima, M., 2007. Microfabricated airflow nozzle for microencapsulation of living cells into 150 micrometer microcapsules. Biomed. Microdevices 9, 91–99. https://doi.org/10.1007/s10544-006-9011-9

Sugiura, S., Oda, T., Izumida, Y., Aoyagi, Y., Satake, M., Ochiai, A., Ohkohchi, N., Nakajima, M., 2005. Size control of calcium alginate beads containing living cells using micro-nozzle array. Biomaterials 26, 3327–3331. https://doi.org/10.1016/j.biomaterials.2004.08.029

Sun, X.T., Liu, M., Xu, Z.R., 2014. Microfluidic fabrication of multifunctional particles and their analytical applications. Talanta 121, 163–177. https://doi.org/10.1016/j.talanta.2013.12.060

Tabeei, A., Samimi, A., Khorram, M., Moghadam, H., 2012. Study pulsating electrospray of non-Newtonian and thixotropic sodium alginate solution. J. Electrostat. 70, 77–82. https://doi.org/10.1016/j.elstat.2011.10.006

Tran, V.T., Benoît, J.P., Venier-Julienne, M.C., 2011. Why and how to prepare biodegradable, monodispersed, polymeric microparticles in the field of pharmacy? Int. J. Pharm. 407, 1–11. https://doi.org/10.1016/j.ijpharm.2011.01.027

Tryggvason, G., Scardovelli, R., Zaleski, S., 2004. Direct Numerical Simulations of Gas-Liquid Multiphase flows. Cambridge University Press, Cambridge. https://doi.org/10.1142/9781860949609_0009

Utada, A.S., Chu, L., Link, D.R., Holtze, C., Weitz, D.A., 2007. Dripping, Jetting, Drops, and Wetting: The Magic of Microfluidics 32, 702–708.

Utada, A.S., Lorenceau, E., Link, D.R., Kaplan, P.D., Stone, H.A., Weitz, D.A., 2005. Monodisperse double emulsions generated from a microcapillary device. Science (80-.). 308, 537–541. https://doi.org/10.1126/science.1109164

Van Steijn, V., Kleijn, C.R., Kreutzer, M.T., 2009. Flows around confined bubbles and

their importance in triggering pinch-off. Phys. Rev. Lett. 103, 1–4. https://doi.org/10.1103/PhysRevLett.103.214501
Vega, E.J., Montanero, J.M., Herrada, M.A., Gañán-Calvo, A.M., 2010. Global and local instability of flow focusing: The influence of the geometry. Phys. Fluids 22, 1–10. https://doi.org/10.1063/1.3450321
Velings, N.M., Mestdagh, M.M., 1995. Physico-chemical properties of alginate gel beads. Polym. Gels Networks 3, 311–330. https://doi.org/10.1016/0966-7822(94)00043-7
Voo, W.P., Lee, B.B., Idris, A., Islam, A., Tey, B.T., Chan, E.S., 2015. Production of ultra-high concentration calcium alginate beads with prolonged dissolution profile. RSC Adv. 5, 36687–36695. https://doi.org/10.1039/c5ra03862f
Weiner, M.L., Salminen, W.F., Larson, P.R., Barter, R.A., Kranetz, J.L., Simon, G.S., 2001. Toxicological review of inorganic phosphates. Food Chem. Toxicol. 39, 759–786. https://doi.org/10.1016/S0278-6915(01)00028-X
Whelehan, M., Marison, I.W., 2011. Microencapsulation using vibrating technology. J. Microencapsul. 28, 669–688. https://doi.org/10.3109/02652048.2011.586068
Whelehan, M., von Stockar, U., Marison, I.W., 2010. Removal of pharmaceuticals from water: Using liquid-core microcapsules as a novel approach. Water Res. 44, 2314–2324. https://doi.org/10.1016/j.watres.2009.12.036
Wikström, J., Elomaa, M., Syväjärvi, H., Kuokkanen, J., Yliperttula, M., Honkakoski, P., Urtti, A., 2008. Alginate-based microencapsulation of retinal pigment epithelial cell line for cell therapy. Biomaterials 29, 869–876. https://doi.org/10.1016/j.biomaterials.2007.10.056
Woo, J.W., Roh, H.J., Park, H.D., Ji, C.I., Lee, Y.B., Kim, S.B., 2007. Sphericity Optimization of Calcium Alginate Gel Beads and the Effects of Processing Conditions on Their Physical Properties. Food Sci. Biotechnol. 16, 715–721.
Wu, J., Kong, T., Yeung, K.W.K., Shum, H.C., Cheung, K.M.C., Wang, L., To, M.K.T., 2013. Fabrication and characterization of monodisperse PLGA-alginate core-shell microspheres with monodisperse size and homogeneous shells for controlled drug release. Acta Biomater. 9, 7410–7419. https://doi.org/10.1016/j.actbio.2013.03.022
Yotsuyanagi, T., Ohkubo, T., Ohhashi, T., Ikeda, K., 1987. Calcium-Induced Gelation of Alginic Acid and pH-Sensitive Reswelling of Dried Gels. Chem. Pharm. Bull. 35, 1555–1563. https://doi.org/10.1248/cpb.35.1555
Yu, W.K., Yim, T. Bin, Lee, K.Y., Heo, T.R., 2001. Effect of skim milk-alginate beads on survival rate of bifidobacteria. Biotechnol. Bioprocess Eng. 6, 133–138. https://doi.org/10.1007/BF02931959
Zhang, J., Li, X., Zhang, D., Xiu, Z., 2007. Theoretical and experimental investigations on the size of alginate microspheres prepared by dropping and spraying. J. Microencapsul. 24, 303–322. https://doi.org/10.1080/02652040701339098
Zhou, C., Yue, P., Feng, J.J., 2006. Formation of simple and compound drops in microfluidic devices. Phys. Fluids 18, 1–14. https://doi.org/10.1063/1.2353116
Zimmermann, H., Hillgärtner, M., Manz, B., Feilen, P., Brunnenmeier, F., Leinfelder, U., Weber, M., Cramer, H., Schneider, S., Hendrich, C., Volke, F., Zimmermann, U., 2003. Fabrication of homogeneously cross-linked, functional alginate microcapsules validated by NMR-, CLSM- and AFM-imaging. Biomaterials 24, 2083–2096. https://doi.org/10.1016/S0142-9612(02)00639-7

3 Matrix Microencapsulation of Active Compounds: Effect of Process Variables on Size Distribution of Microgels

3.1 Introduction

Ionotropic alginate microgel particles (microgels) have been reported to encapsulate a variety of substances, which in their raw form may be sensitive to heat, light, moisture, pH, toxin, oxidation, mechanical shear or pressure. Encapsulation is carried out to prolong the product shelf life, improve/retain the quality of the product, enhance the appearance of the product and/or add value to the product. The microgels are produced via ionotropic cross-linking reaction between calcium cations and alginate chains. Microencapsulation require simultaneous control and tuning of numerous capsule parameters, including their size, permeability and mechanical properties, which can be difficult to achieve with traditional encapsulation techniques. Instead, double emulsion templates made using microfluidics can offer substantial advantages due its inherent precision and control of a wide range of processing variables such as particle size and its distribution, capsules payload. In fact, microfluidic chips are based on microscale channels where in liquids flow, enabling a high control of their movement and dynamics. Beyond the capsule size control, microfluidics can also be used to produce controlled capsules shapes different from spherical, such as cylindrical shapes with a better bioavailability. In summary, microfluidics are a highly advanced tool for tailoring the physical features microcapsules. One of the most popular ways to produce hydrogel beads is by extrusion dripping. In this method, an alginate solution is delivered through a capillary and then is extruded into droplets which detach from the dripping tip by the influence of gravitational force (natural extrusion). The size of a bead produced by simple extrusion dripping is greater than 1,000 μm bigger than the range size of 200–800 μm desired for most encapsulation applications. Beads with diameters smaller than 1,000 μm could be produced through external forces such as vibration, pressurized air and electrostatic charges (Lee et al., 2013). At the same time, the forces may also increase the microgel production rate. The main innovation of this work relies on the choice to develop a technology based on air assisted microfluidic extrusion that has a number of advantages due to easier some post-processing operations like gelation and cleaning. On the other hand the higher velocity and consequently the turbulence flow regime due to high Reynolds numbers involved makes extremely difficult to operate in core-shell configuration (Marra et al., 2017). Moreover, the possible micro pump-micro device integration is up today an open and unresolved problem. The air extrusion method using pressurized air is not complicated and can handle relatively higher viscosity. A typical air extrusion system for alginate microgel formation consists of a pressurized air or gas supply source, an extrusion nozzle and a gelation bath of calcium chloride for gelation process. The use of flow-focusing nozzle to produce microgels was used in which the inner dispersed phase fluid (sodium alginate) and the outer continuous phase fluid (air) flow inside two concentric channels. The fluids meet into the larger outer channel where the focusing air stream generates shear force (which exceeds the gravitation force) that leads to a concentric stretching of the alginate solution jet in the direction of flow. The shear and stretching effect of the air causes the jet to get attenuated and capillary instability breaks up the jet into homogeneous droplets. The size

and the shape of Ca-Alginate beads is influenced by physical properties such as viscosity or surface tension and solution formulation of the alginate and gelling. Dripping tip diameter and collecting distance (between the dripping tip and the gelation bath-air interface) are instead the main factors concerning the experimental set up that may influence the bead size and shape. The principal aims of this work concern (i) the study of a microfluidic device for extrusion of microbeads in matrix configuration by optimising geometric parameters of the device; (ii) analysis of the influence of the process parameters on the microcapsules particle size distribution by varying the dispersed or continuous phase flow rate or the viscosity of alginate solution. In this case the other parameters were keep unchanged.

3.2 Materials and methods

Experimetal Set Up. The microdevice geometry was created using CAE software and printed in methacrylate photopolymer resin with a 3D printer for rapid prototyping (FORMLABS 1+, USA). The device consisted of a support for the extrusion nozzle and an air chamber. In particular the extrusion nozzle consisted of a fused silica polyimide coated capillary with a tip diameter, d_d = 100 μm (MOLEX, USA). This was inserted into a hypodermic needle which ensured the capillary to be always properly centred and aligned. A 700 μm (d_c) inner diameter pipettor tip was used for conveying the air flow, thus focusing the flow of the dispersed phase. The collecting distance between dripping tip and gelation bath was fixed at 5 cm. The co-flow device adopted in the experiments is described in *Figure 22*.

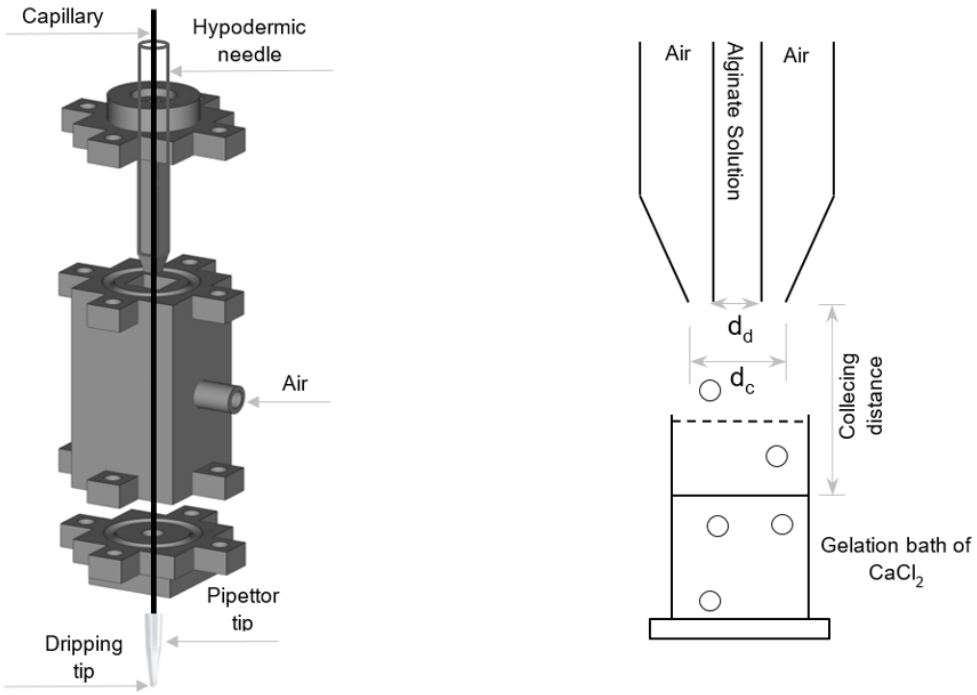

Figure 22. Microdevice design (a) and scheme of extrusion dripping (b).

Materials and Sample Preparation. Sodium alginate and calcium chloride dehydrate was purchased from the Sigma-Aldrich (Milano, Italy). Sodium alginate solutions with

different concentrations (2.0%, 2.5%, 3.0%, 3.5% w/v) were prepared by dissolving a proper amount of powder in 100 mL deionized water; the solutions were mixed by a magnetic stirrer for 24 hours to facilitate degasation and then were transported by a syringe pump (Aladdin 300-220, WPI). The gelation bath was made up of $CaCl_2 \cdot 2H_2O$ in the concentration 0.2 M (Cerveró et al., 2011).
Air flow was controlled by mass flow meter (MASS-VIEW Bronkhorst, The Netherlands) connected to a pressurized air. The microgels were recovered with a filter and then washed with deionized water.
Rheological characterization. Rheological properties of sodium alginate solutions were performed by using a Rotational rheometer (Kinexus lab+, Malvern Instruments). The measurements were carried out at 25 °C using a cone plate configuration (CP4/40) with a 40 mm diameter and a 4° cone angle, the range of shear rate from 1 to 1,000 s^{-1} were applied, viscosity (η) was recorded as a function of shear rate ($\dot{\gamma}$).
Particle Size Analysis. The particle size distributions of microbeads were measured via a Malvern Mastersizer 3000E Hydro, (Malvern Instruments, Worcestershire, U.K.). Each individual particle size measurement was determined from the average of three readings made per sample.

3.3 Results and Discussion

3.3.1 Steady-shear flow measurements

Understanding of the rheological behaviour of sodium alginate aqueous solutions at different concentrations is fundamental to evaluate the influence of viscosity on Ca-alginate beads production in terms of monodispersion, size and shape. In fact, it is generally known that the viscosity of the discontinuous phase is one of the key factors for determining the transition from the dripping regime to the jetting regime. Moreover, the droplets produced in the dripping mode exhibit a more uniform size distribution than ones produced in jetting regime (Moon et al., 2014). The viscous properties for alginate solutions were determined using steady-shear flow test over the range of shear rate ($\dot{\gamma}$) from 1 to 1,000 s^{-1}. The results describe the relationship between viscosity (η) and shear rate ($\dot{\gamma}$) of sodium alginate at different concentrations ranging from 2.0 to 3.5 % (w/v). From the shapes of the flow curves related to 2.5, 3.0 and 3.5 % (w/v) concentrations (*Figure 23*), there was an initial Newtonian plateau region as the shear rate approaches zero. The viscosity exhibited by a material at a shear rate inclining to zero is defined as the zero shear viscosity (η_0) and indicated that the material flows (like liquid) at rest. Above a critical shear rate, all solutions showed a power law region (shear thinning behaviour) where the viscosity decreased with the increase of shear rate. Furthermore, this critical shear rate shifted towards lower values of shear rate as the concentration of sodium alginate increased. According to Ma et al. (2014) the shear data were analysed by fitting the Cross model to the data:

$$\eta = \eta_\infty + \frac{\eta_0 - \eta_\infty}{1 + (k\dot{\gamma})^m} \qquad (13)$$

where η is the viscosity at any specific shear rate $\dot{\gamma}$, η_0 and η_∞ are the viscosity at zero and infinite shear rates, respectively, k is a shear-dependent time constant and its reciprocal 1/ k, corresponds to a critical shear rate that provides a useful indicator of the onset of the shear thinning region. The exponent (m) gives the degree of thinning (0 = no thinning, that is, Newtonian behavior and 1 = maximal thinning). In summary oscillatory frequency sweep test proved that the material is dominated by a viscous component in rest conditions. Based on this dynamic viscoelastic measurements, a Cross model has been chosen to accurately fit the rheological data. The Cross model parameters for the different concentrations of sodium alginate solutions were summarized in *Table 3*.

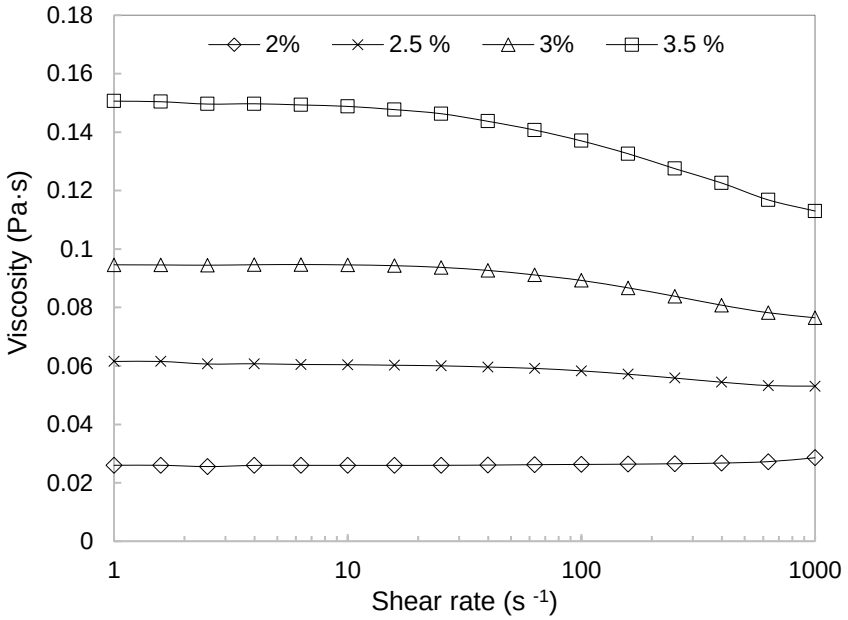

Figure 23. Flow curves of sodium alginate aqueous solutions at different concentrations ranging from 2.0 to 3.5% (w/v).

As shown in *Table 3*, the curve at 2.0 % had a determination coefficient R2 lower than 0.99, which indicated the Cross model was not suitable. In fact, the lowest-concentration solution viscosity was independent of the rate of shear (*Figure 23*) proving the Newtonian behavior of the fluid. *Figure 23* also showed that the viscosity increased with the increase of sodium alginate concentrations. The increase in η could be attributed to the increased intermolecular interactions between polymer molecules.

Table 3. Cross model fitting parameters of sodium alginate at different concentrations ranging from 2.0 to 3.5 % w/v.

concentration (% w/v)	η_0 (Pa·s)	η_∞ (Pa·s)	*k*	*m*	R^2
2.0	0.0373	0.0358	0.0433	0.8034	0.8475
2.5	0.0605	0.0497	0.0126	0.2467	0.9976
3.0	0.0948	0.0733	0.0042	1.2320	0.9998
3.5	0.1506	0.1009	0.0034	0.9282	0.9998

3.3.2 Influence of continuous phase flow rate on size distribution of Ca-alginate beads

Setting flow rate of dispersed phase at 0.0185 ml min^{-1} (concentration 3 % w/v), the production of Ca-alginate beads at different air flow rates, ranging from 0.7 to 2.2 Nl min^{-1} has been investigated. The first tests were carried out at the continuous phase flow rate lower than 0.7 Nl min^{-1} where the shear force generated by air was not enough to obtained desired dripping regime. Starting from 0.7 to 1.6 Nl min^{-1}, size distribution data of the different microbeads samples were depicted both as a density distribution (*Figure 24*) and a cumulative volume curve (*Figure 25*). The cumulative curve describes how many percentages of samples are below a certain size of particles. The D10, D50 and D90 is defined as the size value corresponding to cumulative size distribution at 10%, 50%, or 90%, which represents the size of particles below which 10%, 50%, or 90% of the sample lies. The median diameter D50 was used to compare the results obtained at different air flow rates because it was less affected by presence of secondary populations of particles (secondary peaks). As shown in *Figure 25*, the values of D50 decreased with increasing flow rate of continuous phase ranging from 0.7 to 1.6 Nl min^{-1}. The D50 of samples 0.7, 0.9, 1.1, 1.3 and 1.6 Nl min^{-1} was 87.5, 47.3, 45, 38.1 and 27.1 µm, respectively. This was attributed to the higher share provided by pressurized air as its flow rate increased. Furthermore, secondary peaks could be explained by misalignment of the capillary that affects dripping regime during extrusion. With increasing air flow rate above 1.6 Nl min^{-1} there was no sharp decrease in particle size distributions of microbeads because the interaction between a high speed air jet with an alginate coaxial jet that makes much more difficult to predict and control the extrusion phenomena, including the formation of satellites drop and the effect of "coalescence". More specifically, the discontinuous flow could tend to transit from dripping to jetting regimes as the flow rate of the continuous phase increased. As a result at the end of the jet, the main drop with jet diameter is followed by satellite drops with lower diameters (double whipping). In some instances, air pressure could make faster the drop closer at the tip of the needle than another drop that has detached earlier. As a result, coalescence between the two drops could occur (merging) (Marra et al., 2017).

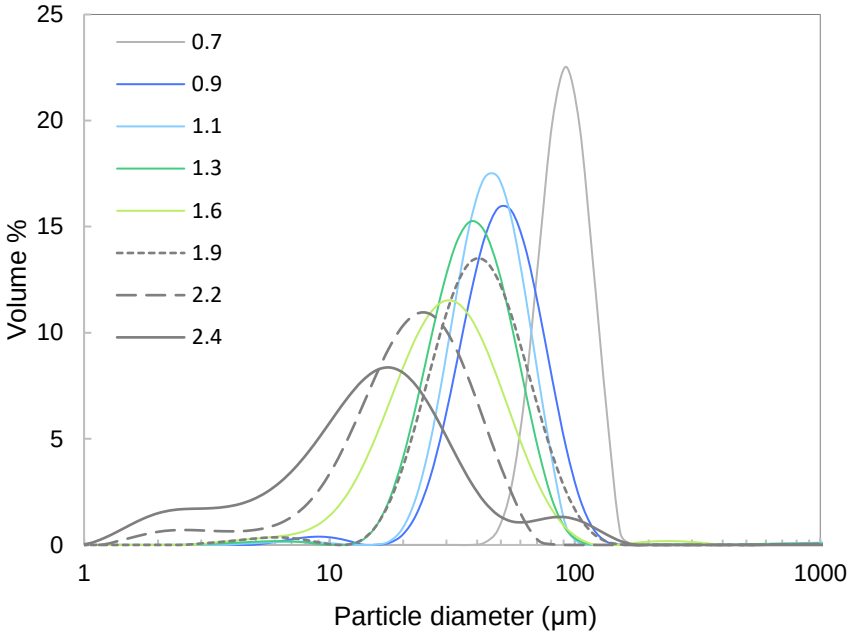

Figure 24. Particle volume distribution of the samples obtained at different flow rates of air, 0.7, 0.9, 1.1, 1.3, 1.6, 1.9, 2.2 and 2.4 Nl min^{-1}.

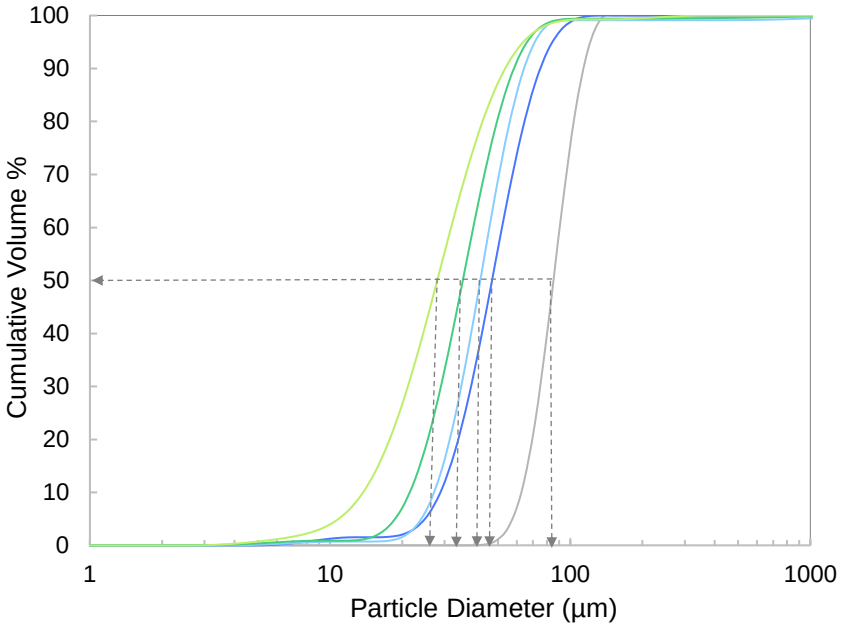

Figure 25. Cumulative volume distribution at 0.7, 0.9, 1.1, 1.3 and 1.6 Nl min^{-1}.

3.3.3 Effect of dispersed phase flow rate

Size distributions of droplets generated at different flow rates of the dispersed phase (7, 11, 15 and 19 µl min^{-1}) are shown in *Figure 26*. The flow rate of the continuous phase was kept at 1.6 Nl min^{-1} based on the results obtained previously because the device exhibited the best performance in terms of capillary stability. There were no significant differences in the D50 of the samples collected at different flow rate of alginate revealing that the droplet formation was primarily affected by the flow rate of the continuous phase.

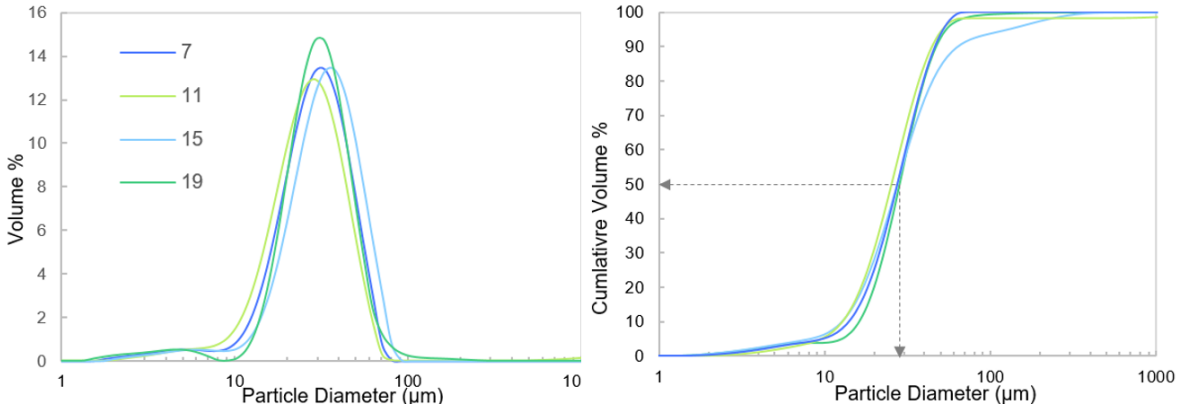

Figure 26. Particle volume distribution of the samples obtained at different flow rates of alginate, 7, 11, 15 and 19 µl min^{-1} (a) and cumulative volume (b).

3.3.4 Effect of alginate solution concentration

The tests were carried out considering four alginate solution concentrations, ranging from 2 to 3.5% (w/v). It was not possible to produce beads using concentration of 2 % (w/v) because the viscous forces within the droplet were unable to compete with the drag forces exerted when the drop hit and entered the gelling bath. Moreover, low viscosities of alginate solution results in higher drop deformation upon impact with the surface of the gelation bath. It has been reported that the viscosity (or concentration) of alginate solution significantly affects the spherical-shaped of the microbeads (Chan et al., 2009). *Figure 27* shows results obtained varying alginate concentration (2.5, 3.0 and 3.5 % w/v) by maintaining constant the value of dispersed phase and air flow rates (values of 7 µl min^{-1} and 1.6 Nl min^{-1}, respectively). The median diameter (D50) of beads decreased slightly (from 43.5 to 29.4 µm) as the concentration increased from 2.5 to 3.0 % w/v. Alginate solution with a concentration of 3.5 % w/v was not suitable for this extrusion method due to difficulties in the bead forming process (pumping and obstruction at the dripping nozzle) (Gombotz and Wee, 1998). This could explain the generation of a bimodal population of beads in correspondence to the alginate concentration of 3.5 % w/v.

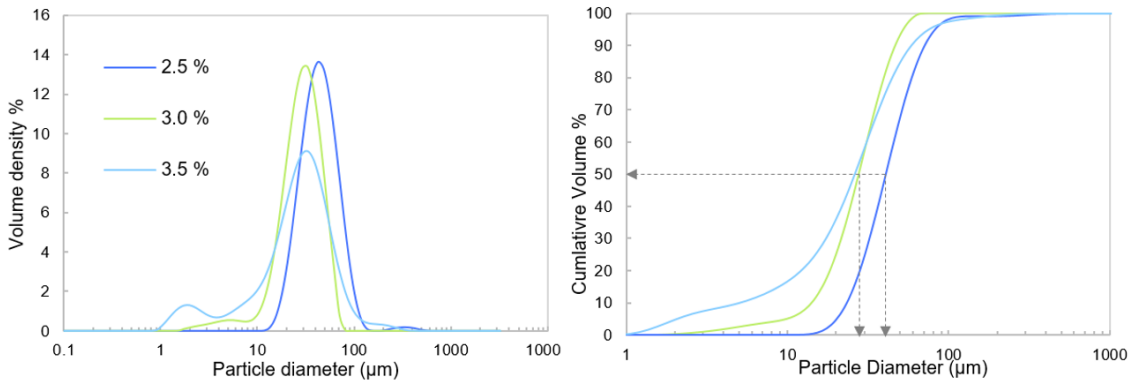

Figure 27. Particle volume distribution of the samples obtained at different concentration of alginate solution, 2.5, 3.0 and 3.5 % (w/v) (a) and cumulative volume (b).

3.4 Conclusions

Experimental test reported in this work demonstrated that size distribution of microbeads is affected by process parameters not only in terms of D50 size, but also in terms of diameter distribution shape. A major effect is played by the flow rate of the continuous phase. Viscosity effects are also quite important, generating a possible change in drop formation pattern when viscosity increase. A more extended experimental set of process parameters is required to fully characterize the possible envelope of microbeads size and characterize it in term of adimensional numbers.

References

Cerveró, J.M., Nogareda, J., Valle, E.M.M. del, Galán, M.A., 2011. Development of a technology to produce monodispersed microparticles based on the formation of drops from viscous non-Newtonian liquids sprayed through a fan jet nozzle. Chem. Eng. J. 174, 699–708. https://doi.org/10.1016/j.cej.2011.09.063

Chan, E.S., Lee, B.B., Ravindra, P., Poncelet, D., 2009. Prediction models for shape and size of ca-alginate macrobeads produced through extrusion-dripping method. J. Colloid Interface Sci. 338, 63–72. https://doi.org/10.1016/j.jcis.2009.05.027

Gombotz, W.R., Wee, S.F., 1998. Protein release from alginate matrices. Adv. Drug Deliv. Rev. 31, 267–285. https://doi.org/10.1016/S0169-409X(97)00124-5

Lee, B.B., Ravindra, P., Chan, E.S., 2013. Size and shape of calcium alginate beads produced by extrusion dripping. Chem. Eng. Technol. 36, 1627–1642. https://doi.org/10.1002/ceat.201300230

Ma, J., Lin, Y., Chen, X., Zhao, B., Zhang, J., 2014. Flow behavior, thixotropy and dynamical viscoelasticity of sodium alginate aqueous solutions. Food Hydrocoll. 38, 119–128. https://doi.org/10.1016/j.foodhyd.2013.11.016

Marra, F., De Vivo, A., Sarghini, F., 2017. Virtualization of fluid-dynamics in micro-air assisted extruders for food microfluidic based encapsulation. J. Food Eng. 213, 89–98. https://doi.org/10.1016/j.jfoodeng.2017.04.030

Moon, S.K., Cheong, I.W., Choi, S.W., 2014. Effect of flow rates of the continuous phase on droplet size in dripping and jetting regimes in a simple fluidic device for coaxial flow. Colloids Surfaces A Physicochem. Eng. Asp. 454, 84–88. https://doi.org/10.1016/j.colsurfa.2014.04.006

4 Core-shell Microencapsulation Using Air Assisted Microfluidic Device

4.1 Introduction

Microencapsulation is a versatile technology applied to numerous disciplines (biological, medical, food). Its successful application requires mono-dispersed, homogenous-shaped capsules, with a narrow distribution because these attributes allow precise manipulation of the loading levels and the release and transport kinetics of the encapsulated substances (Utada et al., 2005).

Despite their fastest growth in the last two decades for pharmaceutical applications, encapsulation and controlled release technologies have only been recently adopted by food industry. The interest by researchers and technologists in the microencapsulation process is growing due to its many existing and potential applications in many food categories such as bakery, dairy products, beverages, packaging (Gouin, 2004). For example, in the baking industry the microencapsulation technologies were adopted for protecting, developing or delaying the release of leaving agents, sweeteners, enzymes, and antimicrobials. Bakery manufacturers, therefore, save on the costs due to the extending shelf life, eliminating long fermentation and the shortening of proofing time (Lakkis, 2016). Different authors investigated the microencapsulation of probiotics for improving their viability in food products and the intestinal tract (Krasaekoopt et al., 2004; Sohail et al., 2012). The probiotics can be incorporated in a wide range of food products like dairy products (milk, ice cream, yogurt, and cheese), meats, baby foods, confectionery, cakes (Champagne et al., 2005).

Moreover, microencapsulation has been applied to add value to the food products by masking the undesirable sensory changes (grittiness or oxidized taste) of calcium, vitamins or poly-unsaturated fatty acids, by protecting heat- or oxidation-labile health actives or volatile ingredients.

The technological framework is variegate, and it involves, for example, several emulsification techniques. In the conventional emulsifying methods for making emulsions, turbulence or shear stress generated by manual or mechanical agitation enhance drop breakup. However, the resultant drops are highly polydisperse and core shell configuration is difficult if not impossible to achieve (Shah et al., 2008).

Microfluidics, the science of designing, manufacturing and operating devices that deal with fluids in nano/pico liter scale, has the potential to control over the size and the size dispersion of the drops (Chu et al., 2007; Sarghini and De Vivo, 2019).

Microfluidics devices can be identified by the fact that they have channels with at least one dimension smaller than 1 mm, and they offer an alternate and versatile route to manipulate with unprecedented accuracy the size of the droplets for core-shell encapsulation structures.

The most widely used wall-forming materials (encapsulating matrix) used for food grade and non-food compounds is alginate, due to its biocompatibility, low cost, easiness in gel formation and resistance to the acidic environment of stomach (Krasaekoopt et al., 2004; Lee et al., 2013; Zhang et al., 2007). It can form thermally stable hydrogel beads in the presence of a divalent calcium cation. Ca-alginate microgels production represents an

interesting technological application allowing encapsulation of microbial cells, enzymes, drugs, oils, herbal extracts, and flavors in both matrix or core-shell configuration.
Droplet extrusion into calcium solutions is a well-known way to produce alginate beads in liquid-air systems. In this method, an alginate solution is delivered through a capillary and forms a pendant droplet at the dripping tip. The droplet detaches under the influence of gravitational force or external force (Lee et al., 2013). However, the droplet mean diameter obtained by natural extrusion under gravity is typically greater than 1000 μm (Fundueanu et al., 1999; Shilpa et al., 2003). The use of an external force rather than simple gravity accelerates the detachment of the alginate solution droplet before it grows to its maximum volume. As a result, the premature bead size is smaller than that of a typical bead produced by natural extrusion dripping.
Drop formation can be greatly improved by replacing gravity with the external forces such as coaxial air jets, electrostatic potential, rotating jet breakage, centrifugal force (Dulieu et al., 1999). These technologies appear to be efficient methods to obtain microcapsules smaller than 1000 μm with limited size dispersion. Among these possibilities and according to our previous work (Sarghini and De Vivo, 2019), we describe the design of a new microfluidic device using a coaxial air jet as external force to control microdroplets extrusion in core-shell configuration. In this approach, air jet is used to generate varicose instabilities into the non-Newtonian liquid jet, providing a jet break-up with different breaking modes and final droplet configurations. The middle fluid (sodium alginate) and the inner encapsulated phase (oil) move in the same direction through two concentric channels and are ejected from their tips at controlled mass flow rate. The air (outer phase) flows in the third capillary outside the inner two, causing the Rayleigh-Plateau instability of the out-going coaxial stream. This fluid dynamics instability is driven by interfacial tension and reduces the total surface area of a fluid system by breaking it into drops(Utada et al., 2005)(Utada et al., 2005)(Utada et al., 2005)(Utada et al., 2005)(Utada et al., 2005). Thus, the jet breaks up prematurely into droplets with a smaller size than those obtained under the influence of simple gravitational force. The main innovation relies on the development of a new technology “industrial oriented” compared with the classical liquid-liquid dual immiscible fluid configuration. In fact, the use of air as continuous phase rather than an immiscible fluid (i.e. oil) overcomes a series of post-processing problems: droplet gelation, oil separation and cleaning. On the other hand, the low values of the air density and viscosity require higher velocities, in order to ensure the appearance of sufficiently high tangential stress and pressure perturbations. At the same time, higher velocity values lead to complex jet break-up dynamics (Errico et al., 2019), including the formation of satellites drops and consequently the increase in size dispersion that makes extremely difficult operating in core-shell configuration.
While most of the works are focused on matrix encapsulation technique, studies focused on core-shell encapsulation in air-assisted microfluidic devices do not exist in literature. Thus, the target of the proposed research is aimed to develop an air-liquid focusing device describing the application of this technique for encapsulating the oil and analyze the effect of the air mass flow rate on the size of the microbeads produced.

4.2 Materials and methods

4.2.1 Micro device design

The novel micro fabricated device is composed of two capillaries that were fed through a support structure, an air chamber (AC) and a pipettor tip (PT). The internal capillary is a fused silica polyimide coated capillary (PI-c) of 100 ± 4 μm internal diameter (ID) and 164 ± 6 μm external diameter (OD) (MOLEX, USA). The external capillary is a medical polyurethane capillary tube (PUR-c) with ID 520 μm and OD 0.7 mm. The pipettor tip ID and OD are 0.83 ± 0.09 mm and 1.57 ± 0.10 mm, respectively. 3D printing technology (FORMLABS 1+, USA) fabricated the AC from the mathematical representation of the three-dimensional surface created using computer-aided design (CAD) software. The design model is shown in *Figure 28*. It was then exported as an STL file readable by print preparation software. The 3D printer produced the AC layer by layer by solidifying of methacrylate photopolymer resin. The printed AC was rinsed in isopropyl alcohol to remove any uncured resin from its surface.

The schematic illustration of the co-flow microcapillary device for making droplets is shown in *Figure 29 a*. The PI-c was inserted into the PUR-c ensuring co-flow geometry since the fluid phases move in the same direction. The PT was inserted under the AC through the provided hole for conveying the air flow entering from the left side, thus flow-focusing the coaxial stream. Capillaries and PT lower ends were not perfectly aligned to facilitate the liquid outlet, as shown in Figure 29. The distance between the PUR-c and PUR-c lower ends (H_1) and the distance between PUR-c and the PT lower ends (H_2) were 20 μm and 50 μm, respectively.

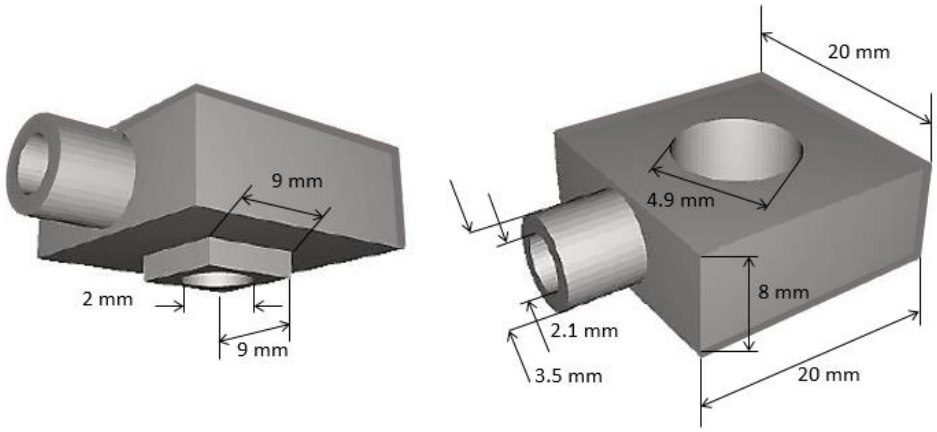

Figure 28. Geometric description of air chamber.

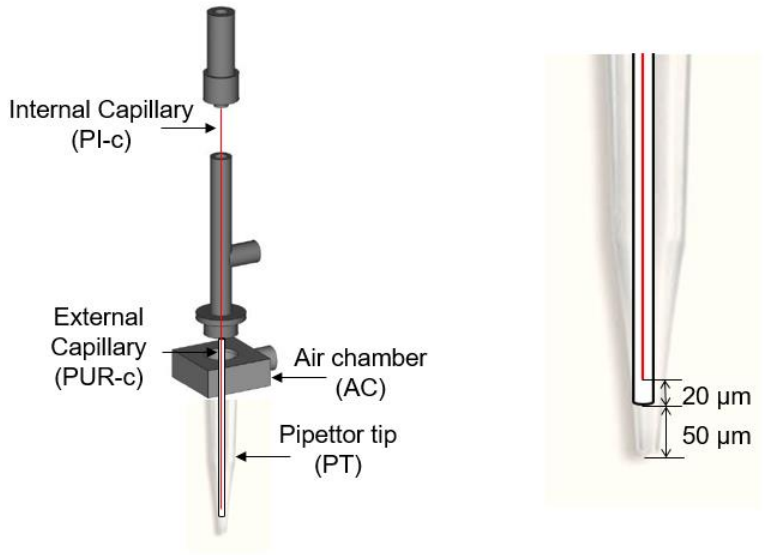

Figure 29. a) Microfluidic device for core-shell encapsulation of alginate beads. b) Orifice details.

4.2.2 Apparatus construction

A technology based on air-assisted microfluidic extrusion has been developed to prepare small core-shell microcapsules. The sketch of the experimental set-up considered in this work is described in *Figure 30*. The inner phase (IP) consisted of sunflower oil, flows through the PI-c, while the middle phase (MP) consisted of sodium alginate, flows through the PUR-c. The fluid phases were injected using syringe pumps (Aladdin 300-220, WPI) through the two concentric capillaries. The PT was used to convey the air flow (outer phase OP) and channel the coaxial stream out of the capillaries. Airflow was controlled by mass flow meter (MASS-VIEW Bronkhorst, The Netherlands) connected to pressurized air. The flow rate of the outer phase (air) usually exceeds that of the outgoing coaxial stream from the concentric capillaries typically by ten to a thousand times. Thus the latter is focused and forced to flow through a small orifice, indicated as "dripping tip" in *Figure 30* (Schneider et al., 2011). High shear stress and the prevailing rapid pressure drop at the orifice result in fluid dynamics instabilities and therefore in a jet break-up into droplets (Marra et al., 2018). The extruded drops fell in a calcium chloride solution for gelation process. The optimum collecting distance between the dripping tip and the gelation bath surface was found to be 24 cm.

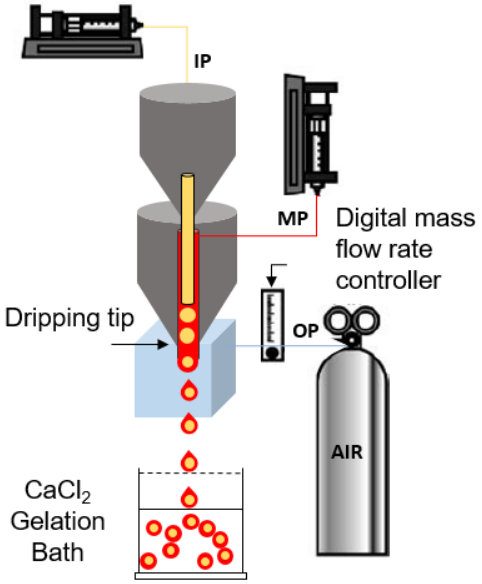

Figure 30. The experimental equipment used in the present study. IP= inner phase; MP= middle phase; OP= outer phase.

4.2.3 Phases formulation and parameter study

Sodium alginate with mannuronic acid to guluronic acid (M/G) ratio equal to 1.56 was provided by Sigma-Aldrich (Milano, Italy). The aqueous solution used in the experiments was prepared by mixing for 12 h at 30 °C distilled water with a 3% w/v concentration of alginate. The surfactant Tween 80 was added until the solution concentration is 8.6% w/w. The concentration of calcium chloride prepared for Ca-alginate bead formation is 0.2 M. The solution was vortex-mixed for 15 min.

The impact of the air flow on microdroplets generation was studied in triplicate experiments. The air flow rate was varied between 1 Nl min^{-1} and 9 Nl min^{-1}. The appropriate experimental parameters for the preparation of microbeads using the technique described above were chosen after many attempts. In fact, it is critical to obtain spherical droplets because of the impact force of the alginate droplet upon hitting the surface of the gelation bath that has a significant effect on the shape of the Ca-alginate beads formed (Lee et al., 2013). Thus, the alginate solution (MP) and sunflower oil (IP) flow rates were maintained at 1 ml min^{-1} and 13 µl min^{-1}, respectively. The main geometrical parameters, i.e. diameters of the internal (PI-c) and external capillaries (PUR-c), and the capillary-to-orifice distances H_1 and H_2, were kept constant for all experiments.

4.2.4 Rheological characterization

Rheological properties of sodium alginate solutions before and after the surfactant addition were performed using a rotational rheometer (Kinexus lab+, Malvern Instruments). The measurements were carried out at 25 °C using a cone plate configuration (CP4/40) with a 40 mm diameter and a 4° cone angle. The shear rate was varied between 1 and 1,000 s^{-1} measuring five samples per decade.

4.2.5 Bead size determination

The resulting alginate droplets fell directly into a $CaCl_2$ solution and calcium alginate beads were formed. After gelation time, the microbeads suspension was filtered and washed three times with deionized water. The stainless steel filter used consists in a double filter construction with the finest mesh available (Brewologist filter).
The alginate solution droplet size is measured by image analysis. The image of the droplet was captured using a high-resolution (digital) camera (Moticam 10+, MOTIC, Hong Kong) connected to an inverted microscope (MOTIC AE31, Hong Kong) and then the bead size is analyzed by image analysis software Motic Image Plus. The sizes of the beads are rather scattered, and the bead size distribution was quantified using a laser light scattering particle sizer (Malvern Instruments, Worcestershire, U.K.). The range of obscuration was 4-6% based on the expected particle size, for wet dispersions; experimental tests were repeated three times for each run, and micro-beads were characterized as milky particles with particle adsorption index equal to 1.51 and particle refraction index equal to 1.36. Results were averaged using at least 20 independent measures.

4.2.6 Encapsulation efficiency calculation

The encapsulation efficiency was calculated according to Devi et al., (2012):

$$\text{Encapsulation efficiency (\%)} = \frac{w_1}{w_2} \cdot 100 \qquad (14)$$

where w_1 is the actual amount of oil encapsulated in a known number of microcapsules and w_2 is the amount of oil introduced in the same amount of microcapsules.
The amount w_1 was measured by liquid-liquid extraction using *n*-Hexane (Sigma-Aldrich, Milano, Italy). 150 ml of distilled water and 30 ml of *n*-Hexane were added to the sample of washed encapsulated microcapsules. The microbeads were obtained from three tests conducted in the same operative conditions. In particular, the flow rates of the inner, middle and outer phase were set to 13 µl min^{-1}, 1 ml min^{-1} and 3 Nl min^{-1}, respectively. The sample was sonicated in an ultrasound bath of 50 kHz frequency (Labsonic LBS1-3, Falc Instruments, Bergamo, Italy) for 80 min followed by a filtration to separate the oil (solvent) fraction from the exhausted alginate matrix. The sample was then transferred to a separatory funnel. The oil actually encapsulated (w_1) was quantified by weight after evaporation of the *n*-Hexane solution (containing the oil) in an oven at a boiling temperature of hexane (69 °C).

4.3 Results and discussion

4.3.1 Basic rheological characteristics of sodium alginate aqueous solution

The viscous properties of aqueous solution of alginate used in a 3% concentration with and without the surfactant, were determined using steady-shear flow measurements. Two distinctive ranges of Newtonian and non-Newtonian shear thinning behaviors were recorded over the range of shear rate $1 < \dot{\gamma} < 1000\ s^{-1}$ .The Cross model has been chosen

to fit more properly the rheological *Table 4*, in agreement with the literature (Ma et al., 2014; Sarghini and De Vivo, 2019):

$$\eta = \eta_\infty + \frac{\eta_0 - \eta_\infty}{1 + (k\dot{\gamma})^m} \qquad (15)$$

where η is the viscosity at any specific shear rate $\dot{\gamma}$, η_0 and η_∞ are the asymptotic values of viscosity at zero and infinite shear rates, respectively, k is a shear-dependent time constant and its reciprocal $1/k$, corresponds to a critical shear rate that provides a useful indicator of the onset of the shear thinning region. The exponent (m) rules the shear dependence in the power-law region. The oscillatory frequency sweep test proved that the material flows in rest conditions and therefore is dominated by a viscous component. In the flow curves depicted on *Figure 31* what has just been highlighted is visible by the initial Newtonian plateau region at a shear rate inclining to zero. The viscosity intercept extrapolated from the plateau continuation is defined as η_0 (zero shear viscosity). Above the critical shear rate $(1/k)$ the material showed a shear thinning region. The viscosity declined with the shear rate increase to fall to a constant value η_∞. For low velocity gradients, the particles brownian motion produces a random distribution, and therefore an isotropic distribution in all the three dimensions. For this reason, the viscosity is assumed constant and equal to η_0. As the gradient is increased, particles line up along the flow lines, leading to a decrease in the viscosity. Finally, the viscosity takes on a constant value η_∞ (Friso, 2017).

Table 4. Cross model fitting parameters of sodium alginate at 3% (w/v) with and without the surfactant at 25°C.

η_0 (Pa·s)	η_∞ (Pa·s)	k	m	R^2
0.0948	0.0733	0.0042	1.232	0.9998
0.1226	0.0902	0.0045	1.133	0.9996

The profile of the sodium alginate solutions with and without the surfactant exhibited similar flow behavior (*Figure 31*). However, by adding the surfactant into the starting solution, the viscosity decreased slightly. This effect can be explained to a reduction in the connectivity of the polymeric matrix caused by the entrapped surfactant micelles, preventing intermolecular interactions between the polysaccharide chains (Fijan et al., 2007).

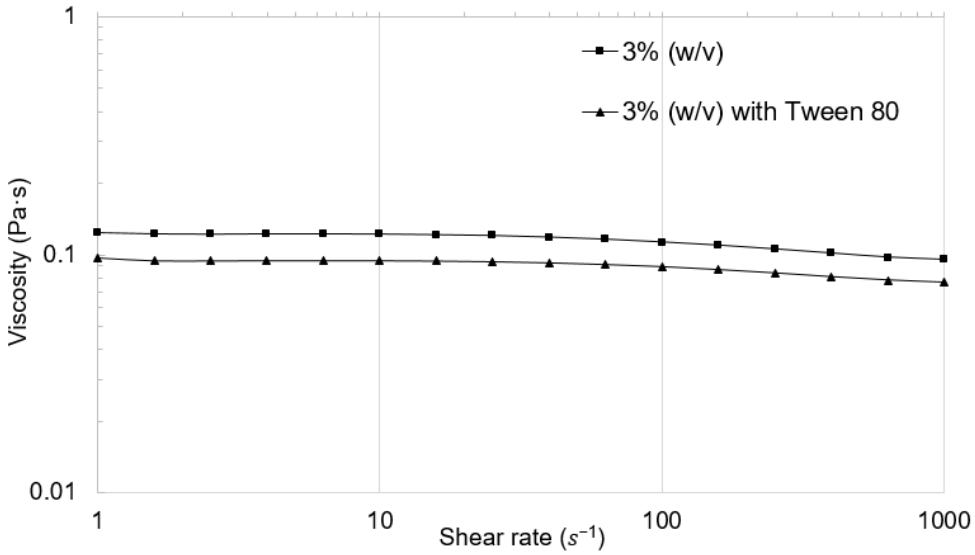

Figure 31. Viscosity as a function of shear rate of sodium alginate solutions at 3% (w/v) at 25°C.

4.3.2 Air generated Rayleigh-Plateau instability: jet break-up dynamic

In the proposed approach the coaxial jet composed in the outer layer by alginates and internal layer by oil is extruded by the inner channels and a jet collision among the jet and skew oriented air jet appears therefore an initial perturbation into the lateral wall of the inner liquid jet is generated. The air jet, given the initial curvature of the lateral liquid jet surface, introduces a series of high-frequency maximum and minimum pressure swirling peaks (*Figure 32)*, further amplifying the break-up mechanism. Such a complex mechanism is strongly inter-influenced by the physical properties of alginate solution, dripping tip diameter, and alginate solution flow rate. This interrelationship can be described by the local characteristics numbers, Reynolds number and Ohnesorge number based on the process variables of sodium alginate solution. In the experiments reported in this paper $Re \cong 10$ and $Oh \cong 1$ demonstrating that the working conditions used to form alginate droplets fall within a regime marked by the growth of long-wavelength, small-amplitude disturbances on the liquid surface promoted by the interaction between the liquid and air (Heinzen et al., 2004). The disturbances are believed to initiate the liquid breakup process. This phenomenon is known as Plateau-Rayleigh instability.

In accordance with this estimate, numerical experiments showed that the effect of the external forced convection due to air-liquid jet interactions generate a series of varicose perturbations represented as periodic displacement sinusoids (Marra et al., 2018). This disturbance grows exponentially causing the breakup of the liquid jet and allowing the production of droplets provided its wavelength is greater than the jet circumference. Thus, the breakup process of a liquid jet is closely associated with the instability of the jet using air as a continuous phase. There is a substantial difference in the liquid-liquid immiscible fluid configuration due to a "physical shaping". In that case, a drop of a liquid is dispersed in the other liquid (continuous phase) by the action of shear forces exerted between the two liquid phases, due to specific capillary tubes geometry (Martins et al., 2017; Sun et al., 2014; Sugiura et al., 2005).

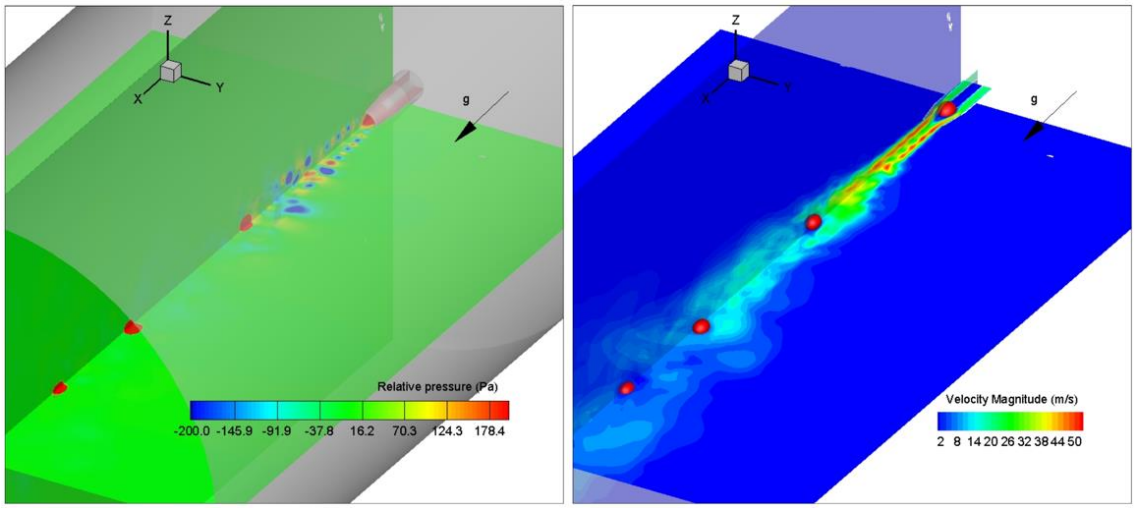

Figure 32. Pressure (left side) and velocity (right side) field generated by the air stream.

4.3.3 Influence of air flow rate on the size distribution of microbeads

Diameter control of calcium alginate beads is an important factor for practical applications. This is because beads with well-defined size allow the development of highly reproducible reactions or controlled-release rates (Gañán-Calvo, 1998). In order to control the bead diameter, we investigated the effect of the flow rate of a continuous phase that has a strong impact on the size distribution of microspheres and the droplet breakup of the coaxial stream (IP + MP) (Sugiura et al., 2007). To investigate this effect, the attention was paid to different values of airflow rate ranging from 1 to 9 Nl min^{-1} in 1 Nl min^{-1} intervals using the experimental setup described in the current study. The oil and alginate flow rate and the geometrical parameters were held constant as described above. The curing time of beads in gelation bath was maintained fixed at 20 min. In agreement with the literature, the time of minimum 15 min is sufficient to reach an equilibrium size and to obtain beads with spherical shape (Peretz, 2004).

A typical size distribution was composed of the main peak and small satellite peaks resulting in a polydispersed microcapsules sample. The example shown in *Figure 33.* Particle size distribution of three replicate beads samples by setting the airflow rate at 9 Nl min-1. *Figure 32* depicts the diameter distribution of the samples obtained at a flow rate of air 9 Nl min^{-1} in which the sample heterogeneity is most apparent due to the high air velocity involving gas flow instabilities and turbulence with a more difficult control of drop size.

Generally, the alginate solution droplet detachment mechanism at the dripping tip can be distinguished into a dripping or jetting process. The transition depends on the capillary number of the outer flow and the Weber number of the inner flow (Utada et al., 2007). In our case, the simple identification of both dripping and jetting regimes is not directly predictable because of the interaction of a high-speed jet of the continuous phase and the consequent instability of a liquid coaxial stream (IP + MP).

According to Si et al., 2009 the dynamics of the jet breakup can be defined by the coexistence of both non-axisymmetric (helical jetting mode) and axisymmetric jetting. For this transition way, liquid jet whips at the end of the elongation due to the effect of

external disturbance. Therefore, both satellites and main droplets whose diameter is comparable with the jet one are formed. This could explain the appearance of the small peaks before the main peak in the drop size characterization shown in *Figure 33*. However, the loss of the jet axial symmetry and thus, the transition between helical and axisymmetric jetting mode could also be justified by the geometrical changes in the device configuration during air-assisted extrusion for example due to a lateral capillary misalignment.

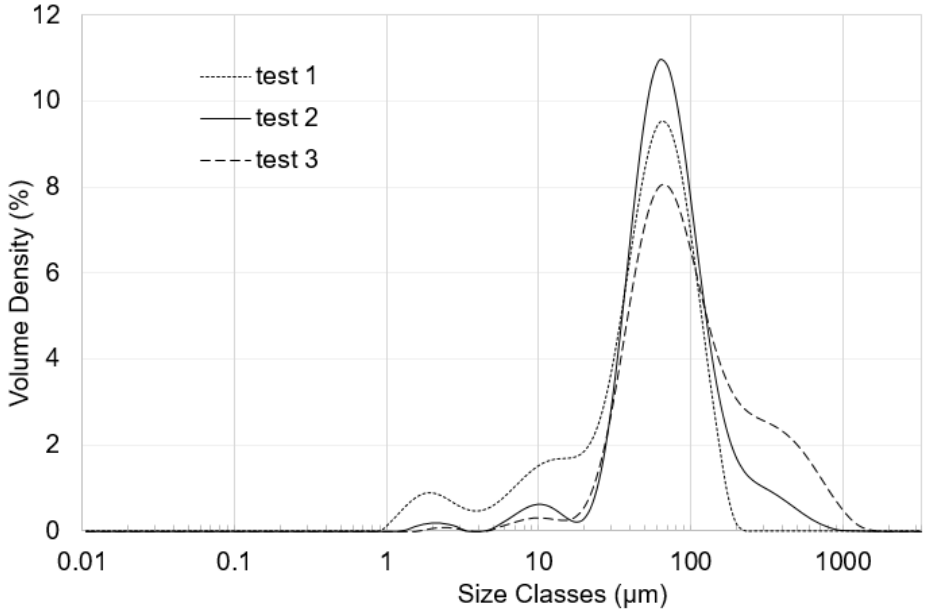

Figure 33. Particle size distribution of three replicate beads samples by setting the airflow rate at 9 Nl min^{-1}.

The liquid jet detached from the tip of the inner capillary undergoes to subsequent elongations and instabilities ending with the periodic droplet's formation. Thus, different velocities are to be found in the droplets immersed into the complex fluid dynamic field leading to the drop merging phenomena (Marra et al., 2017). The faster drop will reach the slower merging in a final drop characterized by a higher diameter compared to that of each of them. Consequently, the particle size distribution was defined by small peaks to the right of the major one.

The most common approach for expressing laser diffraction results is to report the median D50 based on the volume distribution. The D50 is the size in microns that splits the distribution with half above and half below this diameter. This value is one of the easier statistics to understand and also one of the most meaningful for the particle size distributions. However, the single D50 value cannot describe the distribution of the sample and a better approach is to report both a central point of the distribution and the span to express distribution width. The span definition is shown in the equation below:

$$Span = \frac{D90 - \mathrm{D10}}{\mathrm{D50}} \qquad (16)$$

*Differences were not statistically significant in D50 and distribution width by making the comparison between the size distributions of alginate microcapsules with or without the presence of secondary peaks (s.p.). The experimental and numerical results are reported in Table 5 and Table 6*s.p.= secondary peaks

Table 6.

Table 5. D10 and D50 values for different flow velocities of air. Oil and Alginate flow rate were 13 µl min^{-1} and 1 ml min^{-1}, respectively.

Air flow rate (Nl min^{-1})	D10 (µm)		D50 (µm)	
	with s.p.	without s.p.	with s.p.	without s.p.
1	181.35 ± 50.09	250.94 ± 17.64	334.75 ± 18.34	349.43 ± 12.67
2	56.32 ± 4.33	56.32 ± 4.33	202.64 ± 2.73	202.64 ± 2.73
3	58.17 ± 3.45	58.63 ± 4.13	112.18 ± 2.94	112.12 ± 2.86
4	48.31 ± 4.53	49.83 ± 4.81	88.71 ± 4.45	89.30 ± 4.49
5	39.96± 3.97	42.14 ± 3.80	84.67 ± 1.09	85.47 ± 0.62
6	35.48 ± 4.58	37.68 ± 3.88	69.24 ± 2.55	69.01 ± 1.24
7	33.98 ± 13.46	37.31 ± 11.02	76.97 ± 16.48	76.34 ± 16.59
8	24.02 ± 13.69	27.44 ± 11.68	64.56 ± 14.35	66.31 ± 13.47
9	33.18 ± 6.56	35.01 7.16	70.27 ± 2.96	74.14 ± 3.23

s.p.= secondary peaks

Table 6. D90 and span values for different flow velocities of air. Oil and Alginate flow rate were 13 µl min^{-1} and 1 ml min^{-1}, respectively.

Air flow rate (Nl min^{-1})	D90 (µm)		Span	
	with s.p.	without s.p.	with s.p.	without s.p.
1	469.68 ± 12.27	476.40 ± 11.39	0.87 ± 0.17	0.65 ± 0.07
2	386.43 ± 34.68	386.43 ± 34.68	1.63 ± 0.18	1.63 ± 0.18
3	207.44 ± 23.52	205.35 ± 21.64	1.33 ± 0.18	1.31 ± 0.17
4	149.68 ± 1.04	156.85 ± 12.79	1.15 ± 0.11	1.21 ± 0.24
5	174.14 ± 9.23	173.19 ± 11.14	1.59 ± 0.15	1.53 ± 0.17
6	141.10 ± 10.64	124.56 ± 4.46	1.53± 0.06	1.26 ± 0.14
7	186.98 ± 48.89	149.74 ± 26.62	2.00 ± 0.53	1.49 ± 0.17
8	178.33 ± 36.86	160.01 ± 45.83	2.42 ± 0.36	1.98 ± 0.15
9	191.85 ± 7.39	149.20 ± 27.00	2.26± 0.10	1.55 ± 0.49

s.p.= secondary peaks

For this reason, the results shown in *Figure 34* describe the effect of the airflow rate on median value and distribution width, respectively, relate to the appearing of the satellites peaks due to the instability frequencies for Non-Newtonian Rayleigh-Plateau phenomena. Droplet diameter decreased as the airflow rate increased from 1 to 4 Nl min^{-1}.

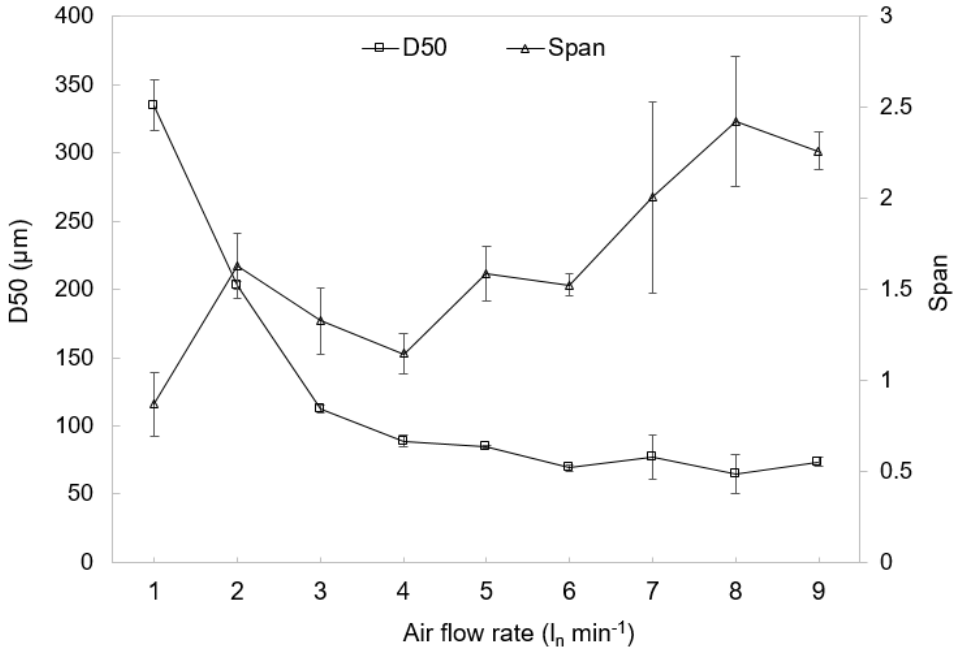

Figure 34. Effect of airflow rate (Nl min^{-1}) on the median diameter D50 (□) and span (△) based on volume distribution of beads produced.

In detail, the device described in the current study enabled to control the size of the calcium alginate beads in the range of 334.75 ± 18.34 μm to 88.71 ± 4.45 μm by increasing the airflow rate up to 4 Nl min^{-1} (see D50 in *Table 5*). These results were in agreement with the work of Sugiura et al. (2007), although referred to development of a different airflow nozzle extrusion technology. A further increase from 5 to 9 Nl min^{-1} was not affecting the size distribution of alginate microcapsules done by air-assisted extrusion. As can be seen by the plateau in *Figure 34* there was no statistically significant change in D50 resulting in a minimum value of 64.56 ± 14.35 μm and a maximum of 84.67 ± 1.09 μm. In addition, a comparison between span values at different air flow rates has been proposed and the results are shown in *Figure 34*. Based on those, the size dispersion increased when the droplet diameter is decreased. The span calculation has proved that the distribution width was not increased by varying the air flow rate from 1 to 6 Nl min^{-1} and was marked by a significant increase from 6 to 9 Nl min^{-1}. According to literature (Poncelet et al., 1993; Lee et al., 2013) if on the one hand, the extrusion dripping systems with the aid of external force (air) reduce the droplet diameter, on the other there was a low control of the production of beads with narrow size distribution.
In *Figure 35* an optical microscope image of core-shell droplets obtained at air flow rate 3 Nl min^{-1} is presented with D50 equal to 112.18 ± 2.94 μm.

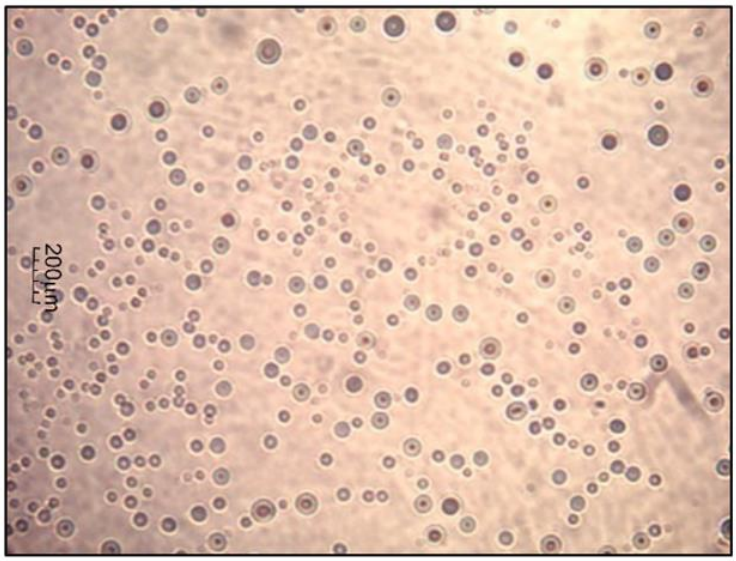

Figure 35. Microscope photograph of prepared Ca-alginate beads. Air flow rate was 3 Nl min^{-1}.

4.3.4 Encapsulation efficiency estimation

The amount of oil initially introduced (w_2) to be encapsulated into the microbeads was 0.721g (approximately 8 ml). The respective amount of that oil actually encapsulated (w_1) measured by *n*-Hexane extraction (described above) was 0.458g. Therefore, equation (1) can be used to estimate the encapsulation efficiency:

$$\text{Encapsulation efficiency (\%)} = \frac{0.458}{0.721} \cdot 100 = 63.5\% \qquad (17)$$

This efficiency is lower than the calculated range 64-89% resulting in the work of Devi et al., 2012. This is firstly because of the different encapsulation technique based on the complex coacervation of gelatin A with sodium alginate, and thus microencapsulation of olive oil in it. Several factors can affect the efficiency of encapsulation. Wu et al. (2013) investigated the influence of the diameter size of microspheres and the shells on the drug content and drug encapsulation efficiency. For example, with spray drying, those are related mainly to the emulsion (solid content, molecular weight, emulsion droplet size, and viscosity) and to the process (feed flow rate, inlet/outlet temperature, gas velocity, and so on). The applied method described in the current study allowed only a rough estimate to be made of the oil encapsulation efficiency considering that the microcapsules have been obtained using the maximum oil flow rate (13 µl min^{-1}) flowing into the inner capillary. A lower oil flow rate could increase the encapsulation efficiency since the shell alginate material would have a greater probability of coating the entire perimeter of the core. As follows, the phenomena of oil loss from microspheres before impact on the surface of the $CaCl_2$ gelation bath could be reduced to a minimum.

4.4 Conclusions

In this work, an innovative industrial oriented technology for core-shell production of alginate microbeads is proposed. The industrial approach is characterized by the simplicity of gelation, cleaning and separation of alginate droplets, and mass production can be obtained by parallelizing the low-cost device adopted in this work. The final size of the droplets can be controlled up to a certain extent as the non-linear droplet break-up mechanisms rely on a certain range of characteristic numbers defining the edges of operative parameters. Nonetheless, droplet production the range of interesting food applications are obtained, paving the way to transfer this technology into real industrial applications.

References

Abraham, S.M., Vieth, R.F., Burgess, D.J., 1996. Novel technology for the preparation of sterile alginate-poly-l-lysine microcapsules in a bioreactor. Pharm. Dev. Technol. 1, 63–68. https://doi.org/10.3109/10837459609031419

Acero, A.J., Montanero, J.M., Ferrera, C., Herrada, M.A., Gañán-Calvo, A.M., 2012. Enhancement of the stability of the flow focusing technique for low-viscosity liquids. J. Micromechanics Microengineering 22. https://doi.org/10.1088/0960-1317/22/11/115039

Aftel, R., Gupta, A.K., Cook, C., Presser, C., 1996. Gas property effects on droplet atomiation and combustion in an air-assist atomier. Symp. Combust. 26, 1645–1651. https://doi.org/10.1016/S0082-0784(96)80388-2

Al-Hajry, H.A., Al-Maskry, S.A., Al-Kharousi, L.M., El-Mardi, O., Shayya, W.H., Goosen, M.F.A., 1999. Electrostatic encapsulation and growth of plant cell cultures in alginate. Biotechnol. Prog. 15, 768–774. https://doi.org/10.1021/bp990069e

Babak, V.G., Skotnikova, E.A., Lukina, I.G., Pelletier, S., Hubert, P., Dellacherie, E., 2000. Hydrophobically associating alginate derivatives: Surface tension properties of their mixed aqueous solutions with oppositely charged surfactants. J. Colloid Interface Sci. 225, 505–510. https://doi.org/10.1006/jcis.2000.6788

Belalia, F., Djelali, N.E., 2014. Rheological properties of sodium alginate solutions. Rev. Roum. Chim. 59, 135–145.

Brandenberger, H., Nüssli, D., Piëch, V., Widmer, F., 1999. Monodisperse particle production: A method to prevent drop coalescence using electrostatic forces. J. Electrostat. 45, 227–238. https://doi.org/10.1016/S0304-3886(98)00052-7

Brandenberger, H., Widmer, F., 1998. A new multinozzle encapsulation/immobilisation system to produce uniform beads of alginate. J. Biotechnol. 63, 73–80. https://doi.org/10.1016/S0168-1656(98)00077-7

Bressel, T.A.B., Paz, A.H., Baldo, G., Lima, E.O.C., Matte, U., Saraiva-Pereira, M.L., 2008. An effective device for generating alginate microcapsules. Genet. Mol. Biol. 31, 136–140. https://doi.org/10.1590/S1415-47572008000100023

Burey, P., Bhandari, B.R., Howes, T., Gidley, M.J., 2009. Gel particles from spray-dried disordered polysaccharides. Carbohydr. Polym. 76, 206–213. https://doi.org/10.1016/j.carbpol.2008.10.001

Burey, P., Bhandari, B.R., Howes, T., Gidley, M.J., 2008. Hydrocolloid gel particles: Formation, characterization, and application. Crit. Rev. Food Sci. Nutr. 48, 361–377. https://doi.org/10.1080/10408390701347801

Ceausoglu, I., Hunkeler, D., 2002. A new microencapsulation device for controlled membrane and capsule size distributions. J. Microencapsul. 19, 725–735. https://doi.org/10.1080/02652040210144261

Cerveró, J.M., Nogareda, J., Valle, E.M.M. del, Galán, M.A., 2011. Development of a technology to produce monodispersed microparticles based on the formation of drops from viscous non-Newtonian liquids sprayed through a fan jet nozzle. Chem. Eng. J. 174, 699–708. https://doi.org/10.1016/j.cej.2011.09.063

Champagne, C.P., Fustier, P., 2007. Microencapsulation for the improved delivery of bioactive compounds into foods. Curr. Opin. Biotechnol. 18, 184–190. https://doi.org/10.1016/j.copbio.2007.03.001

Champagne, C.P., Gardner, N.J., Roy, D., 2005. Challenges in the addition of probiotic cultures to foods. Crit. Rev. Food Sci. Nutr. 45, 61–84. https://doi.org/10.1080/10408690590900144

Chan, E.S., Lee, B.B., Ravindra, P., Poncelet, D., 2009. Prediction models for shape and size of ca-alginate macrobeads produced through extrusion-dripping method. J. Colloid Interface Sci. 338, 63–72. https://doi.org/10.1016/j.jcis.2009.05.027

Chan, E.S., Lim, T.K., Ravindra, P., Mansa, R.F., Islam, A., 2012. The effect of low air-to-liquid mass flow rate ratios on the size, size distribution and shape of calcium alginate particles produced using the atomization method. J. Food Eng. 108, 297–303. https://doi.org/10.1016/j.jfoodeng.2011.08.010

Chen, C., Ye, S., Wang, D., Hatting, J.L., Yu, X., 2014. Alginate embedding and subsequent sporulation of in vitro-produced Conidiobolus thromboides hyphae using a pressurised air-extrusion method. Biol. Control 69, 52–58. https://doi.org/10.1016/j.biocontrol.2013.10.016

Chigier, N., Reitz, R.D., 1996. Regimes of Jet Breakup and Breakup Mechanisms (Physical Aspects), in: Kuo, K. (Ed.), Recent Advances in Spray Combustion: Spray Atomization and Drop Burning Phenomena. American Institute of Aeronautics and Astronautics, Inc., Reston, USA, pp. 109–135.

Ching, S.H., Bhandari, B., Webb, R., Bansal, N., 2015. Visualizing the interaction between sodium caseinate and calcium alginate microgel particles. Food Hydrocoll. 43, 165–171. https://doi.org/10.1016/j.foodhyd.2014.05.013

Chrastil, J., 1991. Gelation of Calcium Alginate. Influence of Rice Starch or Rice Flour on the Gelation Kinetics and on the Final Gel Structure. J. Agric. Food Chem. 39, 874–876. https://doi.org/10.1021/jf00005a012

Chu, L.Y., Utada, A.S., Shah, R.K., Kim, J.W., Weitz, D.A., 2007. Controllable monodisperse multiple emulsions. Angew. Chemie - Int. Ed. 46, 8970–8974. https://doi.org/10.1002/anie.200701358

Cocchietto, M., Blasi, P., Lapasin, R., Moro, C., Gallo, D., Sava, G., 2013. Microencapsulation of Bioactive Principles with an Airless Spray-Gun Suitable for Processing High Viscous Solutions. J. Funct. Biomater. 4, 312–328. https://doi.org/10.3390/jfb4040312

Cohen, I., Li, H., Hougland, J.L., Mrksich, M., Nagel, S.R., 2001. Using selective withdrawal to coat microparticles. Science (80-.). 292, 265–267. https://doi.org/10.1126/science.1059175

Cramer, C., Fischer, P., Windhab, E.J., 2004. Drop formation in a co-flowing ambient fluid. Chem. Eng. Sci. 59, 3045–3058. https://doi.org/10.1016/j.ces.2004.04.006

Cubaud, T., Mason, T.G., 2008. Capillary threads and viscous droplets in square microchannels. Phys. Fluids 20. https://doi.org/10.1063/1.2911716

Cui, J.H., Cao, Q.R., Choi, Y.J., Lee, K.H., Lee, B.J., 2006. Effect of additives on the viability of bifidobacteria loaded in alginate poly-l-lysine microparticles during the freeze-drying process. Arch. Pharm. Res. 29, 707–711. https://doi.org/10.1007/BF02968256

Cui, J.H., Goh, J.S., Park, S.Y., Kim, P.H., Lee, B.J., 2001. Preparation and physical characterization of alginate microparticles using air atomization method. Drug Dev. Ind. Pharm. 27, 309–319. https://doi.org/10.1081/DDC-100103730

Dávalos-Saucedo, C.A., Sarghini, F., Masi, P., 2013. Alginate beads production using a liquid sheet pregelification technique, in: Proc. of the Inside Food Symposium. KU Leuven, Leuven, pp. 1–6.

Deshpande, S.S., Anumolu, L., Trujillo, M.F., 2012. Evaluating the performance of the two-phase flow solver interFoam. Comput. Sci. Discov. 5. https://doi.org/10.1088/1749-4699/5/1/014016

Devi, N., Hazarika, D., Deka, C., Kakati, D.K., 2012. Study of complex coacervation of gelatin a and sodium alginate for microencapsulation of olive oil. J. Macromol. Sci. Part A Pure Appl. Chem. 49, 936–945. https://doi.org/10.1080/10601325.2012.722854

Dimotakis, P.E., 2000. The mixing transition in turbulent flows. J. Fluid Mech. 409, 69–98. https://doi.org/10.1017/S0022112099007946

Dulieu, C., Poncelet, D., Neufeld, R.J., 1999. Encapsulation and Immobilization Techniques, in: Ktihtreiber, W.M., Lanza, R.P., Chick, W.L. (Eds.), Cell Encapsulation Technology and Therapeutics. Springer, New York, pp. 3–17.

Eggers, J., Villermaux, E., 2008. Physics of liquid jets. Reports Prog. Phys. 71. https://doi.org/10.1088/0034-4885/71/3/036601

El-Shanawany, M.S., Lefebvre, A.H., 1980. Airblast Atomization: the Effect of Linear Scale on Mean Drop Size. Am. Soc. Mech. Eng. 4, 184–189.

Errico, A., Lama, G.F.C., Francalanci, S., Chirico, G.B., Solari, L., Preti, F., 2019. Flow dynamics and turbulence patterns in a drainage channel colonized by common reed (Phragmites australis) under different scenarios of vegetation management. Ecol. Eng. 133, 39–52. https://doi.org/10.1016/j.ecoleng.2019.04.016

Fijan, R., Šostar-Turk, S., Lapasin, R., 2007. Rheological study of interactions between non-ionic surfactants and polysaccharide thickeners used in textile printing. Carbohydr. Polym. 68, 708–717. https://doi.org/10.1016/j.carbpol.2006.08.006

Fiszman, G.L., Karara, A.L., Finocchiaro, L.M.E., Glikin, G.C., 2002. A laboratory scale device for microencapsulation of genetically engineered cells into alginate beads. Electron. J. Biotechnol. 5, 279–283. https://doi.org/10.2225/vol5-issue3-fulltext-5

Friso, D., 2017. Meccanica dei solidi e dei fluidi alimentari, in: Friso, D. (Ed.), Ingegneria Dell'industria Agroalimentare. CLEUP sc - Cooperativa Libraria Editrice Università di Padova, Padova, pp. 1–62.

Fundueanu, G., Nastruzzi, C., Carpov, A., Desbrieres, J., Rinaudo, M., 1999. Physico-chemical characterization of Ca-alginate microparticles produced with different methods. Biomaterials 20, 1427–1435. https://doi.org/10.1016/S0142-9612(99)00050-2

Gañán-Calvo, A.M., 1998. Generation of Steady Liquid Microthreads and Micron-Sized Monodisperse Sprays in Gas Streams. Phys. Rev. Lett. 80, 285–288. https://doi.org/10.1103/PhysRevLett.80.285

Gañán-Calvo, A.M., Martín-Banderas, L., González-Prieto, R., Rodríguez-Gil, A., Berdún-Álvarez, T., Cebolla, A., Chávez, S., Flores-Mosquera, M., 2006. Straightforward production of encoded microbeads by Flow Focusing: Potential applications for biomolecule detection. Int. J. Pharm. 324, 19–26. https://doi.org/10.1016/j.ijpharm.2006.05.032

Gañán-Calvo, A.M., Montanero, J.M., 2009. Revision of capillary cone-jet physics: Electrospray and flow focusing. Phys. Rev. E - Stat. Nonlinear, Soft Matter Phys. 79, 1–18. https://doi.org/10.1103/PhysRevE.79.066305

Gåserød, O., Smidsrød, O., Skjåk-Bræk, G., 1998. Microcapsules of alginate-chitosan - I. A quantitative study of the interaction between alginate and chitosan. Biomaterials 19, 1815–1825. https://doi.org/10.1016/S0142-9612(98)00073-8

Gordillo, J.M., Ganán-Calvo, A.M., Pŕez-Saborid, M., 2001. Monodisperse microbubbling: Absolute instabilities in coflowing gas-liquid jets. Phys. Fluids 13, 3839–3842. https://doi.org/10.1063/1.1416188

Gouin, S., 2004. Microencapsulation: Industrial appraisal of existing technologies and trends. Trends Food Sci. Technol. 15, 330–347. https://doi.org/10.1016/j.tifs.2003.10.005

Gundabala, V.R., Martinez-Escobar, S., Marquez, S.M., Marquez, M., Fernandez-Nieves, A., 2013. Celloidosomes® via glass-based microfluidics. J. Phys. D. Appl. Phys. 46. https://doi.org/10.1088/0022-3727/46/11/114006

Haeberle, S., Naegele, L., Burger, R., Stetten, F. Von, Zengerle, R., Ducree, J., 2008. Alginate bead fabrication and encapsulation of living cells under centrifugally induced artificial gravity conditions. J. Microencapsul. 25, 267–274. https://doi.org/10.1080/02652040801954333

Hardikar, A.A., Risbud, M. V., Bhonde, R.R., 1999. A simple microcapsule generator design for islet encapsulation. J. Biosci. 24, 371–376. https://doi.org/10.1007/BF02941251

Hariyadi, D.M., Lin, S.C.Y., Wang, Y., Bostrom, T., Turner, M.S., Bhandari, B., Coombes, A.G.A., 2010. Diffusion loading and drug delivery characteristics of alginate gel microparticles produced by a novel impinging aerosols method. J. Drug Target. 18, 831–841. https://doi.org/10.3109/1061186X.2010.525651

Hariyadi, D.M., Wang, Y., Lin, S.C.Y., Bostrom, T., Bhandari, B., Coombes, A.G.A., 2012. Novel alginate gel microspheres produced by impinging aerosols for oral delivery of proteins. J. Microencapsul. 29, 250–261. https://doi.org/10.3109/02652048.2011.646329

Heinzen, C., Berger, A., Marison, I., 2004. Technology for Jet Break-Up for Encapsulation of Cells and Liquids in Monodisperse Microcapsules, in: Nedovic, V., Willaert, R. (Eds.), Fundamentals of Cell Immobilisation Biotechnology. Kluwer Academic Publishers, pp. 257–275.

Herrada, M.A., Gañán-Calvo, A.M., Ojeda-Monge, A., Bluth, B., Riesco-Chueca, P., 2008. Liquid flow focused by a gas: Jetting, dripping, and recirculation. Phys. Rev. E - Stat. Nonlinear, Soft Matter Phys. 78, 1–16. https://doi.org/10.1103/PhysRevE.78.036323

Herrero, Edgar P., Del Valle, E.M.M., Galán, M.A., 2006. Modelling prediction of the microcapsule size of polyelectrolyte complexes produced by atomization. Chem. Eng. J. 121, 1–8. https://doi.org/10.1016/j.cej.2006.04.003

Herrero, E. P., Martín Del Valle, E.M., Galán, M.A., 2006. Development of a new technology for the production of microcapsules based in atomization processes. Chem. Eng. J. 117, 137–142. https://doi.org/10.1016/j.cej.2005.12.022

Hirt, C.W., Nichols, B.D., 1981. Volume of Fluid (VOF) Method for the Dynamics of Free Boundaries*. J. Comput. Phys. 39, 201–225. https://doi.org/10.1016/0021-9991(81)90145-5

Klokk, T.I., Melvik, J.E., 2002. Controlling the size of alginate gel beads by use of a high electrostatic potential. J. Microencapsul. 19, 415–424. https://doi.org/10.1080/02652040210144234

Kontturi, L.S., Yliperttula, M., Toivanen, P., Määttä, A., Määttä, A.M., Urtti, A., 2011. A laboratory-scale device for the straightforward production of uniform, small sized cell microcapsules with long-term cell viability. J. Control. Release 152, 376–381. https://doi.org/10.1016/j.jconrel.2011.03.005

Krasaekoopt, W., Bhandari, B., Deeth, H., 2004. The influence of coating materials on some properties of alginate beads and survivability of microencapsulated probiotic bacteria. Int. Dairy J. 14, 737–743. https://doi.org/10.1016/j.idairyj.2004.01.004

Lakkis, J.M., 2016. Encapsulation and controlled release in bakery applications, in: Lakkis, J.M. (Ed.), Encapsulation and Controlled Release Technologies in Food Systems. John Wiley & Sons, Inc., United Kingdom, pp. 204–235.

Lasheras, J.C., Hopfinger, E.J., 2000. Liquid Jet Instability and Atomization in a Coaxial Gas Stream. Annual Review of Fluid Mechanics. Annu. Rev. Fluid Mech. 32, 275–308. https://doi.org/10.1146/annurev.genom.1.1.409

Lasheras, J.C., Villermaux, E., Hopfinger, E.J., 1998. Break-up and atomization of a round water jet by a high-speed annular air jet. J. Fluid Mech. 30, 85–105.

Lee, B.B., Bhandari, B.R., Howes, T., 2016. Air Extrusion System for Ionotropic Alginate Microgel Particle Formation: A Review. Chem. Eng. Technol. 39, 2355–2369. https://doi.org/10.1002/ceat.201600088

Lee, B.B., Ravindra, P., Chan, E.S., 2013. Size and shape of calcium alginate beads produced by extrusion dripping. Chem. Eng. Technol. 36, 1627–1642.

https://doi.org/10.1002/ceat.201300230
Lee, J.S., Cha, D.S., Park, H.J., 2004. Survival of freeze-dried Lactobacillus bulgaricus KFRI 673 in chitosan-coated calcium alginate microparticles. J. Agric. Food Chem. 52, 7300–7305. https://doi.org/10.1021/jf040235k
Leong, J.Y., Lam, W.H., Ho, K.W., Voo, W.P., Lee, M.F.X., Lim, H.P., Lim, S.L., Tey, B.T., Poncelet, D., Chan, E.S., 2016. Advances in fabricating spherical alginate hydrogels with controlled particle designs by ionotropic gelation as encapsulation systems. Particuology 24, 44–60. https://doi.org/10.1016/j.partic.2015.09.004
Lin, S.P., Reitz, R.D., 1998. Drop and Spray Formation from a Liquid Jet. Annu. Rev. Fluid Mech. 30, 85–105. https://doi.org/10.1146/annurev.fluid.30.1.85
Lin, T.C., 2012. Performance of a Micro Atomizer Under Single-Fluid and Twin-Fluid Micro-Encapsulation Process. Int. J. Mod. Phys. Conf. Ser. 19, 219–226. https://doi.org/10.1142/s2010194512008781
Ma, J., Lin, Y., Chen, X., Zhao, B., Zhang, J., 2014. Flow behavior, thixotropy and dynamical viscoelasticity of sodium alginate aqueous solutions. Food Hydrocoll. 38, 119–128. https://doi.org/10.1016/j.foodhyd.2013.11.016
Mansour, A., Chigier, N., 1995. Air-blast atomization of non-Newtonian liquids. J. Nonnewton. Fluid Mech. 58, 161–194. https://doi.org/10.1016/0377-0257(95)01356-Z
Marra, F., De Vivo, A., Sarghini, F., 2018. Air Assisted Production of Alginate Beads Using Focusing Flow Microfluidic Devices: Numerical Modeling of Beads Formation. Lect. Notes Bioeng. 119–127. https://doi.org/10.1007/978-3-319-62027-5_11
Marra, F., De Vivo, A., Sarghini, F., 2017. Virtualization of fluid-dynamics in micro-air assisted extruders for food microfluidic based encapsulation. J. Food Eng. 213, 89–98. https://doi.org/10.1016/j.jfoodeng.2017.04.030
Martín-Banderas, L., Flores-Masquera, M., Riesco-Chueca, P., Rodríguez-Gil, A., Cebolla, Á., Chávez, S., Gañán-Calvo, A.M., 2005. Flow focusing: A versatile technology to produce size-controlled and specific-morphology microparticles. Small 1, 688–692. https://doi.org/10.1002/smll.200500087
Martín-Banderas, L., González-Prieto, R., Rodríguez-Gil, A., Fernández-Arévalo, M., Flores-Mosquera, M., Chávez, S., Gaņán-Calvo, A.M., 2011. Application of flow focusing to the break-up of a magnetite suspension jet for the production of paramagnetic microparticles. J. Nanomater. 2011, 1–10. https://doi.org/10.1155/2011/527437
Martins, E., Poncelet, D., Rodrigues, R.C., Renard, D., 2017. Oil encapsulation techniques using alginate as encapsulating agent: applications and drawbacks. J. Microencapsul. 34, 754–771. https://doi.org/10.1080/02652048.2017.1403495
Montanero, J.M., Rebollo-Muņoz, N., Herrada, M.A., Gaņán-Calvo, A.M., 2011. Global stability of the focusing effect of fluid jet flows. Phys. Rev. E - Stat. Nonlinear, Soft Matter Phys. 83, 1–7. https://doi.org/10.1103/PhysRevE.83.036309
Murakami, R., Takashima, R., 2003. Mechanical properties of the capsules of chitosan-soy globulin polyelectrolyte complex. Food Hydrocoll. 17, 885–888. https://doi.org/10.1016/S0268-005X(03)00109-7
Narsaiah, K., Jha, S.N., Wilson, R.A., Mandge, H.M., Manikantan, M.R., 2014. Optimizing microencapsulation of nisin with sodium alginate and guar gum. J. Food Sci. Technol. 51, 4054–4059. https://doi.org/10.1007/s13197-012-0886-6
Nie, Z., Seo, M.S., Xu, S., Lewis, P.C., Mok, M., Kumacheva, E., Whitesides, G.M., Garstecki, P., Stone, H.A., 2008. Emulsification in a microfluidic flow-focusing device: Effect of the viscosities of the liquids. Microfluid. Nanofluidics 5, 585–594. https://doi.org/10.1007/s10404-008-0271-y

Ouwerx, C., Velings, N., Mestdagh, M.M., Axelos, M.A.V., 1998. Physico-chemical properties and rheology of alginate gel beads formed with various divalent cations. Polym. Gels Networks 6, 393–408. https://doi.org/10.1016/S0966-7822(98)00035-5

Peretz, S., 2004. Interaction of alginate with metal ions, cationic surfactants and cationic dyes 49, 857–865.

Perrechil, F.A., Sato, A.C.K., Cunha, R.L., 2011. κ-Carrageenan-sodium caseinate microgel production by atomization: Critical analysis of the experimental procedure. J. Food Eng. 104, 123–133. https://doi.org/10.1016/j.jfoodeng.2010.12.004

Poncelet, D., 2001. Production of Alginate Beads by Emulsification/Internal Gelation. Ann. N. Y. Acad. Sci. 944, 74–82. https://doi.org/10.1111/j.1749-6632.2001.tb03824.x

Poncelet, D., Babak, V.G., Neufeld, R.J., Goosen, M.F.A., Burgarski, B., 1999. Theory of electrostatic dispersion of polymer solutions in the production of microgel beads containing biocatalyst. Adv. Colloid Interface Sci. 79, 213–228. https://doi.org/10.1016/S0001-8686(97)00037-7

Poncelet, D., Poncelet De Smet, B., Beaulieu, C., Neufeld, R.J., 1993. Scale-up of gel bead and microcapsule production in cell immobilization, in: Goosen, M.F.A. (Ed.), Fundamentals of Animal Cell Encapsulation and Immobilization. CRC Press, pp. 113–141.

Prüsse, U., Bilancetti, L., Bučko, M., Bugarski, B., Bukowski, J., Gemeiner, P., Lewińska, D., Manojlovic, V., Massart, B., Nastruzzi, C., Nedovic, V., Poncelet, D., Siebenhaar, S., Tobler, L., Tosi, A., Vikartovská, A., Vorlop, K.D., 2008. Comparison of different technologies for alginate beads production. Chem. Pap. 62, 364–374. https://doi.org/10.2478/s11696-008-0035-x

Rehg, T., Dorger, C., Chau, P.C., 1986. Application of an atomizer in producing small alginate gel beads for cell immobilization. 8, 111–114.

Rodríguez-Rivero, C., Nogareda, J., Martín, M., del Valle, E.M.M., Galán, M.A., 2013. CFD modeling and its validation of non-Newtonian fluid flow in a microparticle production process using fan jet nozzles. Powder Technol. 246, 617–624. https://doi.org/10.1016/j.powtec.2013.05.050

Santa-Maria, M., Scher, H., Jeoh, T., 2012. Microencapsulation of bioactives in cross-linked alginate matrices by spray drying. J. Microencapsul. 29, 286–295. https://doi.org/10.3109/02652048.2011.651494

Sarghini, F., 2015. Microfluidic Encapsulation Process, in: Mishra, M.K. (Ed.), Handbook of Encapsulation and Controlled Release. CRC Press, Boca Raton, USA, pp. 359–378.

Sarghini, F., De Vivo, A., 2019. Effect of process parameters on microencapsulation of active compounds by co-flow air assisted microfluidic extrusion. Chem. Eng. Trans. 75, 439–444. https://doi.org/10.3303/CET1975074

Schneider, T., Chapman, G.H., Häfeli, U.O., 2011. Effects of chemical and physical parameters in the generation of microspheres by hydrodynamic flow focusing. Colloids Surfaces B Biointerfaces 87, 361–368. https://doi.org/10.1016/j.colsurfb.2011.05.040

Schneider, T., Zhao, H., Jackson, J.K., Chapman, G.H., Dykes, J., HaFeli, U.O., 2008. Use of Hydrodynamic Flow Focusing for the Generation of Biodegradable Camptothecin-Loaded Polymer Microspheres. J. Pharm. Sci. 97, 4943–4954. https://doi.org/10.1002/jps.21344

Schoubben, A., Blasi, P., Giovagnoli, S., Rossi, C., Ricci, M., 2010. Development of a scalable procedure for fine calcium alginate particle preparation. Chem. Eng. J. 160, 363–369. https://doi.org/10.1016/j.cej.2010.02.062

Seifert, D.B., Phillips, J.A., 1997. Production of small, monodispersed alginate beads for cell immobilization. Biotechnol. Prog. 13, 562–568. https://doi.org/10.1021/bp9700723

Shah, R.K., Shum, H.C., Rowat, A.C., Lee, D., Agresti, J.J., Utada, A.S., Chu, L.-Y., Kim, J.-W., Fernandez-Nieves, A., Martinez, C.J., Weitz, D.A., 2008. Designer emulsions using microfluidics Open access under CC BY-NC-ND license. Mater. Today 11, 18–27. https://doi.org/10.1016/S1369-7021(08)70053-1

Shilpa, A., Agrawal, S.S., Ray, A.R., 2003. Controlled delivery of drugs from alginate matrix. J. Macromol. Sci. - Polym. Rev. 43, 187–221. https://doi.org/10.1081/MC-120020160

Si, T., Li, F., Yin, X.Y., Yi, X.Z., 2009. Modes in flow focusing and instability of coaxial liquid-gas jets. J. Fluid Mech. 629, 1–23. https://doi.org/10.1017/S0022112009006211

Simpson, N.E., Grant, S.C., Blackband, S.J., Constantinidis, I., 2003. NMR properties of alginate microbeads. Biomaterials 24, 4941–4948. https://doi.org/10.1016/S0142-9612(03)00418-6

Sohail, A., Turner, M.S., Coombes, A., Bostrom, T., Bhandari, B., 2011. Survivability of probiotics encapsulated in alginate gel microbeads using a novel impinging aerosols method. Int. J. Food Microbiol. 145, 162–168. https://doi.org/10.1016/j.ijfoodmicro.2010.12.007

Sohail, A., Turner, M.S., Prabawati, E.K., Coombes, A.G.A., Bhandari, B., 2012. Evaluation of Lactobacillus rhamnosus GG and Lactobacillus acidophilus NCFM encapsulated using a novel impinging aerosol method in fruit food products. Int. J. Food Microbiol. 157, 162–166. https://doi.org/10.1016/j.ijfoodmicro.2012.04.025

Sugiura, S., Oda, T., Aoyagi, Y., Matsuo, R., Enomoto, T., Matsumoto, K., Nakamura, T., Satake, M., Ochiai, A., Ohkohchi, N., Nakajima, M., 2007. Microfabricated airflow nozzle for microencapsulation of living cells into 150 micrometer microcapsules. Biomed. Microdevices 9, 91–99. https://doi.org/10.1007/s10544-006-9011-9

Sugiura, S., Oda, T., Izumida, Y., Aoyagi, Y., Satake, M., Ochiai, A., Ohkohchi, N., Nakajima, M., 2005. Size control of calcium alginate beads containing living cells using micro-nozzle array. Biomaterials 26, 3327–3331. https://doi.org/10.1016/j.biomaterials.2004.08.029

Sun, X.T., Liu, M., Xu, Z.R., 2014. Microfluidic fabrication of multifunctional particles and their analytical applications. Talanta 121, 163–177. https://doi.org/10.1016/j.talanta.2013.12.060

Tabeei, A., Samimi, A., Khorram, M., Moghadam, H., 2012. Study pulsating electrospray of non-Newtonian and thixotropic sodium alginate solution. J. Electrostat. 70, 77–82. https://doi.org/10.1016/j.elstat.2011.10.006

Tran, V.T., Benoît, J.P., Venier-Julienne, M.C., 2011. Why and how to prepare biodegradable, monodispersed, polymeric microparticles in the field of pharmacy? Int. J. Pharm. 407, 1–11. https://doi.org/10.1016/j.ijpharm.2011.01.027

Tryggvason, G., Scardovelli, R., Zaleski, S., 2004. Direct Numerical Simulations of Gas-Liquid Multiphase flows. Cambridge University Press, Cambridge. https://doi.org/10.1142/9781860949609_0009

Utada, A.S., Chu, L., Link, D.R., Holtze, C., Weitz, D.A., 2007. Dripping, Jetting, Drops, and Wetting: The Magic of Microfluidics 32, 702–708.

Utada, A.S., Lorenceau, E., Link, D.R., Kaplan, P.D., Stone, H.A., Weitz, D.A., 2005. Monodisperse double emulsions generated from a microcapillary device. Science (80-.). 308, 537–541. https://doi.org/10.1126/science.1109164

Van Steijn, V., Kleijn, C.R., Kreutzer, M.T., 2009. Flows around confined bubbles and

their importance in triggering pinch-off. Phys. Rev. Lett. 103, 1–4. https://doi.org/10.1103/PhysRevLett.103.214501
Vega, E.J., Montanero, J.M., Herrada, M.A., Gañán-Calvo, A.M., 2010. Global and local instability of flow focusing: The influence of the geometry. Phys. Fluids 22, 1–10. https://doi.org/10.1063/1.3450321
Velings, N.M., Mestdagh, M.M., 1995. Physico-chemical properties of alginate gel beads. Polym. Gels Networks 3, 311–330. https://doi.org/10.1016/0966-7822(94)00043-7
Voo, W.P., Lee, B.B., Idris, A., Islam, A., Tey, B.T., Chan, E.S., 2015. Production of ultra-high concentration calcium alginate beads with prolonged dissolution profile. RSC Adv. 5, 36687–36695. https://doi.org/10.1039/c5ra03862f
Weiner, M.L., Salminen, W.F., Larson, P.R., Barter, R.A., Kranetz, J.L., Simon, G.S., 2001. Toxicological review of inorganic phosphates. Food Chem. Toxicol. 39, 759–786. https://doi.org/10.1016/S0278-6915(01)00028-X
Whelehan, M., Marison, I.W., 2011. Microencapsulation using vibrating technology. J. Microencapsul. 28, 669–688. https://doi.org/10.3109/02652048.2011.586068
Whelehan, M., von Stockar, U., Marison, I.W., 2010. Removal of pharmaceuticals from water: Using liquid-core microcapsules as a novel approach. Water Res. 44, 2314–2324. https://doi.org/10.1016/j.watres.2009.12.036
Wikström, J., Elomaa, M., Syväjärvi, H., Kuokkanen, J., Yliperttula, M., Honkakoski, P., Urtti, A., 2008. Alginate-based microencapsulation of retinal pigment epithelial cell line for cell therapy. Biomaterials 29, 869–876. https://doi.org/10.1016/j.biomaterials.2007.10.056
Woo, J.W., Roh, H.J., Park, H.D., Ji, C.I., Lee, Y.B., Kim, S.B., 2007. Sphericity Optimization of Calcium Alginate Gel Beads and the Effects of Processing Conditions on Their Physical Properties. Food Sci. Biotechnol. 16, 715–721.
Wu, J., Kong, T., Yeung, K.W.K., Shum, H.C., Cheung, K.M.C., Wang, L., To, M.K.T., 2013. Fabrication and characterization of monodisperse PLGA-alginate core-shell microspheres with monodisperse size and homogeneous shells for controlled drug release. Acta Biomater. 9, 7410–7419. https://doi.org/10.1016/j.actbio.2013.03.022
Yotsuyanagi, T., Ohkubo, T., Ohhashi, T., Ikeda, K., 1987. Calcium-Induced Gelation of Alginic Acid and pH-Sensitive Reswelling of Dried Gels. Chem. Pharm. Bull. 35, 1555–1563. https://doi.org/10.1248/cpb.35.1555
Yu, W.K., Yim, T. Bin, Lee, K.Y., Heo, T.R., 2001. Effect of skim milk-alginate beads on survival rate of bifidobacteria. Biotechnol. Bioprocess Eng. 6, 133–138. https://doi.org/10.1007/BF02931959
Zhang, J., Li, X., Zhang, D., Xiu, Z., 2007. Theoretical and experimental investigations on the size of alginate microspheres prepared by dropping and spraying. J. Microencapsul. 24, 303–322. https://doi.org/10.1080/02652040701339098
Zhou, C., Yue, P., Feng, J.J., 2006. Formation of simple and compound drops in microfluidic devices. Phys. Fluids 18, 1–14. https://doi.org/10.1063/1.2353116
Zimmermann, H., Hillgärtner, M., Manz, B., Feilen, P., Brunnenmeier, F., Leinfelder, U., Weber, M., Cramer, H., Schneider, S., Hendrich, C., Volke, F., Zimmermann, U., 2003. Fabrication of homogeneously cross-linked, functional alginate microcapsules validated by NMR-, CLSM- and AFM-imaging. Biomaterials 24, 2083–2096. https://doi.org/10.1016/S0142-9612(02)00639-7

5 Conclusions

The microfluidic technology designed in this work aimed to develop an encapsulation process can be used food in both matrix and core-shell configuration, and it represents a simple and cheap solution at the same time. The industrial scale-up is based on the massive parallelization approach, able to preserve the sensitivity to heat, toxins, oxidation, light, moisture, pH, pressure or mechanical shear of the raw form of a variety of substances, by closing them in microcapsules.

The extrusion system coupled with a micro-air co-flow nozzle allows to produce microgels with a mean diameter (D50) in the range of 27.1–87.5 μm and 64.6–334.8 μm for the matrix and core-shell microencapsulation systems, respectively.

The analysis of the process variables, such as concentration and physical properties, i.e., viscosity of the alginate solution, gelation method, flow rate of the alginate solution and air, collecting distance between nozzle and gelation bath etc. was required to identify the size and size distribution of the Ca-alginate beads formed since those variables affect the extrusion modes and the break up regimes, as mentioned in this thesis.

The study of the air-flow rate influence led to a decrease of the microgels size with the rate of the pressurized air increase. On the other hand, the size distribution of the beads produced increased as the air flow rate increased using coaxial air as external force to break up the pendant droplet prior to its maximum droplet volume.

It has also been demonstrated that a minor capillary misalignment (15°) had a relevant impact on the size and size heterogeneity of the microgels.

In the air extrusion methods, pressurized air is used to break the alginate solution into fine size droplets that is not easily achievable via natural extrusion dripping, but the understanding of the droplet formation dynamics becomes more complex and difficult to predict. This is due to the appearing of the satellites (secondary) droplets resulting in the double whipping and merging phenomena.

An improvement to the air extrusion process could be achieved by deepening understanding of the compressibility effect at air-alginate interface since numerical simulations highlighted air velocity of the order up to 100 m/s

Moreover, in order to extend the application of air extrusion systems to industrial production of Ca-alginate microbeads, future challenges could include the definition of the control system setup in order to reduce the possible redundancy of liquid pumping system and the complexity of control.

Further development of the technology is required to adapt the microfluidic approach to new coating material.

Finally, further innovative modifications could overcome the deformation of the droplet due to the impact on the gelation bath-air interface developing a new gelation process for example based on the crystal gun method described in detail in the introduction of this thesis.